



universität
wien

MASTERARBEIT

Titel der Masterarbeit

Comparison of two *in vitro* neural crest stem cell differentiation systems derived from human induced pluripotent stem cells under defined culture conditions

verfasst von

Song-Hi Kneutgen, BSc

angestrebter akademischer Grad

Master of Science (MSc)

Wien, 2014

Studienkennzahl lt. Studienblatt: A 066 834

Studienrichtung lt. Studienblatt: Masterstudium Molekulare Biologie

Betreut von: Ao. Univ.Prof.Mag. Dr. Ernst Müllner

STATUTORY DECLARATION

"I declare in lieu of an oath that I have written this bachelor's paper myself and that I have not used any sources or resources other than stated for its preparation.

I further declare that I have clearly indicated all direct and indirect quotations. This master thesis has not been submitted elsewhere for examination purposes."

Date:

Signature:

I. ACKNOWLEDGEMENT

First of all I want to thank Dr. Andreas Kurtz that I had the great opportunity to perform this research project in his laboratory at the Berlin-Brandenburg Center for Regenerative Therapies (BCRT) and for supervising this thesis. I want to thank Dr. Harald Stachelscheid who provided me deeper insight in hiPSCs.

Especially, I am deeply grateful to my supervisor Prof. Ernst Müllner in Vienna for his support and advices during my whole study.

Big thanks to the PhD students Krithika Hariharan and Bella Roßbach who introduced and helped me in the hiPSCs culture work and analyzed my samples by FACS. I thank Manfred Roch for his help concerning mesenchymal stem cells. Huge thanks to Linda El-Ahmad, Dr. Julian Braun, Johannes Grünhagen and Maik Stein who supported me with their knowledge in laboratory detection methods. Especially, I want to thank Hanna Lorig who conducted me in the performance of osteogenic detection methods. Thank you, Leila, for working with me on my project. I also want to thank Michael Westphal, Susanne Hildebrandt, Su-Jun Oh, Patrizia Wehler, Isidora Paredes, Stefanie Seltsmann, Fritz Lekschas and Su-Jin Park. It was really nice to work with you in the friendly atmosphere and I enjoyed the time with you.

Special thanks to Hanna Lorig, Dr. Daniela Heeg, and Dr. Jakob Schwendner for correcting my thesis.

And big thanks to my Sandra Kronimus, who accompanied me during my study and the time in the lab. You always helped me out when I lost my mind.

I also want to thank Kevin Gray for his mental support and that he always took care of me.

Finally, I want to thank my stepfather Rüdiger Niemann, who always supported me. Without your moral, emotional as well financial support I would never come to this way.

II. SUMMARY

The neural crest (NC) is a characteristic feature of vertebrates consisting of a transient multipotent embryonic cell population. In early development, NC stem cells (NCSCs) migrate through the body and contribute to various organ systems. Abnormal development of NCSCs can lead to several severe birth defects summarized as neurocristopathies. Generation of human induced pluripotent stem cells (hiPSCs)-derived NCSCs represents a valuable tool for studying the biology of NC development and diseases. Moreover, hiPSCs-derived NCSCs have become a promising technology as patient-specific disease model and availability of unlimited numbers of NCSCs might serve as cell source for cell therapy and tissue engineering.

In this work, we performed *in vitro* NC differentiation systems to investigate the most effective method for producing high amounts of hiPSCs-derived NC-like cells. To this end, two methods that induce NC differentiation through modified signaling pathways under defined culture conditions were tested. Our outcomes revealed that pharmacological inhibition of transforming growth factor- β (TGF- β) combined with activated WNT signaling yields more hiPSCs derived NC-like cells compared to pharmacological inhibition of bone morphogenic protein (BMP) and TGF- β . Activated WNT signaling combined with TGF- β inhibition yielded 68.22 % HNK1⁺p75⁺ cells detected by immunocytochemistry (ICC) staining while fluorescent activated cell sorting (FACS) analyzed 35.2 % HNK1⁺p75⁺ cells. In contrast, dual SMAD blockade produced only 13.68 % HNK1⁺p75⁺ cells monitored by ICC evaluation and 7.4 % HNK1⁺p75⁺ cells determined by FACS analysis. However, both methods required cell-sorting for HNK1 and p75 surface receptors to obtain highly purified NC-like cells.

To proof NC multipotency, osteogenic differentiation was induced with unsorted NC-cells obtained by activated canonical WNT signaling and TGF- β suppression, FACSorted hiPSCs-derived NC-like cells, human mesenchymal stem cells (hMSCs), and human epidermal neural crest stem cells. Alkaline phosphatase (ALP) assay and Alizarin red staining verified that unsorted hiPSCs derived NC-like cells possessed highest potential to differentiate towards osteogenic lineage compared to FACSorted hiPSCs derived NC-like cell population, hMSCs and hEpi-NCSCs.

III. ZUSAMMENFASSUNG

Die Neuralleiste ist ein charakteristisches Merkmal von Vertebraten und besteht aus einer transienten, multipotenten, embryonalen Zellpopulation. Um ihren Bestimmungsort zu erreichen legen diese, ausgehend von ihrem Ursprung, weite Strecken im Körper zurück. In Abhängigkeit von ihrem Bestimmungsort differenzieren die Nachkommen zu einer Vielzahl von unterschiedlichen Zelltypen. Deshalb können Störungen, die während der Entwicklung der Neuralleiste auftreten, zu schweren Geburtskrankheiten führen. Diese Krankheiten werden als „neurocristopathies“ zusammengefasst. Aus diesem Grund, ist die Differenzierung von humanen induzierten pluripotenten Stammzellen (hiPSCs) zu Neuralleistenzellen von großer Bedeutung, um die Entwicklung der Neuralleiste sowie die dazugehörigen Krankheitserscheinungen zu erforschen. Desweiteren erweckt diese Differenzierungsmethode großes Interesse in der Zelltherapie, in Hinblick auf patientenspezifische Krankheitsmodelle, sowohl auch als Modell einer unbegrenzten Quelle von Neuralleistenzellen.

In der vorliegenden Arbeit wurden zwei *in vitro* Zellkulturmodelle miteinander verglichen, um zu untersuchen, welche der beiden die effizienteste Methode darstellt um die größtmögliche Ausbeute von hiPSCs basierenden Neuralleistenzellen zu erreichen. Zu diesem Zweck wurden zwei bereits publizierte Methoden ausgewählt, welche die Differenzierung von hiPSCs zu Neuralleistenzellen induzieren. Dies erfolgte über Modifizierungen von intrazellulären Signalkaskaden unter feederzellfreien, definierten Zellkulturbedingungen. Unsere Ergebnisse bestätigen, dass die pharmakologische Inhibierung von TGF- β in Kombination mit einer Aktivierung von canonical WNT Signalweg eine höhere Ausbeute erzielt, als eine duale Blockade von SMAD Signalwegen. Die Charakterisierung dieser Zellen erfolgt über die Präsenz von zwei Oberflächenrezeptoren der Neuralleisten - HNK1⁺ und p75⁺. Die immunochemische Färbung (ICC) detektierte 68,22 % HNK1⁺p75⁺ Zellen, während via FACS Analyse 35,2 % HNK1⁺p75⁺ Zellen ermittelt wurden. Dem gegenübergestellt ergaben die ICC Auswertungen mittels dual SMAD Inhibierung nur 13,68 % HNK1⁺p75⁺ Zellen. Die FACS Untersuchung zeigte 7,4 % HNK1⁺p75⁺ Zellen. Jedoch benötigten beide Methoden im Anschluss einen Zellsortierungsschritt um eine pure Zellpopulation zu erhalten.

Um die Multipotenz der Zellen der Neuralleiste zu demonstrieren wurde eine osteogene Differenzierung ausgehend von unsortierten HNK1⁺p75⁺ Zellen, FACS sortierten HNK1⁺p75⁺ Zellen, mesenchymale Stammzellen (MSCs) und epidermale Zellen der Neuralleiste (hEpi-NCSCs) initiiert. Der biochemische Nachweis des Enzyms Alkalische Phosphatase sowohl auch die Alizarin Red Färbung haben deutlich gezeigt, dass die höchste Mineralisierung in unsortierten HNK1⁺p75⁺ Zellen stattgefunden hat.

IV. TABLE OF CONTENTS

I. STATUTORY DECLARATION	III
II. ACKNOWLEDGEMENT	V
III. SUMMARY	VII
IV. ZUSAMMENFASSUNG	IX
V. TABLE OF CONTENTS	XI
VI. LIST OF FIGURES	XV
VII. LIST OF TABLES	XVII
1 INTRODUCTION	1
1.1 STEM CELLS	1
1.1.1 HUMAN EMBRYONIC STEM CELLS (hESCs)	2
1.1.2 HUMAN INDUCED PLURIPOTENT STEM CELLS (hiPSCs)	3
1.1.3 ADULT STEM CELLS	6
1.1.4 MESENCHYMAL STEM CELLS (MSCs)	6
1.2 THE NEURAL CREST	7
1.2.1 MAJOR SIGNALING PATHWAYS IN NC FORMATION	9
1.2.2 GENE REGULATORY NETWORK DURING NCSC DEVELOPMENT	10
1.2.3 EXPERIMENTAL METHODS FOR <i>IN VITRO</i> NCSC INDUCTION FROM hiPSC	15
1.2.4 NCSC MULTIPOTENCY REPRESENTED BY OSTEOGENIC DIFFERENTIATION	17
1.2.5 hiPSCs DERIVED NCSCs AND THEIR ROLE IN CELL REPLACEMENT THERAPY	19
2 AIM OF THE PROJECT	21
3 MATERIAL AND METHODS	23
3.1 MATERIALS	23
3.2 CELL CULTURE METHODS	26
3.2.1 CULTIVATION OF CELL LINES	26
3.2.2 FREEZING OF CELLS: hEPI-NCSCs	26
3.2.3 THAWING OF CELL LINES: hEPI-NCSCs	27
3.2.4 CELL PASSAGE OF CELL LINES	27
	XI

3.2.5	CELL COUNTING	29
3.3	NCSC DIFFERENTIATION FROM hiPSC	30
3.3.1	NCSC DIFFERENTIATION FROM hiPSCs BY DUAL SMAD INHIBITION ACCORDING TO GABSANG LEE (2010)	30
3.3.2	NCSC DIFFERENTIATION FROM hiPSCs BY THE ACTIVATION OF WNT SIGNALING AND THE INHIBITION OF SMAD ACCORDING TO LAURA MENENDEZ (2011).	31
3.4	NCSC CHARACTERIZATION	32
3.4.1	RNA ISOLATION	32
3.4.2	CDNA SYNTHESIS	32
3.4.3	POLYMERASE CHAIN REACTION (PCR)	33
3.4.4	GEL ELECTROPHORESIS	35
3.4.5	IMMUNOHISTOCHEMISTRY (ICC)	35
3.4.6	ICC EVALUATION BY COLUMBUS IMAGE DATA STORAGE AND ANALYSIS SYSTEM (PERKIN ELMER)	36
3.4.7	FLUORESCENCE-ACTIVATED CELL SORTING (FACS) ANALYSIS	37
3.4.8	SAMPLE PREPARATION FOR FACSORTING	38
3.4.9	FACSORTING	38
3.4.10	QUANTITATIVE REAL TIME PCR (QRT-PCR)	39
3.5	OSTEOGENIC DIFFERENTIATION	40
3.6	OSTEOGENIC CHARACTERIZATION	41
3.6.1	ALKALINE PHOSPHATASE BIOCHEMICAL ASSAY (ALP-ASSAY)	41
3.6.2	ALKALINE PHOSPHATASE STAINING	42
3.6.3	ALIZARIN RED STAINING	42
3.6.4	STATISTICAL ANALYSIS	43
4	RESULTS	45
4.1	NCSC DIFFERENTIATION	45
4.1.1	PHENOTYPIC CHARACTERIZATION OF hiPSCs DURING NCSC DIFFERENTIATION PROCESS	45
4.1.2	CHARACTERIZATION OF NCSCs BY ANALYZING NCSC MARKERS ON MRNA LEVEL, ICC STAINING, FACS ANALYSIS AND REAL TIME PCR	49
4.2	NCSC MULTIPOTENCY PROOFED BY INDUCED OSTEOGENIC DIFFERENTIATION	58
4.2.1	QUALITATIVE ALP STAINING AND QUANTITATIVE ALP ACTIVITY ASSAY	64
4.2.2	ALIZARIN RED STAINING	66
5	DISCUSSION	69
5.1	NCSC DIFFERENTIATION BY MODIFYING SIGNALING PATHWAYS	69

5.1.1	DUAL SMAD INHIBITION WAS NOT SUFFICIENT FOR ENHANCED PRODUCTION OF NC-LIKE CELL POPULATION	70
5.1.2	INTERMEDIATE BMP LEVEL COMBINED WITH CANONICAL WNT ACTIVATION IMPROVED NC DIFFERENTIATION	72
5.2	SBIO CELLS EXHIBITED HIGHEST POTENTIAL FOR MINERALIZATION	75
6	<u>CONCLUSION</u>	<u>79</u>
7	<u>LITERATURE</u>	<u>82</u>

V. LIST OF FIGURES

Figure 1-1: Hierarchy of stem cells during differentiation process.	1
Figure 1-2: Schematic overview of iPSCs and ESCs generation and in vitro cultivation.....	4
Figure 1-3: NCSC development from neural plate border formation to neural tube closure and NCSC migration.	7
Figure 1-4: NC derivatives emerged from the anterior-posterior axis of the embryo.....	8
Figure 1-5: Schematic representation of the signaling pathways involved in NC formation.....	9
Figure 1-6: Schematic presentation of regulatory steps in NC development.	11
Figure 1-7: Schematic overview of BMP and TGF- β pathways.....	13
Figure 1-8: Schematic representation of canonical Wnt signaling without ligand binding and with ligand binding.	14
Figure 1-9: Schematic overview of NCSC differentiation protocol via Smad inhibition...	16
Figure 1-10: Schematic overview of NCSC differentiation protocol via Smad-2,3 inhibition and canonical Wnt signaling activation conducting NCSC differentiation.	17
Figure 1-11: Osteogenic differentiation derived from mesenchymal stem cells.....	18
Figure 3-1: Experimental set up of NCSC differentiation from hiPSCs according to G. Lee et al (2010).....	30
Figure 3-2: Experimental set up of NCSC differentiation from hiPSCs according to L. Menendez et al (2012).	31
Figure 3-3: FACSorting principle.....	38
Figure 3-4: Experimental set up for osteogenic differentiation.....	40
Figure 3-5: Chemical reaction of BCIP and NBT.	42
Figure 4-1: iPSC growth in colonies and as single cells	45
	XV

Figure 4-2: (A-c) Morphological change of hiPSC to NCSC during 12 days of differentiation induced by dual Smad inhibition.....	47
Figure 4-3: (A-c) Morphological change of hiPSCs to NCSC during 12 days of differentiation induced by Smad-2/-3 inhibition and activation of canonical Wnt signaling.....	48
Figure 4-4: Exemplary demonstration of separated PCR products of neural plate border-, early NCSCs-, late NCSCs-markers, Oct4 and β -Actin through gel electrophoresis in a 1 % agarose gel.....	51
Figure 4-5: Exemplary fluorescence pictures of ICC staining of NSB and SBio treated cells for NCSC marker.....	53
Figure 4-6: Expression of both surface receptors Hnk1 and p75 in NSB and SBio treated cells.	55
Figure 4-7: FACS based characterization of Hnk1 and p75 double positive SBio cells. ...	56
Figure 4-8: Evaluation of Hnk1 and p75 in SBio cells by Real time PCR analysis and ICC staining.....	57
Figure 4-9: Morphological changes of SBio cells during osteogenic differentiation.....	59
Figure 4-10: Morphological changes of SBio FACSsorted cells during osteogenic differentiation.....	60
Figure 4-11: Morphological changes of MSCs during osteogenic differentiation	61
Figure 4-12: Morphological changes of hEpi-NCSCs cells during osteogenic differentiation.....	62
Figure 4-13: Osteogenic differentiation of SBio cells, SBio FACSsorted cells, MSCs and hEpi-NCSCs after 7 days cultivation represented by positive Alkaline phosphatase staining and Alkaline phosphatase activity analysis.....	65
Figure 4-14: Osteogenic differentiation of SBio cells, SBio FACSsorted cells, MSCs and hEpi-NCSCs after 28 days cultivation represented by positive Alizarin red staining.	67

VI. LIST OF TABLES

Table 3-1: Material list.....	23
Table 3-2: Cell culture methods for different cell lines	29
Table 3-3: Media composition for NCSC differentiation.....	31
Table 3-4: cDNA synthesis pipetting scheme.....	33
Table 3-5: cDNA synthesis mix.....	33
Table 3-6: Summary of procedure	33
Table 3-7: Primer list for PCR and qRT-PCR	34
Table 3-8: PCR synthesis mix	33
Table 3-9: PCR procedure.....	35
Table 3-10: Characteristics of antibodies	36
Table 3-11: Exemplary building block for ICC evaluation by Columbus image data storage and analysis system (Perkin Elmer)	37
Table 3-12: qPCR components	39
Table 3-13: qRT-PCR procedure.....	39
Table 3-14: Seeding cell amount of different cell types in a well of a 24-well plate	40
Table 3-15: ALP-1 and ALP-2 buffer composition	41

VII. LIST OF ABBREVIATIONS

Abbreviations	Descriptions
Alk	Activin receptor-like kinase
ALP	Alkaline phosphatase activity
APC	Allophycocyanin
BCIP	5-Bromo-4-chloro-3'-indolyphosphate p - toluidine salt
bFGF	Basic fibroblast growth factor
BMP	Bone morphogenic proteins
BSA	Bovine serum albumin
BSP	Bone sialoprotein
CO ₂	Carbon dioxide
°C	Celsius
cDNA	Complementary deoxyribonucleic acid
C-Myc	Avian myelocytomatosis virus oncogene cellular homolog
DAPI	4', 6'-diamidino-2-phenylindole
DC-media	Defined conditioned media
DMEM	Dulbecco's Modified Eagle Medium
δ	Delta
ECAT1	Embryonic stem cell associated transcript-1
ECM	Extracellular matrix
EDTA	Ethylenediaminetetraacetic acid
EMT	Epithelial to mesenchymal transition
Esg1	Glycine and serine-rich
FACS	Fluorescence activated cell sorting
FBS	Fetal bovine serum
FGF	Fibroblast growth factor
g	Gram
GS	Glycine-serine rich domain
GSK	Glycogen-synthase-kinase
hESC	Human embryonic stem cells
hiPSC	Human induced pluripotent stem cells
hEpi-NCSC	Human epidermal neural crest stem cells
HNK1	Human natural killer-1
ICC	Immunocytohistochemistry
ICM	Inner cell mass
KRS	Knockout-serum replacement
l	Liter
LIF	Leukemia Inhibitor factor
MEF	Mouse-embryonic fibroblasts
ml	Milliliter
mRNA	Messenger ribonucleic acid

MSCs	Mesenchymal stem cells
MSX1	Msh homeobox1
MV	Mean value

Abbreviations	Descriptions
NCSCs	Neural crest stem cells
NBT	Nitro-blue-tetrazolium-chloride
NSB	Noggin SB431542
O ₂	Dioxygen
OCT3/4	Octamer binding transcription factor 3/4
OC	Osteocalcin
PAX3	Paired box-3
PBS w/o Ca ²⁺ /Mg ²⁺	Phosphate buffered saline without Magnesium cations and Calcium cations
pH	Power of hydrogen
PE	Phycoerythrin
p75	Low affinity nerve growth factor receptor
pNPP	Para-nitrophenyl phosphate
qRT-PCR	Quantitative real time polymerase chain reaction
RT	Room temperature
RT-PCR	Reverse transcriptase-polymerase chain reaction
RUNX-2	Runt-related transcription factor 2
rpm	Rounds per minute
SBIO	SB431542 (2'Z, 3'E)-6-bromoindirubin-3'-oxime
SDIA	Stromal derived inducing activity
SLUG	Snail homolog 2 (Drosophila)
SN	Supernatant
SNAIL	Snail homolog 1 (Drosophila)
SOX2/9	SRY-related HMG-box
SSEA4	Stage-specific embryonic antigen-4
STAT3	Signal transducer and activator of transcription
Std	Standard deviation
TGF-β	Transforming growth factor beta
TRA antigens	Tumor rejection antigens
U	Unit
μl	Microliter
μm	Micrometer
WNT	Wingless/Int
ZIC1	Zinc finger of the cerebellum

1 Introduction

1.1 Stem cells

The discovery of stem cells opened new possibilities for regenerative medicine in science and clinical application. The first embryonic stem cells (ESCs) were isolated from human blastocyst in 1998 (Thomson 1998), followed by the generation of induced pluripotent stem cells (hiPSCs) in 2006 (Takahashi & Yamanaka 2006). Beside these two groups, a third subgroup of stem cells - termed adult stem cells - exists. Stem cells are classified by their properties to renew themselves through mitotic cell division (self-renewal) and by possessing the capability to differentiate into diverse range of cell types (Morrison et al. 1997).

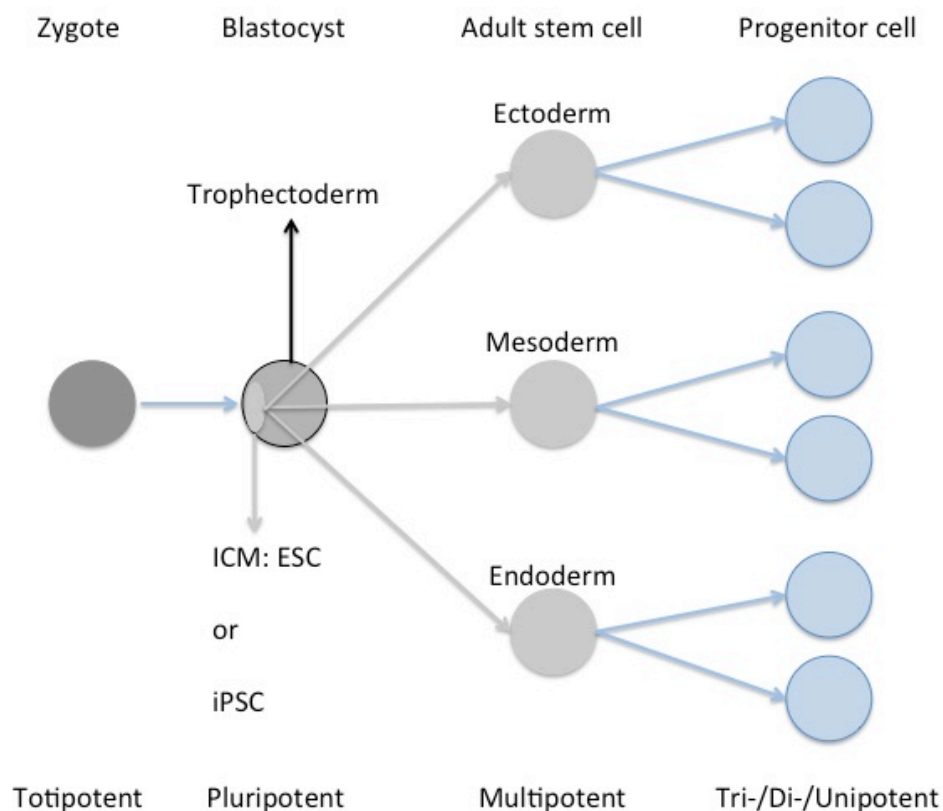


Figure 1-1: Hierarchy of stem cells during differentiation process.

The totipotent zygote differentiates into a blastocyst consisting of ICM and trophectoderm. Pluripotent ICM gives rise to ectodermal, mesodermal and endodermal germ layer. While differentiation potential decreases for each stage, cell specification increases.

In early embryogenesis, a diploid zygote is generated from the fertilized egg, resulting in blastocyst formation by multiple mitotic cell divisions. Only zygotes and blastomeres of early embryos exhibit totipotency. Embryos possess the ability to differentiate into more than 200 cell types that pertain to the three germ layers and to extra embryonic tissues, *in vivo* leading to the formation of new life. During blastocyst stage, blastomeres undergo the first cell fate determination, thereby losing totipotency. In this stage, a minor number of blastomeres evolve into the pluripotent inner cell mass (ICM) called embryoblast, while the remaining blastomeres develop into trophectoderm, generating the extra-embryonic tissue and assisting embryonic growth by giving rise to the placenta, chorion, and the umbilical cord (Vazin & Freed 2010). Pluripotent cells of the ICM are capable to form a multilayered embryo with an outer cell layer (ectoderm), an inner cell layer (endoderm), and an intermediate cell layer (mesoderm). Stem cells, which belong to one of the mentioned germ layers, are classified as multipotent. An example for this are hematopoietic stem cells that belong to mesoderm and can differentiate into various cell types within the same cell lineage. A further subgroup of stem cells are termed unipotent e.g. spermatogonial stem cells that can only differentiate into spermatozoa. Terminal differentiation is correlated with complete loss of developmental potential of cells, which are then defined as somatic cells (Kang & Gao 2012). The first part of this introduction gives a deeper insight in human ESCs (hESCs) and human iPSCs (hiPSCs) and their therapeutic potential in regenerative therapy.

1.1.1 Human embryonic stem cells (hESCs)

The first successful isolation of human embryonic stem cells (hESCs) was reported by Thomson in 1998 (Thomson 1998). For this purpose, he cultivated isolated ICM cells on mitotically inactive mouse-embryonic fibroblasts (MEFs). Thereby, he obtained ESCs, which can be maintained in the same pluripotent state as the ICM. Because of their unlimited potential of self-renewal by symmetric division hESCs are seen as a promising tool for cell-based therapy in patients suffering from diverse degenerative diseases, which are insusceptible to conventional treatment (Daley 2010). A further specialized characteristic of hESCs is their capability of asymmetric division resulting in one daughter cell maintaining pluripotency and a second daughter cell contributing to multiple cell types forming ectodermal, mesodermal and endodermal derivatives. This process can be observed by injecting hESC into immunocompromised mice leading to teratoma formation including derivatives of all germinal sheets (Stojkovic et al. 2004).

However, ESC research also evokes serious moral questions and ethical issues. Generation of hESCs results from the remaining embryos of *in vitro* fertilization, a process in which oocyte and sperm are placed together in a culture dish to enable fertilization (McLaren 2001; reviewed in Austin G Smith 2001). The fact that hESCs derived from the ICM of blastocyst or the primitive gonadal regions of early aborted fetuses include the destroying of human embryos. Laws of hESC research and the regulation of hESC generation differ between countries and are closely related to the history of each country. In Germany for example, hESC research is only allowed with cells, which were established before 1 May 2007 (Stem cell law StZG §4 BGBI. I S. 2277). Besides the ethical compunction additional problems arise from hESCs *in vitro* cultivation. As mentioned previously, maintenance of undifferentiated stem cell phenotype *in vitro* implies co-culturing with MEFs and animal ingredients, whereby hESCs might be exposed to infectious agents (Stojkovic et al. 2004).

It was discovered that MEFs provide cytokines such as Leukemia Inhibitor factor (LIF) which sustain self-renewal and inhibit differentiation in ESCs (reviewed in Austin G Smith 2001). This outcome enabled new opportunities for standardization of ESC culturing through replacement of feeder cells by defined conditioned media (Smith & Hooper 1987). In spite of the establishment towards xenofree hESCs cultivation, several observations report genomic instabilities (Carpenter et al. 2004; Amit et al. 2003) and chromosomal aberrations (Carpenter et al. 2003; Rosler et al. 2004; Draper et al. 2004) in hESCs emerged by prolonged *in vitro* cultivation. In addition, immunosuppression of the acceptor based on the allogenic origin in ESCs transplantation has been reported (Drukker 2006; Sarić et al. 2008). Due to the multitude of disadvantages, it is not clear if hESCs are an ideal tool in regenerative medicine.

1.1.2 Human induced pluripotent stem cells (hiPSCs)

A great opportunity to circumvent ethical issues was the generation of iPSCs. The process for generation of these iPSCs is called reprogramming and implies that a timed expression of master regulators is able to modulate a somatic cell into iPSC (Denker 2009). Three major areas of research conducted the iPSC generation. The first area comprised somatic cell nuclear transfer or cloning (Gurdon 1962; Wilmut et al. 1997; Tada et al. 2001), while the second area dealt with the detection of master transcription factors (Schneuwly et al. n.d.; Davis et al. 1987; Yamanaka & Blau 2010) and the third

area of research covered the culture methods for ESC (Evans & Kaufman 1981; Smith et al. 1988; Thomson 1998). The first two areas of research assumed that a combination of multiple key factors are highly, specifically up-regulated in oocytes or ESC, enabling reprogramming of somatic cells back into the pluripotent state.

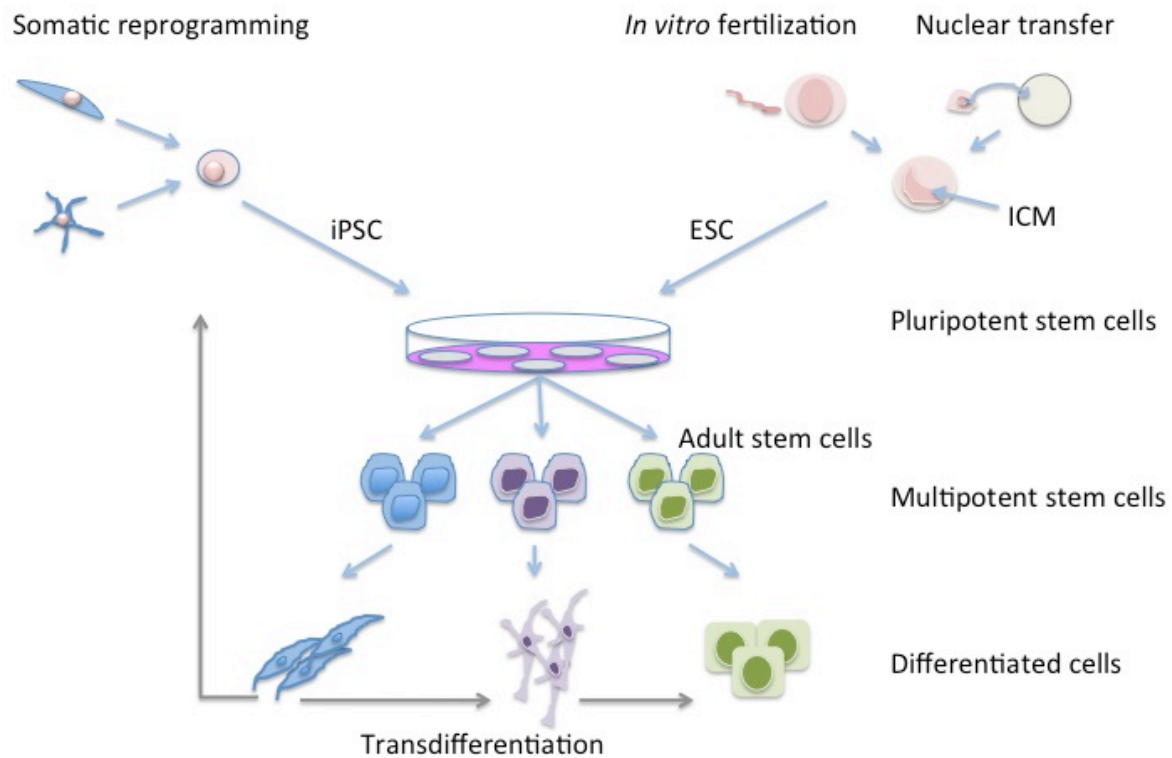


Figure 1-2: Schematic overview of iPSCs and ESCs generation and *in vitro* cultivation.

While somatic reprogramming produces iPSCs from differentiated cells (grey arrow), ESCs are isolated from early embryos obtained by *in vitro* fertilization or nuclear transfer. After *in vitro* cultivation, both cell types give rise to more specialized cells (blue arrows). In addition, reprogramming technology enables lineage conversion between somatic cell types (grey arrows). (Figure adapted from de Peppo & Marolt, 2012). iPSCs: induced pluripotent stem cells, ESC: embryonic stem cells, ICM: inner cell mass.

These key factors were divided into three groups. The first group consisted of genes responsible for the maintenance of pluripotent state (*NANOG*, *OCT3/4* and *SOX2*), while the second group comprised *C-MYC*, *STAT3* and *TC11*, tumor-associated genes and the third group contained factors (*KLF4*, *ECAT1* and *ESG1*), which have a specific role in ESC. Experimental establishment for the identification of this combination of genes was

provided by the knowledge about the maintenance of pluripotency in culture (reviewed by Yamanaka 2012). In 2006, Takahashi and Yamanaka had a breakthrough by reprogramming *in vitro* murine fibroblasts into iPSC with a retroviral vector (Takahashi & Yamanaka 2006), followed by reprogramming of human fibroblasts to hiPSC in 2007 (Takahashi et al. 2007). Remarkably, they demonstrated that the force expression of only 4 transcription factors: *OCT4*, *KLF-4*, *SOX2* and *C-MYC* is sufficient for reprogramming (Takahashi & Yamanaka 2006). hiPSCs feature many properties characteristic for hESCs, implying that morphological appearance, proliferation rate, the reactivation of endogenous pluripotency markers (stage-specific embryonic antigen-4 (SSEA4), TRA antigens and transcription factors such as OCT3/4 and Nanog) (Adewumi et al. 2007) *in vivo* and *in vitro* (Kim et al. 2009) obey to the down-regulation of transgenes applied for reprogramming. Due to these characteristics hiPSC are a very promising tool to study human development, genetic diseases, and to serve as cell culture model for the application of toxicological and pharmaceutical substances (Mollamohammadi et al. 2009). To assess pluripotency of hiPSCs, teratoma assay or high throughput screening (reviewed in Kang & Gao 2012) are performed. However, iPSC technology also bears severe drawbacks as the risk of insertional mutagenesis is increased by application of retro- or lenti viruses during reprogramming, which might cause severe side effects in gene therapy (Hacein-Bey-Abina et al. 2003). The second drawback is the low efficiency of iPSCs generation which is less than 1 % gathered by reprogramming (Takahashi et al. 2007). Furthermore several studies report accumulation of epigenetic and genetic aberrations in iPSCs evolved by reprogramming and subsequent long-term cultivation (Hussein et al. 2011; Gore et al. 2011; Lister et al. 2011). In correlation of oncogenic potential, one study observed that injection of hiPSCs into blastocysts lead to 20 % tumor formation in chimeric mice (Okita et al. 2007). Besides these negative aspects, further extensive studies are crucial to gain more comprehensive knowledge of hiPSCs as the generation of patient and disease-specific stem cells offers great potentials for regenerative therapies in clinical applications.

1.1.3 Adult stem cells

Adult stem cells, also termed somatic stem cells, are undifferentiated, multipotent stem cells within clusters of specialized cells located in several tissues or organs. In contrast to ESC, adult stem cells are defined by limited self-renewal and were conventionally believed to produce a limited number of cell types restricted to the tissue in which they reside (Körbling et al. 2003). However, this assumption was contradicted by numerous findings that adult stem cells are able to overcome lineage barriers by differentiating into cell types aberrant from their tissue of origin, an occurrence termed stem cell transdifferentiation (Lagasse et al. 2000). The function of adult stem cells is to maintain, generate and regenerate tissue damage due to injury or physiologic cell turnover. Hematopoietic stem cells are the most well characterized adult stem cells related to their clinical application for bone marrow transplantation in order to treat malignant diseases (Körbling et al. 2003). Other studies in adult stem cell research focus on mesenchymal stem cells (MSCs), which can be easily isolated and cultured (Friedenstein et al. 1974).

1.1.4 Mesenchymal stem cells (MSCs)

MSCs were first isolated in 1974 from bone marrow (Friedenstein et al. 1974), and since then several findings discovered other MSCs locations such as fetal, perinatal and adult tissue, umbilical cord Wharton's jelly, adipose tissue, peripheral blood, circulatory system, fetal liver, lungs, synovium and amniotic fluid (reviewed in Neirinckx et al. 2013). In these tissues, MSCs function as supportive cells and regulate the maintenance of tissue homeostasis (Uccelli et al. 2008; Caplan & Correa 2011). Furthermore, it was detected that these MSCs are able to transdifferentiate into endodermal and ectodermal lineages including neuron-like cells (Sanchez-Ramos et al. 2000; Woodbury et al. 2000). These multipotent adherent cells possess the typical fibroblast-like morphology that is characterized by a long, thin, spindle like cell body. Regarding their multipotency, transdifferentiation and high proliferation rate, MSC evoked great interest in tissue engineering and regenerative medicine.

1.2 The neural crest

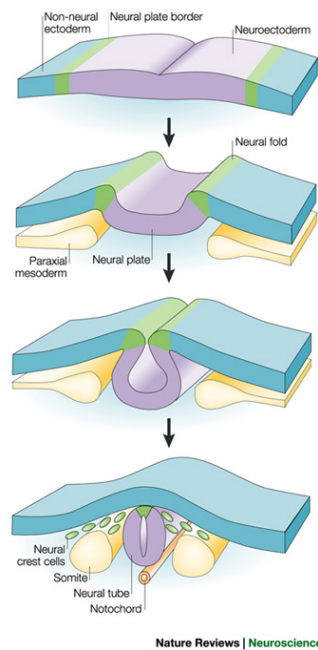


Figure 1-3: NCSC development from neural plate border formation to neural tube closure and NCSC migration.

Figure adapted from L.S. Gammill et al, 2003.

The neural crest (NC) consists of a transient embryonic, multipotent cell group, creating a unique structure to the vertebrate embryo. Wilhelm His first reported NC in chick embryos in 1868 as a small, multipotent cell population positioned between the developing neural tube and presumptive epidermis (reviewed in X. Huang & Saint-Jeannet 2004). This cell population is termed NC because it is located at the “crest” of the closing neural tube (Bronner & LeDouarin 2012). Neural crest stem cells (NCSCs) exhibit stem-cell-like properties in case of multipotency, capable of leading to the formation of a variety of different tissue and organs. Therefore, the NC is sometimes considered as ectomesenchyme and regarded as the 4th germ layer from an evolutionary perspective (Hall 2000). By epithelial to mesenchymal transition (EMT) this cell population is individualized, which occurs in embryonic stage 9, around the third to 4th week of pregnancy in humans (O’Rahilly & Müller 2007). After delamination from neuroepithelium, NCSCs migrate along defined pathways through the body until they reach their final destination (reviewed in Le Douarin et al. 2004). The NC is divided in

4 major segments based on their anatomic position at the neuraxis and differentiation capability: cranial, cardiac, vagal, and trunk NC.

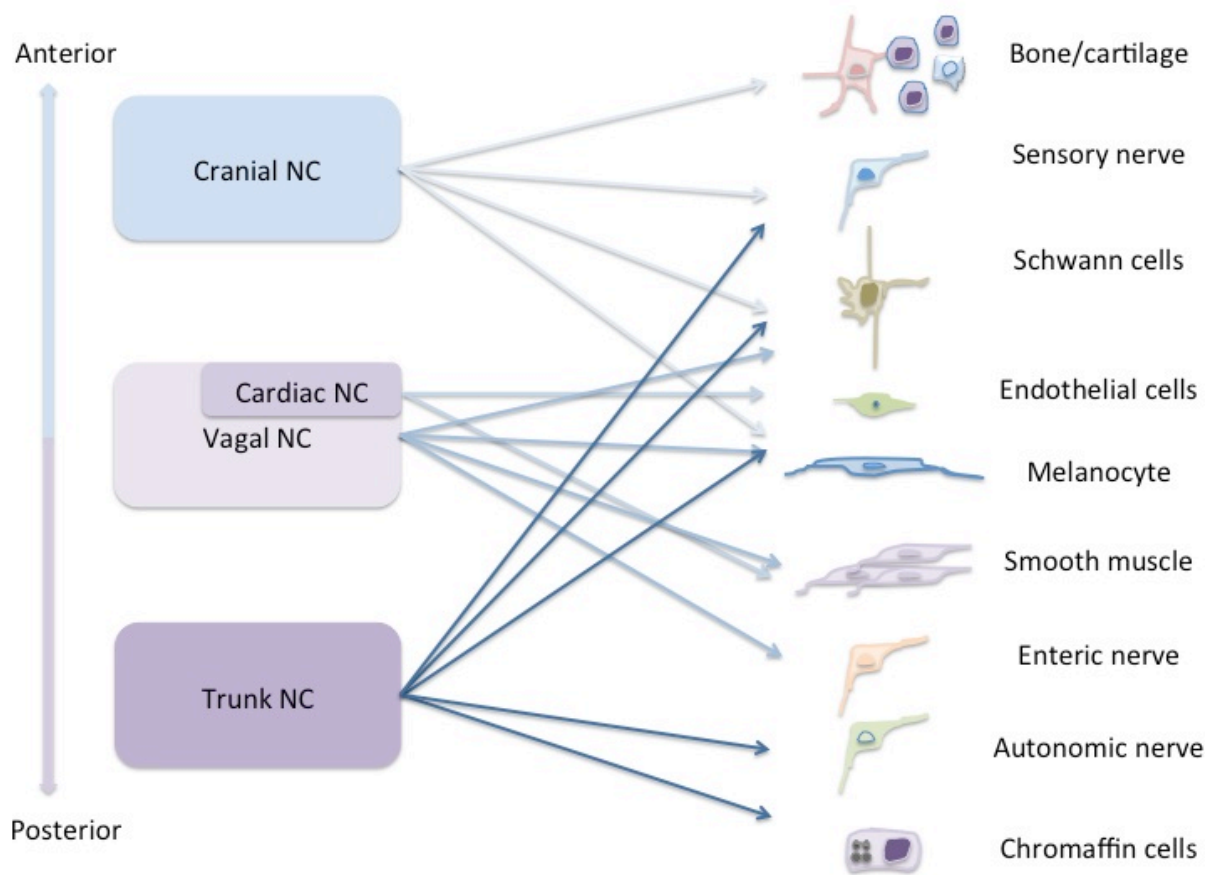


Figure 1-4: NC derivatives emerged from the anterior-posterior axis of the embryo.

Figure was adapted from G. Lee et al, 2009.

The majority of head connective tissue and skeletal structures, nerves and pigment cells arise from the cranial NCSCs, while cells from the vagal region contribute to the formation of the enteric ganglia of the gut. Within the vagal region, cardiac NCSCs are incorporated and regulate cardiac development by generating the aorticopulmonary septum and conotruncal cushions. Finally, trunk NCSCs have to be mentioned, which serve as source for adrenal chromaffin cells, sensory and sympathetic ganglia (Shakhova & Sommer 2010). Beside the high multipotent potential, the NC also possesses regenerative capabilities after tissue ablation. This regenerative efficiency is provided by the remaining neural tube cells and adjacent NC but is reduced with age (reviewed in Sauka-Spengler & Marianne Bronner-Fraser 2008).

1.2.1 Major signaling pathways in NC formation

Induction of the NC is a multistep procedure, starting from early gastrulation to late organogenesis. In the first step, signals induce the thickening of the ectoderm sheet, resulting in its dissociation from the rest of the embryonic ectoderm. This nervous system precursor location is defined as the neural plate. At the border between future neural and non-neural ectoderm a gene regulated network is triggering the presumptive NC territory. Several studies examined the NC initiation process in different model organisms, whereby outcomes are inconsistent (reviewed in Sauka-Spengler & Bronner-Fraser 2008).

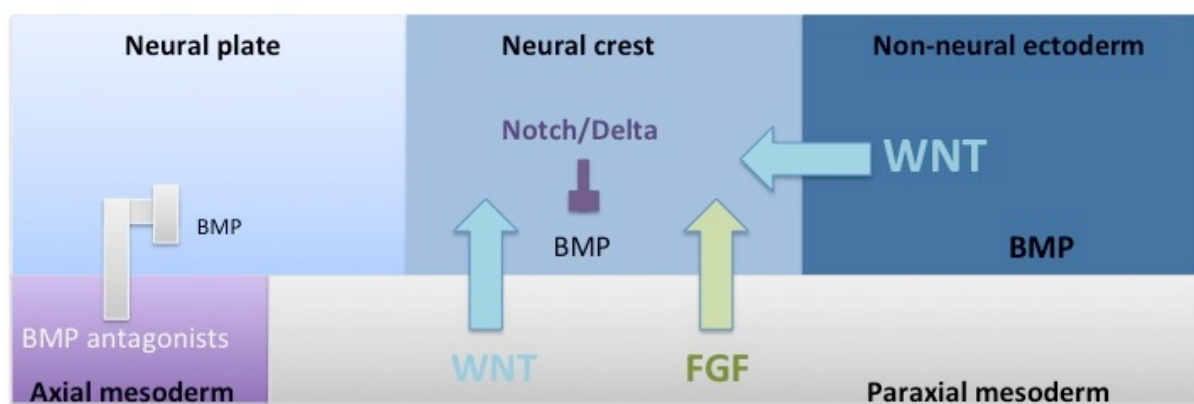


Figure 1-5: Schematic representation of the signaling pathways involved in NC formation.

BMP antagonists secreted by the axial mesoderm inhibit BMP signaling leading to neural plate formation. Activated FGF and WNT signaling, provided by paraxial mesoderm and low BMP level, regulated by δ -notch signaling, induce neural crest formation. Figure adapted from Xiao Huang et al, 2004.

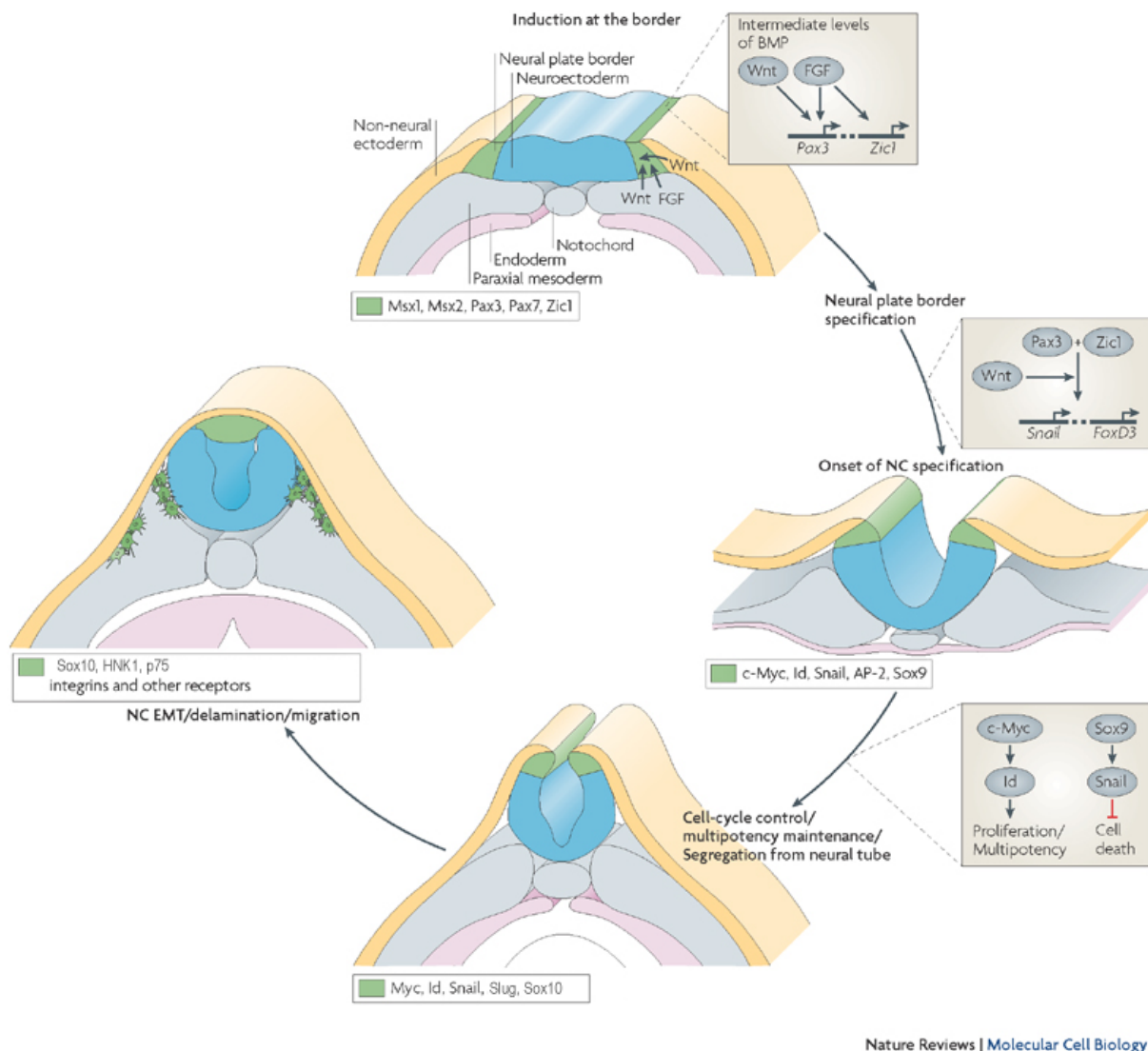
The major signaling pathways involved in NC initiation are bone morphogenic proteins (BMPs), fibroblast growth factors (FGFs), delta (δ)-notch and WNT signaling. Secreted BMPs proteins are members of the transforming growth factor- β (TGF- β) superfamily and participate in dorsoventral patterning during early development of the embryo. It is suggested that intermediate level of BMPs partly initiates NC induction. The establishment of intermediate BMP signaling is regulated by BMP antagonists such as noggin, follistatin or chordin, which are delivered by the underlying paraxial mesoderm (Raven 1945; Marchant et al. 1998). Moreover, it is assumed that the maintenance of newly induced NCSCs depends on intermediate BMP level (Selleck et al. 1998). Studies

in *Xenopus laevis* showed that FGF-2 in correlation with low BMP level is able to induce NC formation (Mayor et al. 1995; Mayor et al. 1997). Interestingly, transient NC initiation was afforded by secreted FGF-8 from the paraxial mesoderm (Monsoro-Burq 2003). Further studies in birds and frogs showed that δ -notch signaling acts upstream of BMP expression to support NC formation and to border the NC to the neural plate border (Endo et al. 2002; Glavic et al. 2004). However, the principle NC initiator is activated canonical WNT signaling, secreted from the mesoderm and adjacent non-neural ectoderm (García-Castro et al. 2002; Yanfeng et al. 2003; Sauka-Spengler & Bronner-Fraser 2008), which is also believed to participate in NC lineage specification (LaBonne & Bronner-Fraser 1998; Lewis et al. 2004; Wu et al. 2005; Jones & Trainor 2005).

1.2.2 Gene regulatory network during NCSC development

NC is first initiated at the neural plate border by signal molecules, implying intermediate BMP level, FGFs and WNTs. To establish the neural plate border, these signals regulate expression of neural plate border specifiers *MSX1*, *PAX3* and *ZIC1*. Expression of neural plate border specifiers induces bending of the neural plate border, leading to the formation of neural folds. Within the neural folds, *PAX3* and *ZIC1* act synergistically in a WNT dependent manner, and as the neural folds fuse, in the dorsal part of the neural tube. This synergistic activity up-regulates early NC specifiers such as *SNAIL*, *SLUG*, *ID*, *C-MYC*, *SOX10* and *SOX9* in a subset of precursor cells (Sato et al. 2005; Sauka-Spengler & Bronner-Fraser 2008; Liu & Xiao 2011). Expression of these early NC specifiers in NC precursor cells will define a new regulatory network to direct differentiation towards NC fate. For example, *C-MYC-ID* network is mediating cell-fate decisions by controlling cell cycle (Bellmeyer et al. 2003) and by keeping the NC progenitor pool in a multipotent state (Kee & Bronner-Fraser 2005; Light et al. 2005), while *SOX9* promotes cell survival by *SNAIL* expression, which has an anti-apoptotic effect (Cheung et al. 2005). Further, premigratory NCSCs undergo an EMT before the neural tube closures (O’Rahilly & Müller 2007), in which epithelial properties are replaced by a migrating, mesenchymal morphology (Duband et al. 1995). These delaminating and migrating NCSCs maintain *SOX10* expression, which partly regulates their migration by mediating expression of downstream effector genes such as type II cadherin and integrins. Today, there are no specific late NC specifiers defined, however, many articles refer to the expression of two surface receptors, the carbohydrate epitope HNK1 and the low affinity nerve growth

factor p75^{NTR}, as well as the transcription factor *SOX10*, that is used for NCSC classification (Sauka-Spengler & Bronner-Fraser 2008; Stuart M. Chambers 2009; Lee et al. 2010a; Menendez et al. 2011).



Nature Reviews | Molecular Cell Biology

Figure 1-6: Schematic presentation of regulatory steps in NC development.

Intermediate BMP level, FGF and WNT induce neural plate border by activating expression of neural plate border specifiers *PAX3* and *ZIC1*. These neural plate border specifiers act synergistically in a WNT dependent manner, leading to up-regulation of NC specifiers such as *C-MYC*, *ID*, *SOX9* and *SNAIL* in cells committed to NC fate in the neural folds and/or dorsal neural tube. Before the neural tube closures, premigratory NCSCs undergo EMT and pinch off from neuroepithelium. Early migratory NCSCs start to migrate and express *SOX10*, HNK1 and p75. Figure adapted from T. Sauka-Spengler et al, 2008.

1.2.2.1 SMAD-1, -5 and -8 signaling

BMPs are multi-functional growth factors and belong to the TGF- β superfamily. Studies in rats first identified BMPs as bone and cartilage inducers when implanted at ectopic sites. Dimeric BMPs bind to transmembrane receptors that possess serine/threonine kinase domains in their intracellular regions. Upon ligand binding, these receptors form a heteromeric complex consisting of two type I and two type II BMP receptors (Miyazono et al. 2010). Type I receptor is transphosphorylated by the constitutively active type II receptor in the GS (glycine and serine-rich) domain located N-terminal to the serine/threonine kinase domains (Cárcamo et al. 1994; Wrana et al. 1994). Phosphorylation induces conformational changes of type I receptor, whereby its steric inhibited catalytic center becomes unblocked. Activated type I receptor transduce intracellular signals by phosphorylation of the C-terminal domain of SMAD-1, -5 and -8 in the cytoplasm. Phosphorylation of SMAD-1, -5 and -8 initiates interaction with the mediator molecule SMAD-4, forming a hetero-oligomeric complex. This hetero-oligomeric complex in turn enters the nucleus in conjunction with other nuclear factors and induces the expression of specific target genes (Shi & Massagué 2003; Miyazono et al. 2010). Various downstream pathways are dependent on BMP signaling, regulating broad spectra of biological activities in different tissues in human development (Miyazono et al. 2010).

1.2.2.2 SMAD-2, -3 signaling

The TGF- β superfamily consists of a wide range of signaling members including TGF- β , Nodal, and Activin A that mediate a variety of biological processes such as cell growth arrest, development, and differentiation (Miyazono et al. 2010). Also in this pathway, dimeric ligand binding of transmembrane serine/threonine kinase receptors (type I and II) leads to heterotetrameric complex formation. Upon ligand binding, activated type I receptor transduce intracellular signals by phosphorylation of SMAD-2/-3, resulting in the assembling of a heteromeric complex consisting of phosphorylated SMAD-2/-3 and SMAD-4 that enters the nucleus to activate target genes (Lagna et al. 1996).

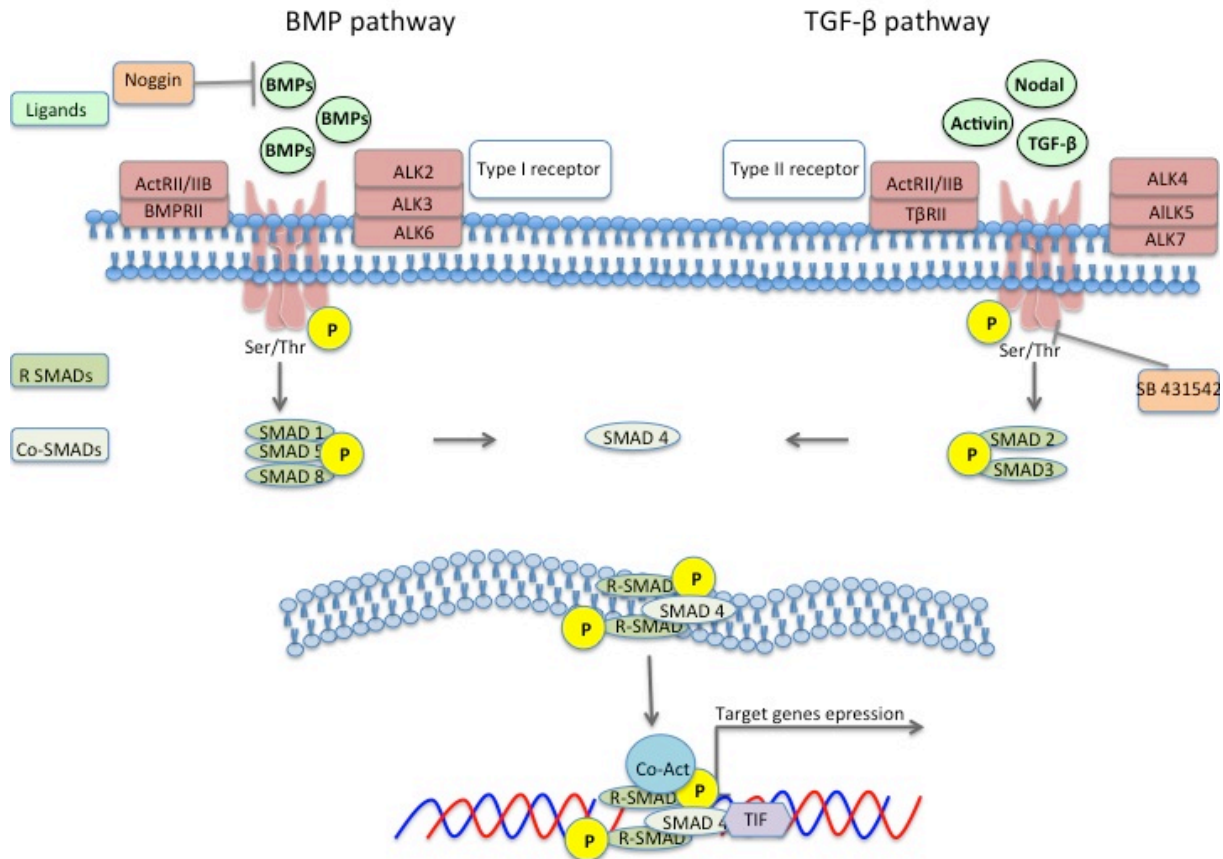


Figure 1-7: Schematic overview of BMP and TGF-β pathways.

After ligand binding to its respective receptor, R-SMADs are phosphorylated by their related receptors. A phosphorylated heteromeric complex is formed with SMAD-4, which enters the nucleus and induces target gene expression. Alternatively, Noggin inhibits BMP pathway by direct binding to BMP ligands, while the small molecule SB431542 inhibits TGF- β pathway by binding to the ATP-binding site of the receptor. Figure adapted from M. Kandasamy et al., 2011.

1.2.2.3 Canonical WNT signaling

WNT signaling is involved in maintenance and cell fate decision of stem cells, cell proliferation, cell migration, and generation of tissue polarity (van Amerongen & Nusse 2009). In unexcited cells, the transcription factor β -catenin interacts with the destruction complex in the cytoplasm consisting of APC and AXIN scaffold proteins, which bind β -catenin, while the kinases CKI and GSK3 β phosphorylate β -catenin. Phosphorylated β -catenin is ubiquitinated, followed by its rapid degradation in the proteasome. This process is discontinued upon WNT ligand binding to a Frizzled family receptor and to its co-receptor of the LRP-5/-6 arrow family. Ligand binding initiates inhibition of the APC/AXIN/CK1/GSK β destruction complex, leading to

hypophosphorylated β -catenin release. The characteristic of canonical WNT signaling is cytoplasmic accumulation of β -catenin that in turn translocates into the nucleus. Binding of β -catenin to TCF proteins provides a transcription activation domain, enabling expression of β -catenin /TCF target genes. Without WNT ligands, TCF/LEF factors form with other factors (Groucho, histone deacetylase) a complex and act as a transcriptional repressor (Eisenmann 2005; Clevers 2006).

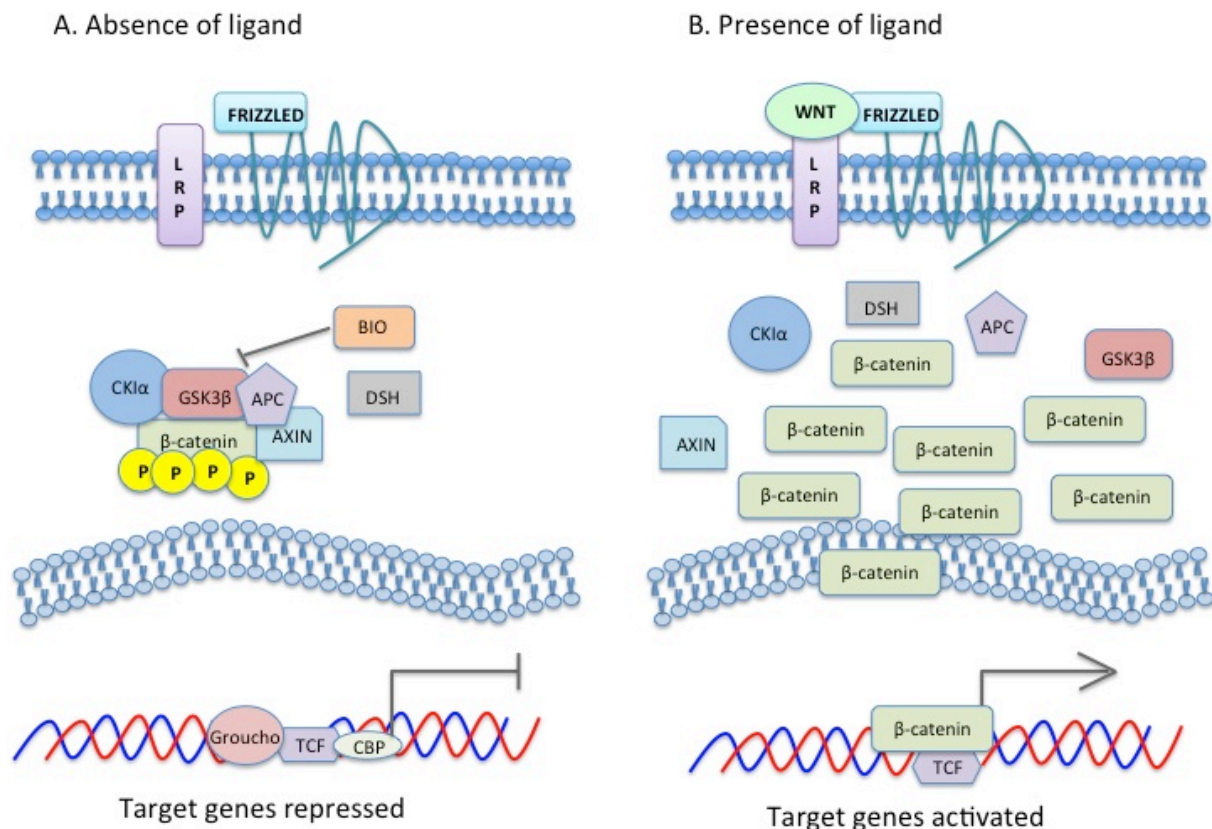


Figure 1-8: Schematic representation of canonical WNT signaling without ligand binding and with ligand binding.

A. In the absence of WNT ligand, β -catenin is captured, phosphorylated, ubiquitinated by the degradation complex and further degraded. B. Binding of the WNT ligand enables release of β -catenin from the degradation complex and its entering into the nucleus to activate target genes. Alternatively, small molecule BIO inhibits ATP binding site of GSK3 β , leading to canonical WNT signaling activation. Figure adapted from D.M Eisenmann et al, 2005.

1.2.3 Experimental methods for *in vitro* NCSC induction from hiPSC

As disorders during NCSC development lead to severe diseases and the isolation of NCSC from embryos is related to ethical questions, the differentiation of NCSC from human pluripotent stem cells became a very important tool in regenerative medicine. Most induction protocols imply the use of stromal feeder-layers (Mizuseki et al. 2003; Pomp et al. 2005; Motohashi et al. 2007; Brokhman et al. 2008; Pomp et al. 2008a; Jiang et al. 2009) termed stromal derived inducing activity (SDIA) method and more recently the technique of neural rosettes (Lee et al. 2007; Lazzari et al. 2006). These quite long and low efficiency methods are combined with flow cytometry to select NCSCs expressing p75 and HNK1 from cell populations. Other methods for NCSC differentiation imply the formation of neurospheres (Jiang et al. 2009) or embryoid bodies (Rathjen et al. 2002; Zhou & Snead 2008). A further source for NC cells is the isolation from adult tissue such as hair-follicles (Clewes et al. 2011). Recent outcomes present two methods for deriving NCSC from hESCs/hiPSCs by modifying signaling pathways under defined culture conditions, which are presented below.

1.2.3.1 NCSC differentiation from hiPSC according to Gabsang Lee

In 2010, Gabsang Lee published an *in vitro* method for NCSC induction from hiPSCs (Lee et al. 2010b). This method is based on dual SMAD inhibition, induced by the two inhibitors Noggin and SB431542. As mentioned in section 1.2.2 Noggin is an endogenous inhibitor, secreted by the paraxial mesoderm and inhibits BMP by its direct binding. This leads to the inhibition of SMAD-1, -5 and -8 signaling pathway. The second inhibitor SB431542 is a small molecule that directly binds to the ATP binding site of the BMP receptors, thereby inhibiting the autophosphorylation of the receptors and in turn the phosphorylation of SMAD-2 and -3. In addition to dual SMAD inhibition, which should direct iPSCs towards NCSC lineage, cells are also cultivated in Knock-out-replacement serum (KRS), which replaces fetal bovine serum (FBS) and enables maintenance of ESC and iPSCs in culture. During 12 days NCSC differentiation protocols, KSR media is slightly replaced by N2 media that is in general applied for neural differentiation.

Dual SMAD inhibition

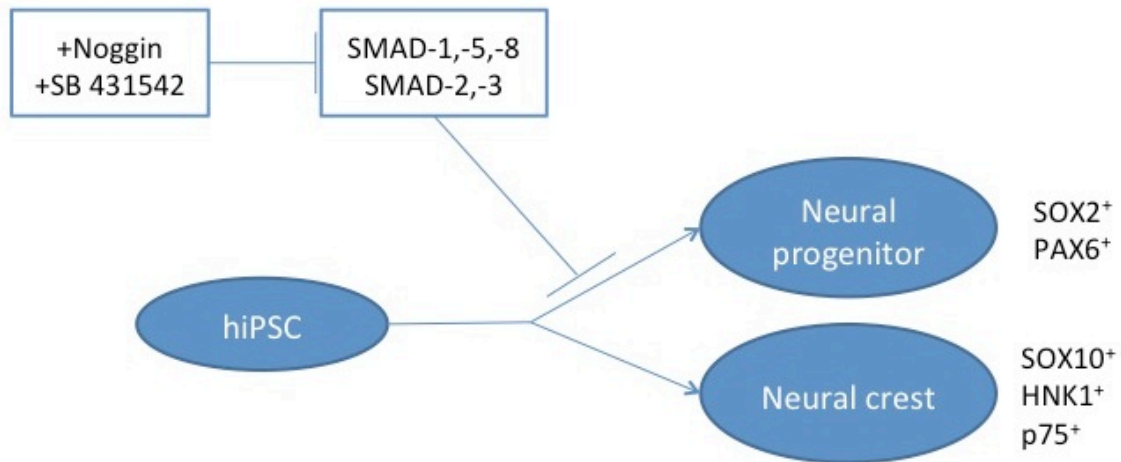


Figure 1-9: Schematic overview of NCSC differentiation protocol via SMAD inhibition.

hiPSCs-derived NCSC differentiation is induced by Noggin that inhibits SMAD-1, -5 and -8, whereas SB431542 blocks SMAD-2, -3 signaling according to G. Lee, 2010. Figure adapted from L. Menendez, 2011.

1.2.3.2 NCSC differentiation from hiPSC according to Laura Menendez

In 2011, Laura Menendez published a feeder free NCSC differentiation protocol, based on SMAD-2, -3 inhibition and the activation of the canonical WNT pathway (Menendez et al. 2011). For this purpose, Menendez applied the small inhibitor molecule SB431542 for SMAD-2, -3 inhibition, and (2'Z, 3'E)-6-bromoindirubin-3'-oxime (BIO) for the activation of WNT signaling. BIO is a small molecule that directly binds to the ATP binding site of the glycogen-synthase-kinase (GSK) of the β -catenin destruction complex. Thus, β -catenin is no longer phosphorylated by GSK and instead released from the degradation complex. As mentioned in section 1.2.1, low BMP level and activation of the canonical WNT signaling should push iPSCs into NCSC lineage. In contrast to the G. Lee protocol, Menendez' iPSC cells are further maintained in stem cell media except activin as cultivation with the two inhibitors should be sufficient for NC differentiation within 12 days.

SMAD -2,-3 inhibitions combined with canonical WNT activation

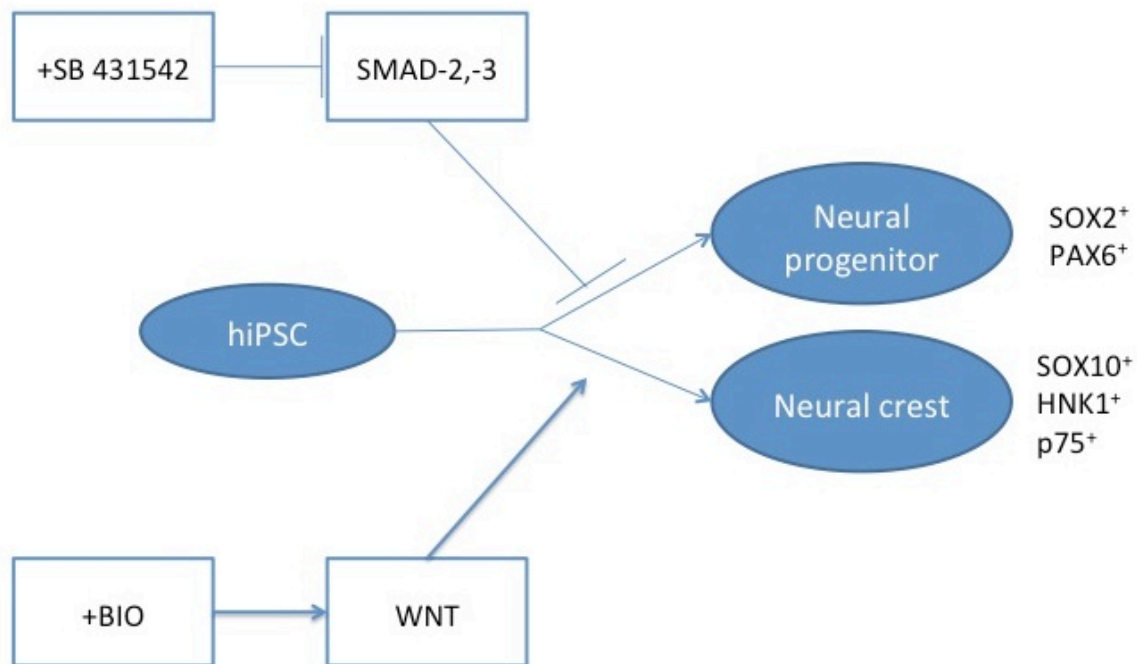


Figure 1-10: Schematic overview of NCSC differentiation protocol via SMAD-2,-3 inhibition and canonical WNT signaling activation conducting NCSC differentiation.

hiPSCs-derived NCSC differentiation is induced by (2'Z, 3'E)-6-bromoindirubin-3'-oxime (BIO) that activates canonical WNT signaling, whereas SB431542 inhibits SMAD-2, -3 signaling according to L. Menendez, 2011. Figure adapted from L. Menendez, 2011.

1.2.4 NCSC multipotency represented by osteogenic differentiation

In order to demonstrate NCSC multipotency, cells obtained from the NCSC differentiation protocols are further applied to osteogenic differentiation. A standard osteogenic differentiation protocol for mesenchymal stem cells (MSC) can be applied. The mineralization media consists of basal media and mineralization catalyzers β -glycerolphosphat, dexamethasone and ascorbic acid. *In vitro* osteogenic differentiation from MSCs can be divided in two developmental phases. The first developmental stage occurs in general within the first to second week, while the second maturation is observed between the second or third week (Miron & Zhang 2012). During the transformation from MSCs to osteoprogenitor cells, expression of Runt-related transcription factor 2 (*RUNX2*) (Banerjee et al. 1997; Ducy et al. 1997) and *OSTERIX* (Nakashima et al. 2002) is up-regulated. Mitotic osteoprogenitors start to synthesize

collagen I that allocates the structural framework by enabling distribution of tension, turn, pressure evolving from normal activity and moving (Boskey et al. 1999). From this population, some cells differentiate into mitotic pre-osteoblasts, which express alkaline phosphatase (ALP). ALP is a hallmark of osteoblast differentiation due to the outcomes of *in vitro* studies, where ALP participated in the induction of mineralization (Tenenbaum 1987; Wennberg et al. 2000).

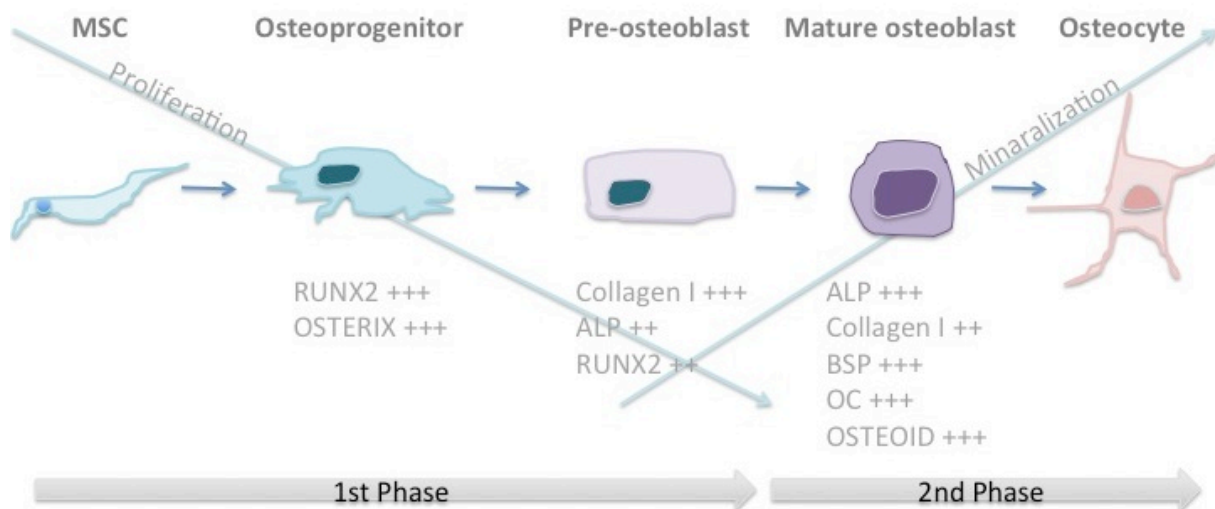


Figure 1-11: Osteogenic differentiation derived from mesenchymal stem cells.

RUNX2 and *OSTEORIX* mediate MSCs towards osteoprogenitor differentiation and afterwards into pre-osteoblast lineage. Decreased proliferation and up-regulation of alkaline phosphatase (ALP) and collagen I characterize pre-osteoblast state. Mature osteoblasts up-regulate bone sialoprotein (BSP), osteocalcin (OC) and osteoid resulting in osteocyte differentiation. Figure adapted from R.J. Miron, 2012.

In the second maturation phase, fully non-mitotic matured osteoblasts arise from pre-osteoblasts. Fully matured osteoblasts are characterized by elevated expression of non-collagenous proteins such as bone sialoprotein (BSP) and osteocalcin (OC), which regulate bone formation and bone turnover. A further hallmark of fully matured osteoblasts is the OSTEOD synthesis, which is the organic phase of bone matrix. Formation of hydroxyapatite (Burger & Klein-Nulend 1999) mineralizes osteoid. Terminal differentiation of an osteocyte is indicated when an osteoblast is surrounded by its own matrix and participates in cell communication as well as in the regulation of bone remodeling (Burger & Klein-Nulend 1999).

As previously mentioned, the principle of osteogenic differentiation of MSCs is generally based on the addition of β -glycerophosphate, dexamethasone and ascorbic acid to the basal media. Each component is known to support the development of mineralization in MSC *in vitro*. Dexamethasone is a synthetic corticosteroid, which mimics the actions of various glucocorticoids and induces the binding of activator proteins to glucocorticoid receptors in the cell nucleus. In turn, the activated glucocorticoid receptor will bind to the regulatory region of the osteoblast-specific genes and will induce its expression (Bellows et al. 1990; Cheng et al. 1994; Peter et al. 1998; Atmani et al. 2002; Nuttelman et al. 2004). It is known that constant treatment with dexamethasone *in vitro* improves alkaline phosphatase activity, which is prerequisite for the mineralization process (Cheng et al. 1994). In addition, morphology transformation of MSCs from spindle-shaped to cuboidal is also related to the influence of dexamethasone (Cheng et al. 1994). The second component for osteogenic differentiation is ascorbic acid, which is essential for the survival of osteoblasts *in vitro*. In addition it facilitates the proliferation of osteoblasts and increases the total protein, collagen synthesis and alkaline phosphatase activity to maintain the osteoblastic phenotype of the cells (Koshihara et al. 1987; Hitomi et al. 1992). In contrast to the first two components, the exact mechanism of β -glycerophosphate in osteogenic differentiation induction is still unclear. It is supposed that β -glycerophosphate serves as a local source for inorganic phosphate ions. This released inorganic phosphate supplies the chemical potential for promoting mineralization on the surface of extracellular matrix (ECM) (Fortuna et al. 1980; Nuttelman et al. 2004).

1.2.5 hiPSCs-derived NCSCs and their role in cell replacement therapy

One major problem in studying the biology of these important cells is their transient nature. As mentioned in section 1.2, human induction and differentiation of NC occurs during early embryogenesis leading to technical and ethical problems concerning isolation of early embryonic tissues. Due to this, only few data is available of human NC development (Thomas et al. 2008; Betters et al. 2010) while most current knowledge has arisen from studies of lower organisms (Mayor et al. 1997; Endo et al. 2002; Glavic et al. 2004). Because of their contribution to multiple organs and tissues (Hall 2000), detailed study of events occurring during early NC development is very significant in embryological research. In addition, investigations of NC-related pathologies emerged from inherited or acquired aberrant development (Hansen et al. 2000; Antony & Hansen

2000), collectively defined as neurocristopathies (Bolande 1997), also attracted great attention in science. These NC-related pathologies include DiGeorge (craniofacial and heart defects), frontonasal dysplasia (multiple craniofacial defects), Waardenburg-Shah syndrome (hypopigmentation and aganglionic megacolon) (reviewed in Huang & Saint-Jeannet 2004), Hirschsprung disease (with abnormal innervation of the posterior gut), congenital heart defects (mainly in the outflow tract) and several cancers such as neuroblastoma, melanoma and pheochromocytoma (reviewed in Le Douarin et al. 2004). A further specialized characteristic of NCSC is the mechanism of EMT and cell invasion in association with fibrotic diseases (Zeisberg & Kalluri 2004) and cancer metastasis (Thiery 2002).

As previously mentioned, *in vitro* strategies of hiPSCs-derived NCSCs are an ideal tool in NC-research due to their property of self-renewal and their potential of producing a limitless pool of parental cells (Kreitzer et al. 2013). Additionally, prospective *in vitro* models might enable the gain of huge numbers of hNCSC derivatives, which are required for high throughput screening of substances to design and test novel therapeutical strategies (Münst 2012). Especially, patient-specific cells could be reprogrammed to hiPSCs and further differentiated in NC-derived tissue to replace damaged or lost tissue (Kreitzer et al. 2013). In particular, examination of the mechanism of NC biology and associated neurocristopathies in a patient-specific manner could be a further facility to develop new drugs and therapeutic approaches to treat NC disorders (Münst 2012; Kreitzer et al. 2013). In this manner, two publications reported from the production of patient-specific iPSCs-derived NCSCs for Familial Dysautonomia (Lee et al. 2009; Lee & Studer 2011) and Treacher-Colins Syndrome (Menendez et al. 2013).

2 Aim of the Project

NCSCs are a transient embryonic cell population unique to vertebrates. This cell population evoked great interests in the scientific community due to its contribution to a variety of NCSC derivatives and more interestingly based on the neurocristopathies that emerged from developmental disorders. The reason for our low level of knowledge in human NCSCs development is the inaccessibility of this cell population. To overcome this obstacle, the establishment of NCSCs differentiation methods from hiPSCs is of crucial importance. This project was concerned with the differentiation of hNCSCs, applying hiPSCs as a cell source. The aim of this project was to investigate whether dual SMAD inhibition combined with neural differentiation media is more successful than SMAD-2, -3 inhibition combined with activated canonical WNT signaling for NCSC differentiation from hiPSCs. Successful characterization of NCSC-like cells was to be performed on mRNA level and by confirmation of the presence of surface markers HNK1 and p75. Finally, FACSorting should yield a purified, homogenous, stable hNCSC population. Multipotency was to be investigated by successful osteogenic differentiation. This project aimed to give insight into the generation of hiPSCs-derived NC-like cells, which could serve in future as a further step towards regenerative research in a patient-specific manner.

3 Material and Methods

3.1 Materials

Table 3-1: Material list

Antibody	Manufacturer/Supplier
HNK1 antibody	BioLegend®, London (UK)
Nerve growth factor p75 CD271 (LNGFR)-APC human Orde-No. 130-091-884	MACS Miltenyl Biotec, Bergisch Gladbach (Germany)
Buffer for ICC-staining	Manufacturer/Supplier
BD Perm/Wash™	BD Biosciences, Franklin Lakes (USA)
BD Cytifix™	Biochrom AG, Berlin (Germany)
Donkey Serum	Sigma Aldrich, St. Gallen (Switzerland)
Chemicals	Manufacturer/Supplier
1 x PBS (Dulbecco's Phosphate Buffered Saline) with or without Mg ²⁺ /Ca ²⁺	Gibco®, Life Technologies GmbH, Darmstadt (Germany)
4', 6-diamidino-2-phenylindole (DAPI)	Invitrogen™, Life Technologies GmbH, Darmstadt (Germany)
Agarose Standard	CARL ROTH GmbH, Karlsruhe (Germany)
Alizarin Red	Sigma Aldrich, St. Gallen (Switzerland)
CELLstart™	Life Technologies™ GmbH, Darmstadt (Germany)
Cetylpyridiniumchloride	CARL ROTH GmbH, Karlsruhe (Germany)
Dimethyl sulfoxide (DMSO)	Sigma Aldrich, St. Gallen (Switzerland)
DNA-Ladder 100 bp (0.1 µg/µl)	Solis BioDyne Tartu, (Estonia)
Ethidium Bromide	Sigma Aldrich, St. Gallen (Switzerland)
Geltrex	Gibco®, Life Technologies GmbH, Darmstadt (Germany)
Glycine	CARL ROTH GmbH, Karlsruhe (Germany)
Para-nitrophenyl phosphate (pNPP)	New England BioLabs, Ipswich (USA)
Roti®-Histofix 4 %	CARL ROTH GmbH, Karlsruhe (Germany)
SB-Buffer 1 x 5 M Na ₂ B ₄ O ₇ ×10H ₂ O	Sigma Aldrich, St. Gallen (Switzerland)
Magnesium chloride (MgCl ₂)	CARL ROTH GmbH, Karlsruhe (Germany)
NBT/BCIP	Sigma Aldrich, St. Gallen (Switzerland)
NP40	CARL ROTH GmbH, Karlsruhe (Germany)
Trypan blue	Gibco®, Life Technologies GmbH, Darmstadt (Germany)
Ultra Pure™ 0.5M EDTA, pH8.0	Gibco®, Life Technologies GmbH, Darmstadt (Germany)
Zinc chloride (ZnCl ₂)	CARL ROTH GmbH, Karlsruhe (Germany)
Culture dishes	Manufacturer/Supplier
Falcon tubes	BD Biosciences, Heidelberg (Germany)
BD Falcon™ 6-well Multiwell Plate	BD Biosciences, Heidelberg (Germany)
BD Falcon™ 12-well Multiwell Plate	BD Biosciences, Heidelberg (Germany)
BD Falcon™ 24-well Multiwell Plate	BD Biosciences, Heidelberg (Germany)
BD Falcon™ 96-well Multiwell Plate, flat bottom	BD Biosciences, Heidelberg (Germany)
Perkin Elmer 96-well Multiwell Plate	Perkin Elmer, Waltham (USA)
Falcon tubes	BD Biosciences, Heidelberg (Germany)

Enzyme	Manufacturer/Supplier
Alkaline Phosphatase	New England BioLabs, Ipswich (USA)
Dispase in DMEM/F-12 (1mg/ml)	StemCell™ Technologies, Grenoble (France)
StemPro® Accutase®	Gibco®, Life Technologies GmbH, Darmstadt (Germany)
Trypsin/EDTA, 0.05 %/0.02 %	Biochrom AG, Berlin (Germany)

Equipment	Manufacturer/Supplier
Agarose gel chamber	Peqlab, Erlangen (Germany)
Allegra™ Centrifuge X-22	Beckman Coulter GmbH, Krefeld (Germany)
BD FACSAria™ III	BD Biosciences, Heidelberg (Germany)
BD LSR Fortessa	BD Biosciences, Heidelberg (Germany)
Cell Scraper	TPP® Techno Plastic Products AG, Trasadingen (Switzerland)
Centrifuge Allegra X15R	Beckman Coulter, Krefeld (Germany)
Cryovials	Sigma Aldrich, St. Gallen (Switzerland)
Gel electrophoresis equipment	Peqlab, Erlangen (Germany)
Duomax 1030	Heidolph Instruments GmbH&Co. KG, Schwabach (Germany)
Freezing Container, Nalgene® Mr. Frosty	Thermo Scientific, Dreieich (Germany)
Heating Block Dri-Block DB 2A	Techne, Staffordshire (UK)
Heraeus Fresco 211 centrifuge	Thermo Scientific, Dreieich (Germany)
Heraeus Multifuge X3R centrifuge	Thermo Scientific, Dreieich (Germany)
Heraeus Pico 17 centrifuge	Thermo Scientific, Dreieich (Germany)
Incubator 11-13625	BINDER GmbH, Tuttlingen (Germany)
Mastercycler epgradient S	Eppendorf, Hamburg (Germany)
Microtubes	Eppendorf, Hamburg (Germany)
NanoDrop 1000 spectrophotometer	Peqlab Biotechnology GmbH, Erlangen (Germany)
Neubauer cell counting chamber	Celeromics, Grenoble (France)
Operetta High Content Screener	Perkin Elmer, Waltham (USA)
PCR cycler FlexCycler	Analytik Jena (Germany)
PCR cycler Gene Amp PCR System 9700	Peqlab, Erlangen (Germany)
Phase-Contrast Microscope: Axiovert 40CFL	Zeiss, Jena (Germany)
pH-measurement PB11	Sartorius Stedim Biotech GmbH, Göttingen (Germany)
Real time-PCR	Applied Biosystems®, Life Technologies GmbH, Darmstadt (Germany)
Applied Biosystems 7500 device	Applied Biosystems®, Life Technologies GmbH, Darmstadt (Germany)
Scout™ Pro 2000g	Ohaus®, Nänikon (Switzerland)
Sonifier 450 Cell disrupters	Branson Ultrasonics, Dietzenbach (Germany)
Stereo microscope SMZ 1000	Nikon GmbH, Düsseldorf (Germany)
Spectra max 340PC384	Molecular Devices GmbH, Biberach an der Riss (Germany)
Thermomixer 5436	Eppendorf, Hamburg (Germany)
UV-Gel documentation system NightHawk	Berthold Technologies GmbH & Co. KG, Bad Wildbad (Germany)
XR 205SM-DR	Precisa Instruments Ltd. (Switzerland)
Vortex-2 Genie	Scientific Industries, Inc, New York (USA)
Waterbath	GFL, Burgwedel (Germany)
Workstation L226IVF	HD Scientific, Wetherill Park (Australia)

Inhibitors	Manufacturer/Supplier
BIO	InSolution™ GSK-3 Inhibitor IX , Calbiochem, Merck KGaA, Darmstadt (Germany)
Noggin	R&D systems GmbH, Wiesbaden (Germany)

SB431542	Tocris, R&D systems GmbH, Wiesbaden (Germany)
Y-27632 (ROCK inhibitor)	StemCell™ Technologies, Grenoble (France)
Media	Manufacturer/Supplier
DMEM/F12	
Knockout™ DMEM/F-12 (1X)	Gibco®, Life Technologies GmbH, Darmstadt (Germany)
mTeSR™1	StemCell™ Technologies, Grenoble (France)
NeuroCult XF	StemCell™ Technologies, Grenoble (France)
StemPro® hESC SFM	StemCell™ Technologies, Grenoble (France)
Kits	Manufacturer/Supplier
Rneasy®Micro/Mini Kit (Qiagen)	Qiagen®, Hilden (Germany)
TopTaq™MasterMixKit	Qiagen®, Hilden (Germany)
SuperScript® III First-Strand Synthesis System	Invitrogen™, Life Technologies GmbH, Darmstadt (Germany)
SYBR® Green PCR Master Mix	Applied Biosystems®, Life Technologies GmbH, Darmstadt (Germany)
Supplements	Manufacturer/Supplier
Ascorbic Acid	Sigma Aldrich, St. Gallen (Switzerland)
β -2-Mercaptoethanol	Invitrogen™, Life Technologies GmbH, Darmstadt (Germany)
β-Glycerolphosphat	Sigma Aldrich, St. Gallen (Switzerland)
Dexamethasone	Sigma Aldrich, St. Gallen (Switzerland)
Glutamax	Invitrogen™, Life Technologies GmbH, Darmstadt (Germany)
Heregulin-β-1	PeproTech, Hamburg (Germany)
Human insulin	Sigma Aldrich, St. Gallen (Switzerland)
Human transferrin	Sigma Aldrich, St. Gallen (Switzerland)
Fetal calf serum	Biochrom AG, Berlin (Germany)
Knockout Serum Replacement for ES cells	Gibco®, Life Technologies GmbH, Darmstadt (Germany)
LONGR3 IGF-I human	Sigma Aldrich, St. Gallen (Switzerland)
MEM non-essential amino acids	Life Technologies™ GmbH, Darmstadt (Germany)
N2 –media supplement	Life Technologies™ GmbH, Darmstadt (Germany)
Pen Strep 10000 Units/ml	Gibco®, Life Technologies GmbH, Darmstadt (Germany)
Recombinant human basic fibroblast growth factor (bFGF2)	PeproTech, Hamburg (Germany)
Recombinant human basic epidermal growth factor (EGF2)	PeproTech, Hamburg (Germany)
Trace elements A, B, C	Cellgro, Mediatech, Inc. A Corning Subsidiary, Manassas (USA)
Software	Manufacturer/Supplier
Columbus Image Data System	Perkin Elmer, Waltham (USA)
FlowJo Version 8.8.2	Tree Star, Inc., Ashland (USA)
GraphPad Prism	GraphPad Software, California (USA)
Real Time Analysis software	Applied Biosystems®, Life Technologies GmbH, Darmstadt (Germany)
SoftMaxPr0 software Version 5.4	Molecular Devices GmbH, Biberach an der Riss (Germany)

3.2 Cell culture methods

3.2.1 Cultivation of cell lines

3.2.1.1 hiPSCs cultivation

The used hiPSC line was derived from human cord blood somatic stem cells (Zaehres et al. 2010). Cells were grown as colonies in 6-well plates (BD Biosciences) and cultivated with 2 ml mTeSR-1 media (StemCell™ Technologies) per well at 37 °C and 5 % CO₂ supply. Media change was performed every day.

3.2.1.2 Human epidermal neural crest stem cells (hEpi-NCSCs)

HEpi-NCSCs were isolated from human hair follicles by the research group of Sieber Blum (Clewes et al. 2011). Cells were cultivated in NeuroCult XF media (StemCell™ Technologies) and incubated under hypoxic conditions (5 % O₂) at 37 °C and 5 % CO₂ supply. 80 % media change occurred every two to three days.

3.2.1.3 Mesenchymal stem cells (MSCs)

Manfred Roch at the Charité Berlin segregated hMSCs from human adipose tissue. Cells were cultivated in basal media consisting of DMEM low glucose media (1 g/l) (Dulbecco's Modified Eagle Medium, Gibco®), 10 % FCS (Fetal calf serum, Biochrom AG) and 1 % Pen/Strep (Penicillin Streptomycin, Gibco®) and incubated at 37 °C with 5 % CO₂ supply. Media change was carried out two to three times a week.

3.2.1.4 S462 Cell line

S462 cell line isolated from cancer Schwann cells derived from NF1 patients, were cultivated in basal media and incubated at 37 °C with 5 % CO₂ supply. 80 % media change was carried out two to three times a week.

3.2.2 Freezing of cells: hEpi-NCSCs

Media was discarded, and cells washed twice with PBS w/o Ca²⁺/Mg²⁺ (Dulbecco's Phosphate Buffered Saline, Biochrom AG). For cell detachment 0.05 % trypsin/EDTA (Biochrom AG) was added and incubated for 1 minute at 37 °C. Trypsin reaction was stopped by adding the double amount of used NeuroCult XF media and transferred to a 50 ml falcon (BD Biosciences). Cells were pelleted at 300 x g for 5 minutes at 4 °C. Media was discarded and cell pellet was resuspended in freezing media consisting of 10 %

DMSO (Dimethyl sulfoxide, Sigma) mixed with 90 % FCS and transferred to cryovials (Sigma). First, cryovials were collected in a freezing container “Mr. Frosty” (Thermo Scientific) and stored at -80 °C for at least 6 h. The next day, cryovials were conveyed to gaseous nitrogen tanks (-180 °C) for long-term storage.

3.2.3 Thawing of cell lines: hEpi-NCSCs

Cryovial was thawed quickly by swirling the vial in a 37 °C waterbath until there was only a small amount of ice left. After disinfection of the cryovial, the cell suspension was immediately transferred into a 50 ml falcon. A volume of 5 ml pre-warmed NeuroCult XF media was added drop-wise to the cell suspension while gently swirling the falcon to decrease osmotic shock caused by the cryoprotectant. Cell suspension was centrifuged at 300 x g for 5 minutes at room temperature (RT) in order to remove the DMSO. Supernatant (SN) was discarded and the cell pellet was gently resuspended in 20 ml pre-warmed NeuroCult XF media. SN of pre-coated CELLstart™ (Life Technologies™) wells were discarded, 2 ml of cell suspension was transferred into a well of 6-well plate and incubated under hypoxic conditions (5 % O₂) at 37 °C and 5 % CO₂ supply.

3.2.4 Cell passage of cell lines

3.2.4.1 hiPSC colony cell passage

When cells were 60 – 80 % confluent, the media was aspirated, cells were washed with 2 ml pre-warmed KO DMEM/F12 (Gibco®) media, and dispase (1 mg/ml, StemCell™ Technologies) was added for cell detachment and incubated for 5 - 7 minutes at 37 °C. When the edges of cell colonies were detached, dispase was removed and cells were washed with pre-warmed KO DMEM/F12. A volume of 2 ml pre-warmed mTeSR-1 was added and cell colonies were scratched off the surface with a cell scraper (TPP® Techno Plastic Products AG). The cell suspension was collected in a 50 ml falcon and mixed with 7 ml pre-warmed mTeSR-1 media. The SN of GelTrex (Gibco®) pre-coated wells was removed and 1.5 ml of cell suspension was placed into each well. When cells showed a cell confluence of 80 %, a 1 to 6 split ratio was performed.

3.2.4.2 hiPSC single cell passage

The media was removed and cells were washed with pre-warmed KO DMEM/F12. For single cell passaging, 1 ml of accutase (Gibco®) was added and cells were incubated for 3 to 5 minutes at 37 °C. When all cells were rendered to single cells, the enzymatic

reaction was stopped by addition of 2 ml mTeSR-1 supplemented with 5 μ M Rock Inhibitor Y-27632 (StemCell™ Technologies). The cell suspension was harvested into a 50 ml falcon, pelleted at 300 x g for 5 minutes at RT and resuspended in 1 ml mTeSR-1 supplemented with 5 μ M Rock Inhibitor Y-27632. After cell count, an aliquot of the desired cell amount was taken and mixed with the corresponding amount of pre-warmed mTeSR-1. Before cell seeding, the SN of the GelTrex pre-coated well was discarded.

3.2.4.3 hEpi-NCSC

Cell passage of hEpi-NCSCs was performed with 0.05 % trypsin/EDTA as described in sections 3.2.2 and 3.2.3.

3.2.4.4 MSC and S462 cell passage

After media removal, cells were washed twice with 5 ml pre-warmed PBS w/o Ca^{2+} / Mg^{2+} and detached by 2.5 ml 0.05 % trypsin/EDTA treatment for two minutes at 37 °C. When the majority of cells were detached, the trypsin reaction was terminated by addition of 10 ml basal media. Cell suspension was harvested in a 50 ml falcon, pelleted at 300 x g for 5 minutes at RT and SN was aspirated. Cell pellet was resuspended in 1 ml pre-warmed basal media and cell count was performed. After cell count, the appropriate cell amount was pipetted to 10 ml pre-warmed DMEM low glucose (1 g/l) media, 10 % FCS and 1 % Pen/Strep in a 75 cm² culture flask.

3.2.5 Cell counting

To seed the exact amount of cells for each cell passaging, counting of cells was performed by using a haemocytometre (Neubauer). For this purpose 10 µl of cell suspension was pipetted into each of the two haematocytometre chambers and visualized under a light microscope with a 10 x magnification. Cells were counted in 8 fields of grid lines each containing a volume of 1 mm³. Number of cell per milliliter was counted by following formula:

$$\text{Cells per millimeter} = \left[\frac{\text{Total number of cells}}{\text{number of fields}} \times \text{Dilution factor} \times 10^4 \right]$$

Table 3-2: Cell culture methods for different cell lines

	hiPSCs	MSC	S462	hEpi-NCSC
Culture vessel	6-well plate	75 cm ² flask	75 cm ² flask	6-well plate
Cell coating	1 ml GeTrex	-	-	0.75 ml CeLLStart
Cell amount	1:6 split ratio	1 x 10 ⁵ cells	3.75 x 10 ⁵ cells	5 x 10 ³ - 1 x 10 ⁴ cells
Media	2 ml mTeSR-1	10 ml basal media	10 ml basal media	2 ml NeuroCult XF media
Cell wash buffer	2 x 2 ml KO DMEM/F12	2 x 5 ml PBS w/o Ca ²⁺ /Mg ²⁺	2 x 5 ml PBS w/o Ca ²⁺ /Mg ²⁺	2 x 2 ml PBS w/o Ca ²⁺ /Mg ²⁺
Enzymatic cell detachment reagent	1 ml dispase/ 1ml accutase	2.5 ml 0.05 % trypsin/EDTA	2.5 ml 0.05 % trypsin/EDTA	0.5 ml 0.05 % trypsin/EDTA
Freezing media	-	-	-	7 x 10 ⁴ - 10 ⁵ cells in 0.5ml Freezing media (10 % DMSO, 90 % FCS)
Media for cell thawing	-	10 ml basal media	10 ml basal media	5 ml NeuroCult XF media

3.3 NCSC differentiation from hiPSC

3.3.1 NCSC differentiation from hiPSCs by dual SMAD inhibition according to Gabsang Lee (2010)

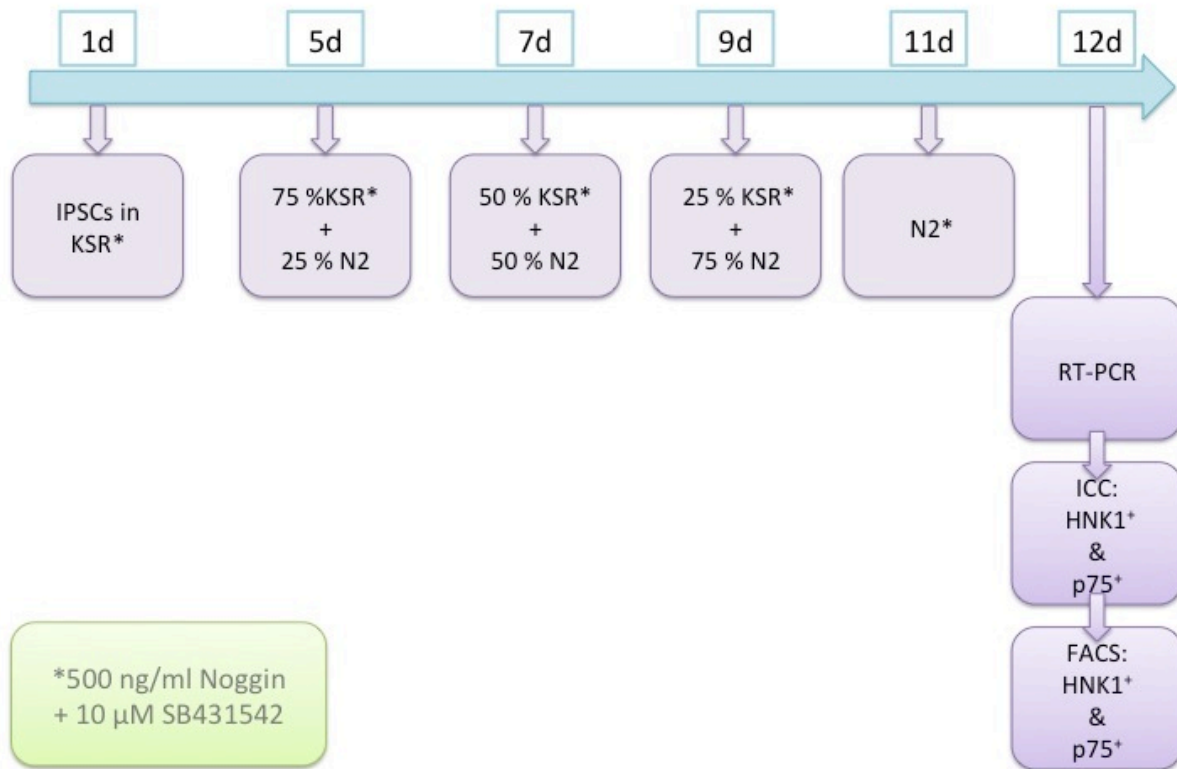


Figure 3-1: Experimental set up of NCSC differentiation from hiPSCs according to G. Lee et al (2010).

When hiPSCs were 60 – 80 % confluent, cells were harvested as single cells (as described in section 3.2.4.2), plated on GelTrex-coated wells of 12-well plate at 1×10^4 cells per cm^2 and cultured in 1 ml mTeSR-1 media containing 5 μ M Rock Inhibitor Y-27632 per well. Media change was performed the next day. After two days of cultivation in mTeSR-1 combined with 5 μ M Rock Inhibitor Y-27632, cell confluence should range between 50 - 70 %. NCSC differentiation was initiated by the replacement of mTeSR-1 media to KSR media containing 10 μ M SB431542 (Tocris) and 500 ng/ml Noggin (R & D System). As a control, cells were cultivated under the same conditions as the Noggin SB431542 (NSB) sample but without the inhibitors. Media replacement and slow switch from KSR (Knockout Serum Replacement) to N2 media were performed on days 2, 3, 5, 7, 9 and 11 as detailed described in Figure 3-1. Cells were incubated at 37 °C and 5 % CO₂ supply.

Table 3-3: Media composition for NCSC differentiation

NCSC differentiation media according to G. Lee		NCSC differentiation media according to L. Menendez
KSR-media	N2-media	Defined conditioned media (DC-media)
KO DMEM/F12	DMEM/F12	DMEM/F12
15 % KSR	2.5 µg/ml Insulin	2 % BSA FAA
1 x Glutamax	0.1 mg/ml Apotransferin	1 x Pen/Strep
1 x Pen/Strep	3 nM Sodium selenite	1 x Glutamax
0.1 mM β-Mercaptoethanol	10 µM Putrescine	1 x MEM non-essential amino acids
	2 nM Progesterone	1 x Trace elements A, B & C
	1 x Pen/Strep	0.1 mM β-Mercaptoethanol
		50 µg/ml Ascorbic acid
		10 µg/ml Transferrin
		10 ng/ml Heregulin β-1
		200 ng/ml LONGR3-IGF-I
		8 ng/ml bFGF2

3.3.2 NCSC differentiation from hiPSCs by the activation of WNT signaling and the inhibition of SMAD according to Laura Menendez (2011).

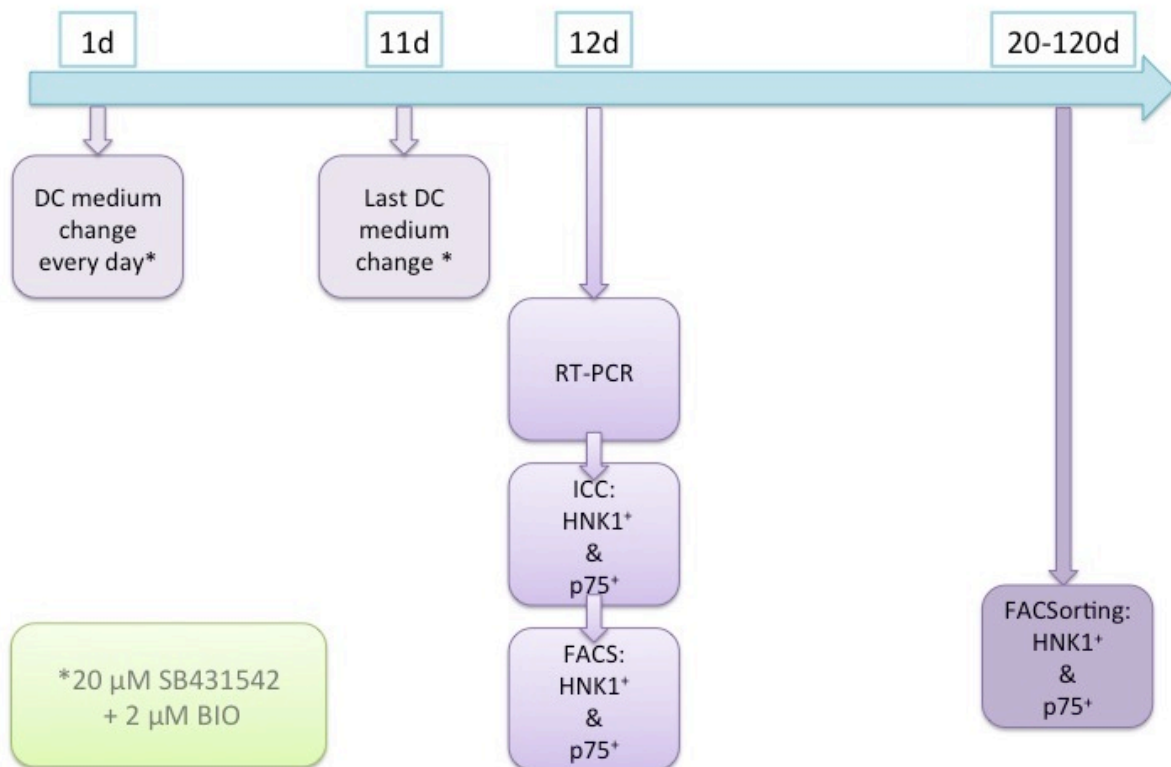


Figure 3-2: Experimental set up of NCSC differentiation from hiPSCs according to L. Menendez et al (2012).

When hiPSCs were 60 – 80 % confluent, cell harvest was performed by accutase treatment as described in section 3.2.4.2. Cells were plated on GelTrex coated wells of a 12-well plate. 1×10^5 cells per cm^2 were seeded and cultured in 1 ml mTeSR-1 media supplemented with 5 μM Inhibitor Y-27632 per well. Media switch to StemPro media (StemCell™ Technologies) was carried out the next day. NCSC differentiation was induced on the third day. Cells were cultivated in defined media without activin supplemented with 20 μM SB431542 and 2 μM BIO (Calbiochem) for 11 days and media change occurred every day. As a control, cells were cultivated under the same conditions but without inhibitors. In general, cells had to be passaged every 3 to 4 days with 0.5 μM EDTA. For this purpose, media was discarded, cells were washed twice with 1 ml PBS w/o $\text{Ca}^{2+}/\text{Mg}^{2+}$ and 0.5 ml of 0.05 μM EDTA was used for cell detachment. Incubation time at 37 °C ranged between 3 - 5 minutes and cells were washed with 0.1 % BSA (Bovine serum albumin, Merck Millipore) wash buffer. Cell suspension was collected in a 15 ml falcon and centrifuged at 300 x g for 5 minutes at RT. SN was removed and the cell pellet was resuspended in pre-warmed defined media supplemented with 20 μM SB431542 and 2 μM BIO. A total of 1×10^5 cells was plated on GelTrex-coated wells of a 12-well plate and incubated at 37 °C. The same procedure for cell passage was applied for the control sample.

3.4 NCSC characterization

3.4.1 RNA isolation

After 12 to 14 days of NCSC differentiation, RNA was isolated from cultures derived from both NCSC differentiation systems (G. Lee and L. Menendez). For this purpose RNeasy®Micro Kit (Qiagen) was used. The procedure was performed as described in the manufacture's protocol (RNeasy®Micro Mini Handbook (09/2012) page 27 - 30).

3.4.2 cDNA synthesis

A total of 1 μg of the yielded RNA was reverse transcribed into cDNA using the kit SuperScript® III First-Strand Synthesis System (Invitrogen). For a First-Strand cDNA synthesis the components were mixed and incubated with the related incubation times and temperatures as depicted in Table 3-4, Table 3-5, and Table 3-6.

Table 3-4: cDNA synthesis pipetting scheme

Components	Amount
1 µg RNA	<i>n</i> µl
50 µM oligo (dT)	1 µl
10 mM dNTP Mix	1 µl
DEPC treated water	To 10 µl

Table 3-5: cDNA synthesis mix

Components	1 x Sample
10 x RT Buffer	2 µl
25 mM MgCl ₂	4 µl
0.1 M DTT	2 µl
Rnase Out	1 µl
SuperScriptIII (200 U/µl)	1 µl

Table 3-6: Summary of procedure

Step	Procedure
Denaturing	RNA + Primer + dNTPs (10 µl) at 65 °C for 5 minutes
	Place on ice for at least 1 minutes
Annealing	Add 10 µl of cDNA Synthesis Mix
cDNA synthesis	50 °C for 50 minutes
Terminate reaction	85 °C for 5 minutes
Remove RNA	Add 1 µl of RNase H at 37 °C for 20 minutes

3.4.3 Polymerase chain reaction (PCR)

PCR served as a molecular biological method to amplify specific areas of the yielded cDNA by the application of certain primers (Metabion) listed in Table 3-8. The components of the TopTaq™MasterMixKit (Qiagen®) were mixed with the yielded cDNA as shown Table 3-7. For each primer set an additional negative control was applied (without cDNA). Due to the fact that beta-actin (β-Actin) is highly conserved in every cell type, it is referred as a positive control for PCR reaction. The function of this housekeeping gene is the regulation of cell motility, structure and integrity

Table 3-7: PCR synthesis mix

Components	1 x Sample (μl)
10 x TopTaq PCR	5
cDNA template	<i>n</i>
dNTP mix (10 mM)	1
10 x Coral load	5
Forward Primer (10 pmol)	1
Reverse Primer (10 pmol)	1
TopTaq DNA polymerase	0.25
RNase free H ₂ O	Fill up to 50

Table 3-8: Primer list for PCR and qRT-PCR

Primer	Sequence	Annealing temperature (°C)	PCR product length (bp)
SOX10 F	tgc agc aca aga aag acc ac	59.2	213
SOX10 R	gcc aca tca aag gtc tcc at		
ZIC1 F	cac gcg gga ctt tct gtt c	58.9	198
ZIC1 R	tgc ccg ttg acc acg tta g		
PAX3 F	agc cgc atc ctg aga agt aa	57	202
PAX3 R	ttc tgc gct gtt tcc tct tt		
MSX1 F	cct tcc ctt taa ccc tca cac	61.1	284
MSX1 R	ccg att tct ctg cgc ttt tct		
p75 F	agc caa cca gac cgt gtg t	61.1	663
p75 R	ttg cag ctg ttc cac ctc tt		
HNK1 F	gca aga agg gct tca ctg ac	61.1	165
HNK1 R	gcc ccc aga ata gaa agg ag		
SNAIL F	ctg ctg ctg agc tga atg ac	57	210
SNAIL R	ggacagagtcccagatgagc		
SLUG F	cct tcc tgg tca aga agc at	57	225
SLUG R	atc cgg aaa gag gag aga gg		
SOX9 F	aga agg acc acc cgg att ac	57	313
SOX9 R	aag tcg ata ggg ggc tgt ct		
OCT4 F	tgt ctc cgt cac cac tct	56	164
OCT4 R	ttc cca att cct tcc tta		
β-ACTIN F	aga gcta cga gct gcc tga c	55	350
β-ACTIN R	agc act gtg ttg gcg tac ag		

Table 3-9: PCR procedure

Step	Temperature (°C)	Time (minutes)	Cycles (#)
Initial melting	95	5	
Denaturing	95	0.5	35-40
Primer annealing	<i>n</i>	0.5	
Elongation	72	0.5	
Dinal elongation	72	10	
Cooling	4	∞	

3.4.4 Gel electrophoresis

Visualization of the PCR products was performed by gel electrophoresis. For this approach a 1 % Agarose gel (CARL ROTH GmbH) in SB-buffer (Sigma) containing 1 % Ethidium bromide (500 µg/ml, Sigma) was prepared. A volume of 20 µl of each PCR product was added in one gel pocket. A 100 bp DNA ladder (Solis Bio Dyne Tartu) enabled product size determination. Gel running was carried out at 220 V for 15 minutes in order to separate the cDNA fragments. The cDNA visualization was effected by Ethidium bromide due to its property to intercalate into the major groove of DNA.

3.4.5 Immunohistochemistry (ICC)

In conjunction with the G. Lee Protocol, NCSC differentiation was performed directly in the wells of a 96-well plate (Perkin Elmer). In contrast, for the L. Menendez protocol, NCSC differentiation occurred in the wells of a 12-well plate and cells were harvested by EDTA passaging. Approximately 3×10^4 cells were seeded in a well of a 96-well plate and cultivated until a cell confluence of 70 - 80 % was reached. Media was removed and cells were washed with 200 µl PBS with $\text{Ca}^{2+}/\text{Mg}^{2+}$ (Gibco®). For cell fixation 100 µl 3.7 % BD Cytofix™ (Biochrom AG), which contains formaldehyde was added and incubated for 10 minutes. Formaldehyde preserves the cells by crosslinking amino groups with nearby nitrogen atoms. After the removal of fixation buffer cells were washed with 200 µl PBS with $\text{Ca}^{2+}/\text{Mg}^{2+}$. Unspecific antibody binding was prevented by adding 100 µl of 10 % Donkey Serum Blocking buffer (Sigma) and incubating for 30 minutes at RT. After the removal of Blocking buffer, cells were washed and cell permeabilization was performed by adding 100 µl 1 x Perm/Wash buffer (BD Biosciences) to each well. The compound Saponin is included in Perm/Wash buffer

and forms pores in cell membrane bilayers. During the 25 minutes incubation time of cells in Perm/Wash buffer, antibodies were diluted to optimal working concentration in 1 x Perm/Wash buffer and stored on ice in the dark. For detailed information about the dilution of the antibodies see Table 3-10. Due to the fact that the antibodies HNK1 and p75 were already labeled a one-step staining was performed. For this purpose 50 µl of the diluted antibody was pipetted to each well and incubated for 30 minutes in the dark at RT. After removal of the antibodies, cells were washed with 100 µl/well Perm/Wash buffer. In the last step, nuclei staining was carried out by adding 50 µl of DAPI diluted (4',6'-diamidino-2-phenylindole, 1:1000, Invitrogen™) in PBS with $\text{Ca}^{2+}/\text{Mg}^{2+}$. After 30 minutes incubation time, DAPI was discarded and cells were stored within 200 µl PBS w/o $\text{Ca}^{2+}/\text{Mg}^{2+}$ at 4 °C until imaging.

Table 3-10: Characteristics of antibodies

Antibody	Location of marker	Species	Fluorochrome	Isotype	Dilution
HNK1	surface	Mouse	PE	IgM, κ	1:20
P75	surface	Mouse	APC	IgG1	1:20

3.4.6 ICC evaluation by Columbus image data storage and analysis system (Perkin Elmer)

The Operetta High Content Screener (Perkin Elmer) represents a new modern imaging technology, which is a fully automated fluorescence microscope containing 8 excitation and 8 exchangeable emission filters. Several different fluorescently labeled cell components can be visualized and measured in parallel by applying fluorescent tags with different absorption and emission maxima. Thereby the effect of substances on cells can be monitored in a detailed molecular and phenotypic picture, enabling to produce and collect complex data. Screening of stained wells of fixed NSB or SBio cells of a 96-well plate were carried out with three channels (Brightfield, DAPI, APC and PE) and an objective 20 x magnification. The screened pictures were further analyzed with the Columbus Image Data Storage and Analysis System (Perkin Elmer). To analyze the received data, a pipeline was established, consisting of different building blocks with specific functions. The applied building blocks are presented in Table 3-11. To quantify the total amount of cells, nuclei were counted through DAPI intensity detection. The filtering of artifacts is enabled due to their brighter intensity compared to the DAPI

signal. For each marker, the range was manually adjusted to calculate and filter intensity. In the next step, intensities for HNK1-PE and p75-APC double positive cells were set and inserted in the formula to calculate the amount of double positive cells in percent related to the total cell number. The pipeline was adjusted for both experiments to ensure that all cell nuclei were captured and that solely cells of interest were filtered.

Table 3-11: Exemplary building block for ICC evaluation by Columbus image data storage and analysis system (Perkin Elmer)

Building Block	Output
Nuclei detection by DAPI intensity	Number of nuclei for a specific area
Filter by DAPI intensity to exclude very bright objects (dividing nuclei, artifacts)	Number of non-dividing nuclei (a) for a specific area
Intensity calculation of respective marker (HNK1 and p75)	Mean intensity of respective marker for a specific area
Filter by marker intensity range to determine the number of cells positive for respective marker and positive for all markers	Number of marker positive cells ($b_{\text{HNK1}}, b_{\text{p75}}, b_{\text{both marker}}$) for a specific area
Calculating the percentage of marker positive cells ($b_{\text{both marker}} \cdot 100 / a$)	Number of marker(s) positive cells in % for a specific area

3.4.7 Fluorescence-activated cell sorting (FACS) analysis

FACS enables to sort a heterogeneous cell mixture into two or more containers based on its specific light scattering and fluorescent properties of each cell. In the first step of FACS, cell suspension is soaked into an entrained rapidly flowing stream of liquid. The flow is adjusted to separate the cells from each other relative to their diameter. The stream of cells breaks into individual droplets by a vibrating mechanism. In order to reduce the probability of more than one cell per droplet, the system is arranged in a specific manner. Before the stream breaks into droplets, the flow passes through a fluorescence measuring station where the fluorescent property of interest for each cell is analyzed. The computer defines how the cells will be sorted before the stream breaks into droplets. An electrical charge is applied to the stream during the formation of the drop leading to its new charge. This newly formed charged drop is further deflected left or right by charged electrodes and collected into tubes based upon their charge. The fluorescence for each cell is recorded and the cell number in each collection tube is analyzed.

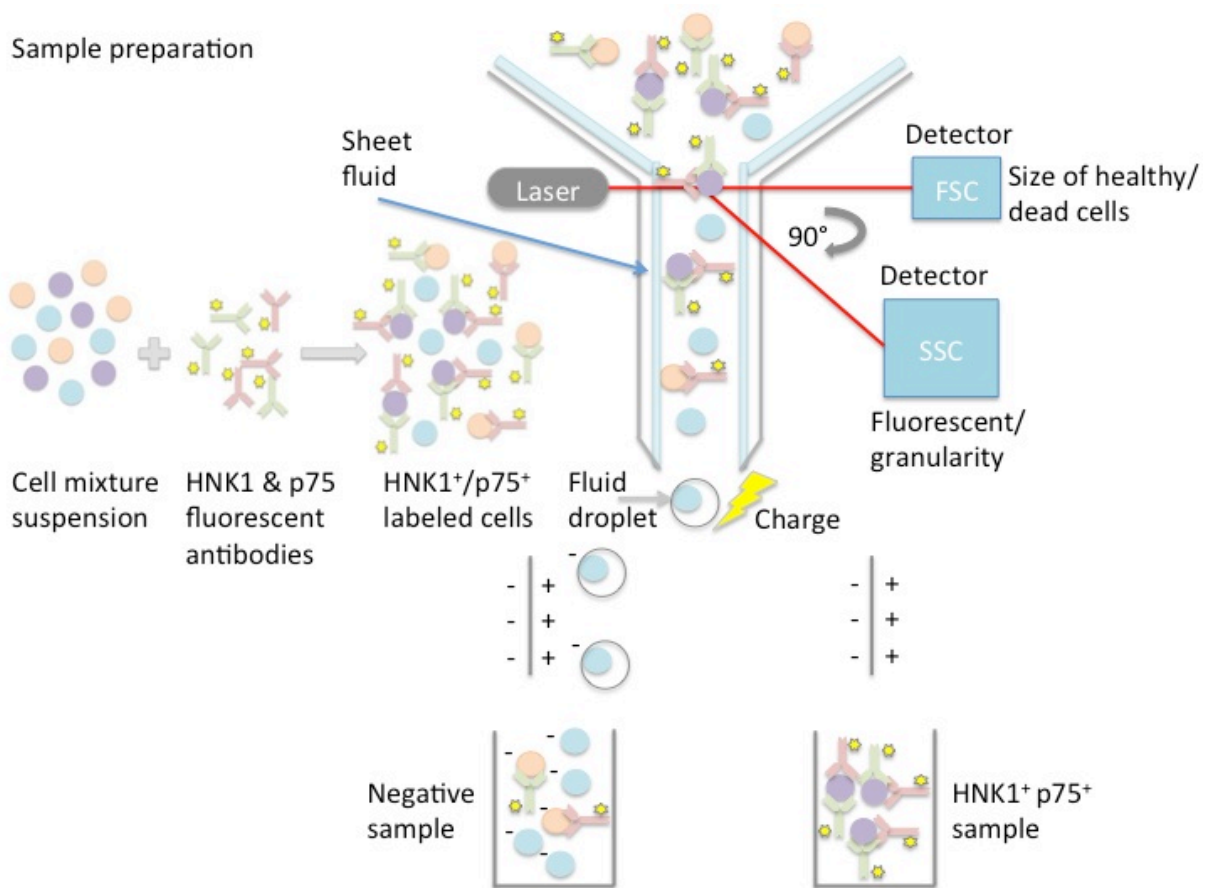


Figure 3-3: FACS sorting principle

Cells are incubated with HNK1-PE and p75-APC antibodies before FACS-analysis is carried out. Figure adapted from Sabban, S. et al. (2011).

3.4.8 Sample preparation for FACS sorting

Cell harvest was performed by 0.05 % EDTA passage or by 0.05 % trypsin/EDTA. Cells were washed with 2 ml chilled PBS with $\text{Ca}^{2+}/\text{Mg}^{2+}$ and pelleted at 300 x g for 5 minutes at 4 °C. SN was removed and cells were stained with a primary antibody mixture at 4 °C for 30 minutes in the dark. Afterwards cells were washed with chilled PBS w/o $\text{Ca}^{2+}/\text{Mg}^{2+}$ and pelleted at 300 x g for 5 minutes at 4 °C. SN was discarded and cells were resuspended and FACS measured/sorted immediately.

3.4.9 FACS sorting

FACS sorting was carried out by the Flow Cytometry Core Facility BD FACSaria™ III (BD Bioscience) of the DRFZ Berlin with the help of Désirée Kunkel. The first step of the sorting strategy always implied exclusion of dead cells by gating of forward and side scatter, and second gating on HNK1⁺p75⁺ cells. To verify high purity cell sorting,

Re-FACS analysis was carried out. After FACSorting p75 and HNK1 double positive cells were plated on GelTrex coated wells and cultivated in defined media supplemented with 20 μ M SB431542 and 2 μ M Bio. Cells were incubated at 37 °C with 5 % CO₂ supply until they reached 60 - 80 % confluence.

3.4.10 Quantitative real time PCR (qRT-PCR)

Total RNA from SBio cells was purified with RNeasy®Micro Kit and transcribed into cDNA with SuperScript® III First-Strand Synthesis System as described in section 3.4.1 and 3.4.2. To analyze mRNA expression of human genes qRT-PCR was applied. The mechanism of qRT-PCR is based on the PCR technique, which amplifies a target DNA molecule. In addition, qRT-PCR enables detection and quantification of specific sequences in a DNA sample, which gives the relative expression amount when normalized to a housekeeping gene like *GAPDH*. The qRT-PCR was performed in an Applied Biosystems 7500 device and PCR product of the reaction is detected at its end by non-specific fluorescent dyes like SYBR green that intercalate with any double stranded DNA. The components of SYBR® Green PCR Master Mix (Applied Biosystems®) were mixed with cDNA and primers as depicted in Table 3-12. Analysis was performed using the Real Time Analysis software (Applied Biosystems®). To calculate the relative expression ratio [R] following formula was applied:

$$[R] = 2^{-[\Delta CP_{Sample} - \Delta CP_{Control}]}$$

Table 3-12: qPCR components

Components	1 x Sample
SYBR Green master mix	1.5 μ l
Forward Primer (10 pmol)	0.5 μ l
Reverse Primer (10 pmol)	0.5 μ l
cDNA (1 μ g)	<i>n</i> μ l
RNase free H ₂ O	Fill up to 25 μ l

Table 3-13: qRT-PCR procedure

Step	Temperature (° C)	Time (minutes)	Cycles (#)
Initial melting	50	2	42
Melting	95	10	
Primer annealing	95	0.25	
Elongation	60	1	

3.5 Osteogenic differentiation

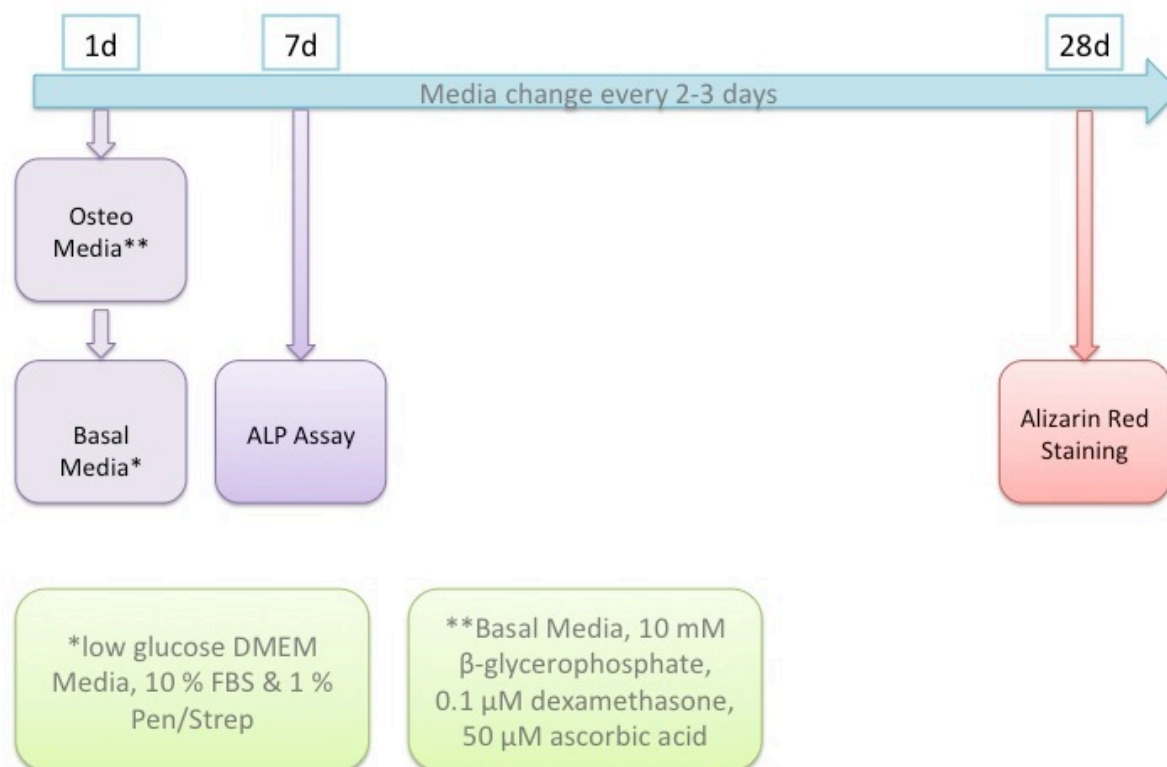


Figure 3-4: Experimental set up for osteogenic differentiation.

In the first step of osteogenic differentiation, SBio cells, MSCs and hEpi-NCSCs were harvested and seeded at high cell density (1×10^5 cells/well of SBio cells, 3×10^3 cells/well of MSCs and hEpi-NCSCs as shown in Table 3-14) in 24-well plates. For each cell type 6 wells of a 24-well plate were seeded and cells were cultured under their normal conditions until 90 % cell confluence was reached. In three wells of each cell type osteogenic differentiation was initiated by media switch to osteogenic media (DMEM low glucose, 10 % FBS, Pen/Strep, 10 mM β-glycerophosphate (Sigma), 0.1 μM dexamethasone (Sigma) and 50 μM ascorbic acid (Sigma)). The remaining three wells of each cell type were further cultivated in the DMEM low glucose, 10 % FBS and Pen/Strep and served as negative control. Cells were cultured at 37 °C and 5 % CO₂ supply for 28 days. Media change was performed every two to three days.

Table 3-14: Seeding cell amount of different cell types in a well of a 24-well plate

	1. SBio	MSC	hEpi-NCSC	S462
24-well plate	1×10^5 cells/well	3×10^3 cells/well	3×10^3 cells/well	1×10^5 cells/well

3.6 Osteogenic characterization

3.6.1 Alkaline phosphatase biochemical assay (ALP-assay)

Table 3-15: ALP-1 and ALP-2 buffer composition

Substances	100 ml ALP1	100 ml ALP2
0.1 M Glycine	0.75 g	0.75 g
1 % NP40	1 ml	-
1 mM MgCl ₂	0.00952 g	0.00952 g
1 mM ZnCl ₂	0.013629 g	0.013629 g

The substance Para-nitrophenyl phosphate (pNPP) (New England BioLabs) enables activity detection of alkaline phosphatase. In this reaction, pNPP is hydrolyzed to p-nitrophenol and phosphate which results in a color change from colorless to yellow. The absorbance is measured at a wavelength of 405 nm in a plate reader. In the first step of the experiment, media was discarded and cells were washed with 1 ml 1 x PBS w/o Ca²⁺/Mg²⁺ per well. Cell lysis was performed with 0.5 ml ALP1 buffer per well on a shaker for one hour at 4 °C. Afterwards, the cell lysis solution was collected in 1.5 ml microcentrifuge tubes and sonicated for 10 cycles within chilled glycine in order to break the cell membrane. Cell debris was pelleted at 12000 x rpm for 10 minutes at 4 °C and the SN was transferred into new chilled 1.5 ml microcentrifuge tubes. The assay was carried out in a 96-well plate (BD Biosciences). A volume of 100 µl of each sample was pipetted into a well of a 96-well plate in duplicate. By adding 100 µl of 2 mg/ml pNPP dissolved in ALP2 buffer the ALP-activity reaction was induced. Samples were incubated for 30 minutes at RT in the dark and further incubated at 37 °C for the whole experiment. Absorbance of all assay and control wells was read out on a plate reader at 405 nm every 30 minutes for three hours. The absorbance values obtained at each time point were converted into alkaline phosphatase activity (U/µl) using an alkaline phosphatase standard dilution series (stock concentration = 0.5 U/µl, 1:2, 1:4, 1:8, 1:16, 1:32, 1:64, 1:128, 1:256, 1:512, 1:1024, 1:2048, 1:4096). ALP activity was measured on the 7th, 21st, and 28th day of osteogenic differentiation.

3.6.2 Alkaline phosphatase staining

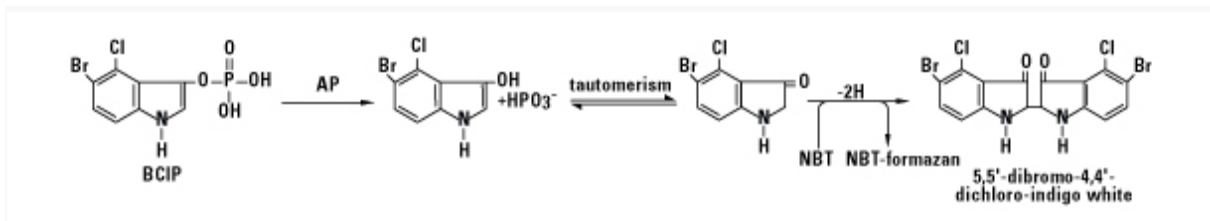


Figure 3-5: Chemical reaction of BCIP and NBT.

Figure adapted from L. J. Stuyver et al. (2003).

The two compounds BCIP (5-bromo-4-chloro-3'-indolylphosphate p -toluidine salt) and NBT (nitro-blue-tetrazolium-chloride) permit detection of alkaline phosphatase activity. In the first step of this reaction, BCIP is hydrolyzed by alkaline phosphatase to an intermediate that will further undergo a dimerization leading in an indigo color change. In addition, NBT is reduced to the NBT-formazan due to the two reducing equivalents produced by the dimerization. First, media was aspirated and cells were carefully washed with 1 x PBS w/o $\text{Ca}^{2+}/\text{Mg}^{2+}$. To each well 0.5 ml Histofix (Carl Roth) was added and incubated for 20 minutes at RT to fix cells. The fixation solution was carefully removed and cells were washed three times with distilled water. 0.5 ml BCIP/NBT (Roche) dissolved in distilled water was pipetted to each well and incubated at RT in the dark. After 5 minutes incubation, pictures were taken every 10 minutes for 40 minutes.

3.6.3 Alizarin Red staining

Formation of calcified ECM during osteogenesis is analyzed by Alizarin Red S staining (Sigma). Alizarin red is an organic compound that forms a chelate with Ca^{2+} cations. In the first step, media was aspirated and cells were carefully washed with 1 ml 1 x PBS w/o $\text{Ca}^{2+}/\text{Mg}^{2+}$. To each well, 0.5 ml Histofix were added and incubated for 30 minutes at RT. Histofix was carefully removed, cells were washed three times with 1 ml distilled water and aspirated. A volume of 0.5 ml of 2 % Alizarin red (pH 4.1 - 4.3) was transferred to each well and incubated for 10 minutes at RT in the dark. Afterwards Alizarin red was carefully removed and unbound Alizarin red was carefully washed off with distilled water until the distilled water remained colorless. Discoloration of Alizarin Red was carried out by adding 400 μl 10 % Cetylpyridiniumchlorid to each well and incubated at RT on a plate shaker for one hour. SN was diluted with 1 x PBS w/o

Ca²⁺/Mg²⁺ in a 1:8 dilution ratio and transferred to a 96-well plate. Each sample was pipetted in triplicate and samples were measured at 562 nm.

3.6.4 Statistical analysis

Statistical tests were calculated by using GraphPad Prism. Analysis between two groups was carried out using Mann-Whitney U test and within one group, parameters were compared by Wilcoxon test.

4 Results

4.1 NCSC differentiation

4.1.1 Phenotypic characterization of hiPSCs during NCSC differentiation process

To establish a robust method for producing hiPSCs derived NC-like cells to investigate NC biology in comparison to NC disorders, we tested whether dual SMAD inhibition or concurrent SMAD-2/-3 inhibition combined with activated canonical WNT signaling is the most effective method of choice. hiPSCs were cultured and expanded on GelTrex coated 6-well plates in mTeSR-1 medium. The round shaped cells possess characteristic appearance of pluripotent stem cells, forming compact colonies with defined borders and a low nucleus cytoplasm ratio (Figure 4-1 A). In order to obtain the defined amount of hiPSCs for each method (section 3.3.1 and section 3.3.2), single cell passaging was performed as described in section 3.2.4.2. Morphology changes appearing during NCSC differentiation are presented in Figure 4-2 A-C for the dual SMAD inhibition protocol, while Figure 4-3 A-C show concomitant SMAD-2/-3 inhibition combined with activation of the canonical WNT signaling. Treated samples of both methods were always referred to their related untreated control samples (Figure 4-2 a-c and Figure 4-3 a-c).

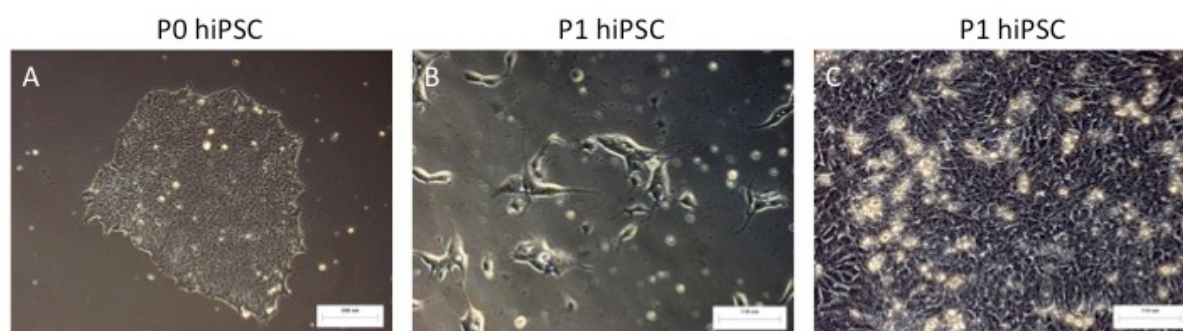


Figure 4-1: iPSC growth in colonies and as single cells

(A) hiPSC colony in mTeSR-1 media, (B) 1 day after single cell passage 10 x in mTeSR-1 media supplemented with Rock inhibitor Y-27632 and two days after single cell passage in StemPro media. Cells were documented by phase contrast microscopy, (A) is shown in 10x magnification, (B-C) in 20 x magnification. Scale bar = 200 μ m in A and 110 μ m in B, C.

Before NCSC induction via dual SMAD inhibition, dissociated single cells hiPSCs were re-plated on GelTrex-coated 12-well plates in mTeSR-1 medium supplemented with Rock inhibitor Y-27632 as described in section 3.3.1. The spiky single cells began to form star shaped small colonies, which is typical for Rock inhibitor cultivation (Figure 4-1 B) 24 hours after accutase passaging. After 48 hours, cells were switched from mTeSR-1 media to KSR media containing Noggin and SB431542.

NSB sample: After two days, cells treated with Noggin and SB431542 (NSB) showed morphological distinctions from hiPSCs (fibroblast-like cell bodies formed loosened colonies with undefined borders where single cells evolved from; shown in Figure 4-2 A). Stable survival of cells under new cultivation conditions might have arisen by differentiation towards NC fate (as mentioned in section 1.2.2 activation of Snail inhibits apoptosis; shown in Figure 4-2 B). Elevated cell proliferation was indicated by raised metabolism (yellow color change of the media) and high cell density observed on day 5 (data not shown). In addition, high cell density led to 3-dimensional cell growth forming clusters from which various morphological cell types developed (clusters of epithelial-like cell bodies; indicated by white arrows in Figure 4-2 B-C). On day 12, a complete overgrown 3-dimensional heterologous cell plate was yielded (Figure 4-2 C).

NSB control sample: Regarding the fact that hiPSCs are very sensitive to any changes concerning cultivation conditions, untreated hiPSCs were exposed to higher selection pressure compared to NSB samples. This was marked by high cell death followed by low cell density through media switch from mTeSR-1 media to KSR and N2 media (Figure 4-2 a, and b) until day 9. Different cell types with different cell morphology were also observed on day 5 (fibroblast-like as well as epithelial-like cell bodies; indicated by white arrows in Figure 4-2 B-C). From day 9, cell growth was stable and cells also grew in 3-dimensional heterologous cell clusters (indicated by white arrows in Figure 4-2 c). The heterologous cell types growing in 3-dimensional clusters were similar to the NSB sample on day 12 (Figure 4-2 C and c).

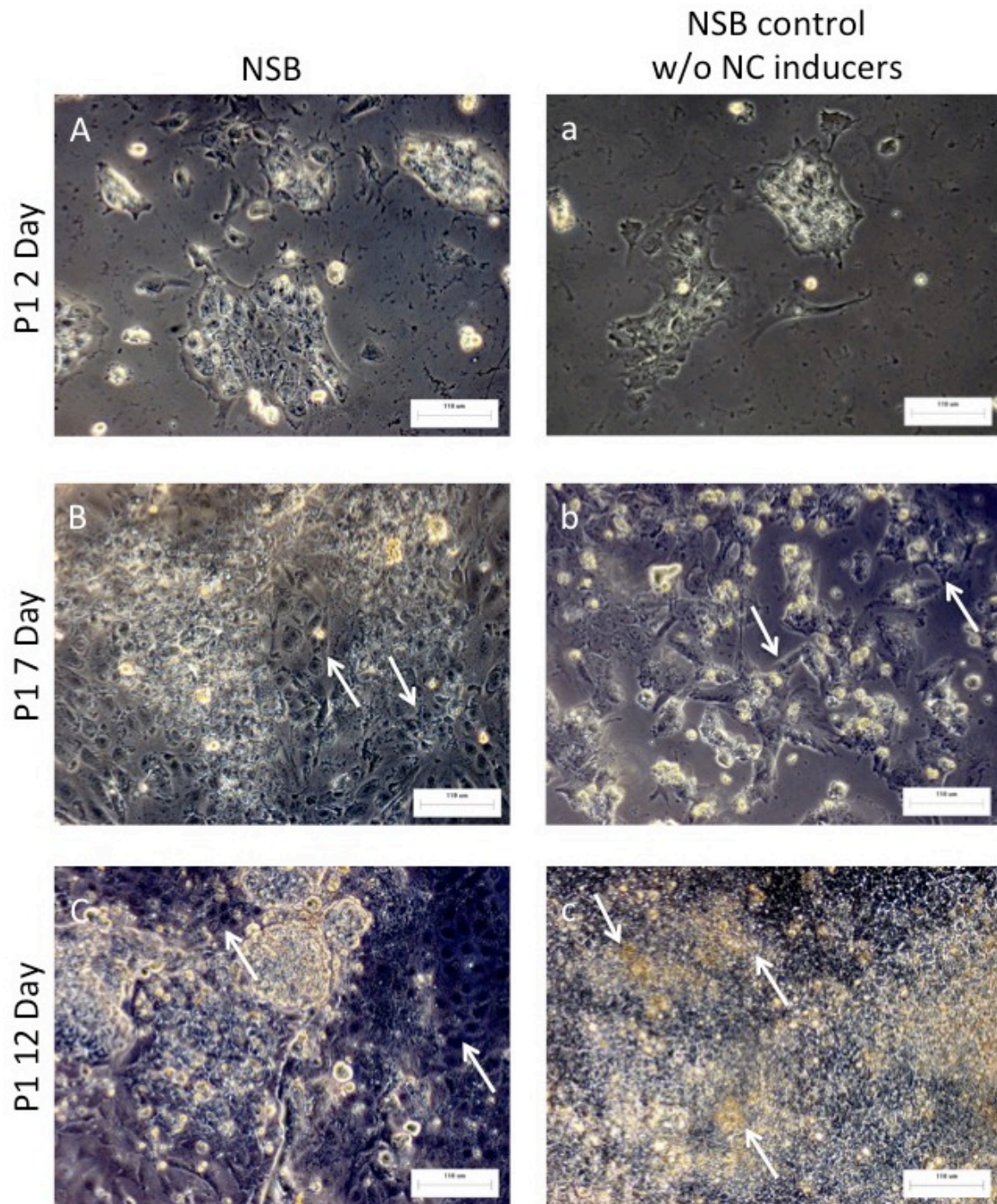


Figure 4-2: (A-c) Morphological change of hiPSC to NCSC during 12 days of differentiation induced by dual SMAD inhibition.

(A) NSB treated cells and (a) untreated NSB control cultivated in KSR media on the second day of differentiation protocol. (B) NSB and (b) untreated NSB control w/o NC inducers exposed to 50 % KSR and 50 % N2 media on the 7th day. (C) NSB and (c) untreated control maintained in N2 media on the 12th day of NCSC differentiation, documented by phase contrast microscopy. All pictures are shown in 20 × magnification. Scale bar = 110 μm in all pictures.

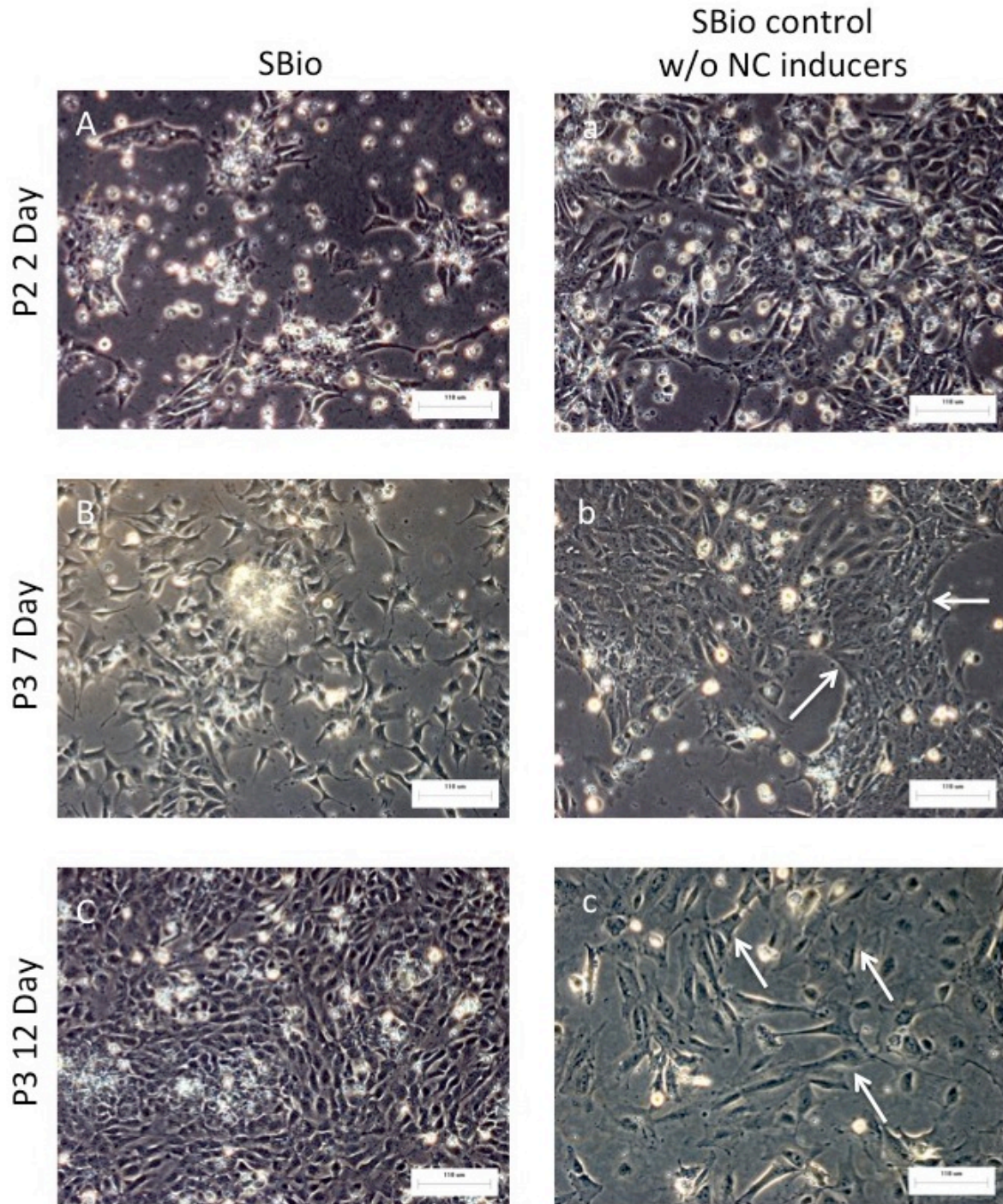


Figure 4-3: (A-c) Morphological change of hiPSCs to NCSC during 12 days of differentiation induced by SMAD-2/-3 inhibition and activation of canonical WNT signaling.

(A) SBio cells and (a) untreated SBio control cells after EDTA passage on the second day, (B) SBio cells and (b) untreated control cells after second EDTA passage on the 7th day and (C) SBio and (c) untreated SBio control cells after 12 days of NCSC differentiation, documented by phase contrast microscopy. All pictures are shown in 20 × magnification. Scale bar = 110 µm in all pictures.

The cell amount for the NCSC differentiation protocol according to L. Menendez was by a factor of ten higher (section 3.3.2) than the cell amount applied for the dual SMAD inhibition method (section 3.3.1). As a result NCSC differentiation was induced at very high cell density (Figure 4-1 C). Another difference to the dual SMAD method was further application of hiPSC conditioned media (StemPro) but without Activin A termed defined conditioned media (DC-media). Differentiation of hiPSCs towards NCSC-lineage was conducted under iPSC conditioned media without Activin A containing SB 431542 and (2'Z, 3'E)-6-bromoindirubin-3'-oxime (BIO).

SBio sample: Cell proliferation of SBio treated cells was very high allowing EDTA passage (section 3.3.2) to be performed on the second day of NCSC differentiation (Figure 4-1 C). Fibroblast-like SBio treated cells still grew in clusters (indicated by white arrows in Figure 4-3 A), which was observed 8 hours after passaging. Surprisingly, after the second cell passage on day 5 (Figure 4-3 B) the majority of cells grew as single cells and only a few loose cell clusters were observed. On the last day of NCSC differentiation, a high yield of cells was harvested (Figure 4-3 C).

SBio control sample: Cell growth of untreated hiPSCs resembled growth behavior of SBio samples but had a slightly lower growth rate after EDTA passage on the second day (Figure 4-3 a). The major difference to the SBio sample was monitored after the third cell passage on day 7, where cell survival was rigorously reduced for untreated hiPSCs. These cells tend to grow in clusters in contrast to the single growing SBio treated cells (indicated by white arrows in Figure 4-3 b). On day 12, the few cells that survived appeared in fibroblast-like structures forming cell clusters, which seemed flatter compared to the SBio sample (indicated by white arrows in Figure 4-3 c).

4.1.2 Characterization of NCSCs by analyzing NCSC markers on mRNA level, ICC staining, FACS analysis and Real Time PCR

Characterization of NCSCs was not based on one marker, but on a combination of different markers. To analyze, which of the NCSC differentiation experiments resulted in an improved yield of NCSC-like cells, reverse transcription PCR for different markers was carried out for qualitative analysis, while ICC staining and FACS analysis of late NCSC markers HNK1 and p75 served for quantitative evaluation. Finally, a real time PCR for the markers HNK1 and p75 was conducted to investigate if the obtained results comply with the results obtained from previously mentioned methods.

4.1.2.1 Comparison of NCSC markers expression on mRNA level after NCSC differentiation of both methods

Reverse transcription PCR was performed with mRNA isolated after 12 days of NC differentiation. Isolated mRNA proofed that the respective gene expression occurred in these cells and was further converted into cDNA as described in section 3.4.2. Each experiment was performed in triplicate and mRNA was isolated from NSB treated cells, untreated control cells (termed NSB control) and SBio cell samples. Due to low cell survival of SBio-untreated control cells (defined as SBio control sample), only one sample of three experimental approaches could be gathered. The mRNA of undifferentiated hiPSC was extracted to analyze in what extend treated cells changed their expression pattern for different markers compared to their pluripotent origin. MSC functioned as control due to their expression of some of the investigated markers. With respect to the origin of S462 cells, it was still expected that some genes of NCSC markers might be active (section 3.2.1.4).

Figure 4-4 A-B represents the PCR products from the samples mentioned above. Appearance of β -*ACTIN* cDNA fragments was qualitatively detected by the presence of bands, revealing that PCR succeeded for all samples, shown in Figure 4-4 A.

Examination of the neural plate border genes *PAX3* and *MSX1* showed strong expression in all NSB samples, NSB controls, S462 sample and MSC sample. This assumption was conducted by the occurrence of a large intense band from each sample. Only samples of isolated mRNA from the 12th days of NCSC differentiation (2.SBio, 3.SBio and 3.SBio control) showed strong expression of the *MSX1* gene, while these cells expressed lower *PAX3* gene, which was notable by a faint band (Figure 4-4 B). For SBio FACSorted cells low expression for both neural plate border genes was detected, whereas no signal was observed in hiPSCs cells (Figure 4-4 A-B).

Early NCSC marker expression of *SOX9*, *SNAIL* and *SLUG* were discovered in all samples and their respective controls of both NCSC differentiation methods, except for the 1.SBio FACSorted sample which only expressed the gene *SLUG*. S462 cells evidenced signals for *SOX9* and *SLUG* expression, but no signal for *SNAIL*, whereas MSCs solely expressed gene *SLUG*; and hiPSC was only positive for the gene product *SNAIL*.

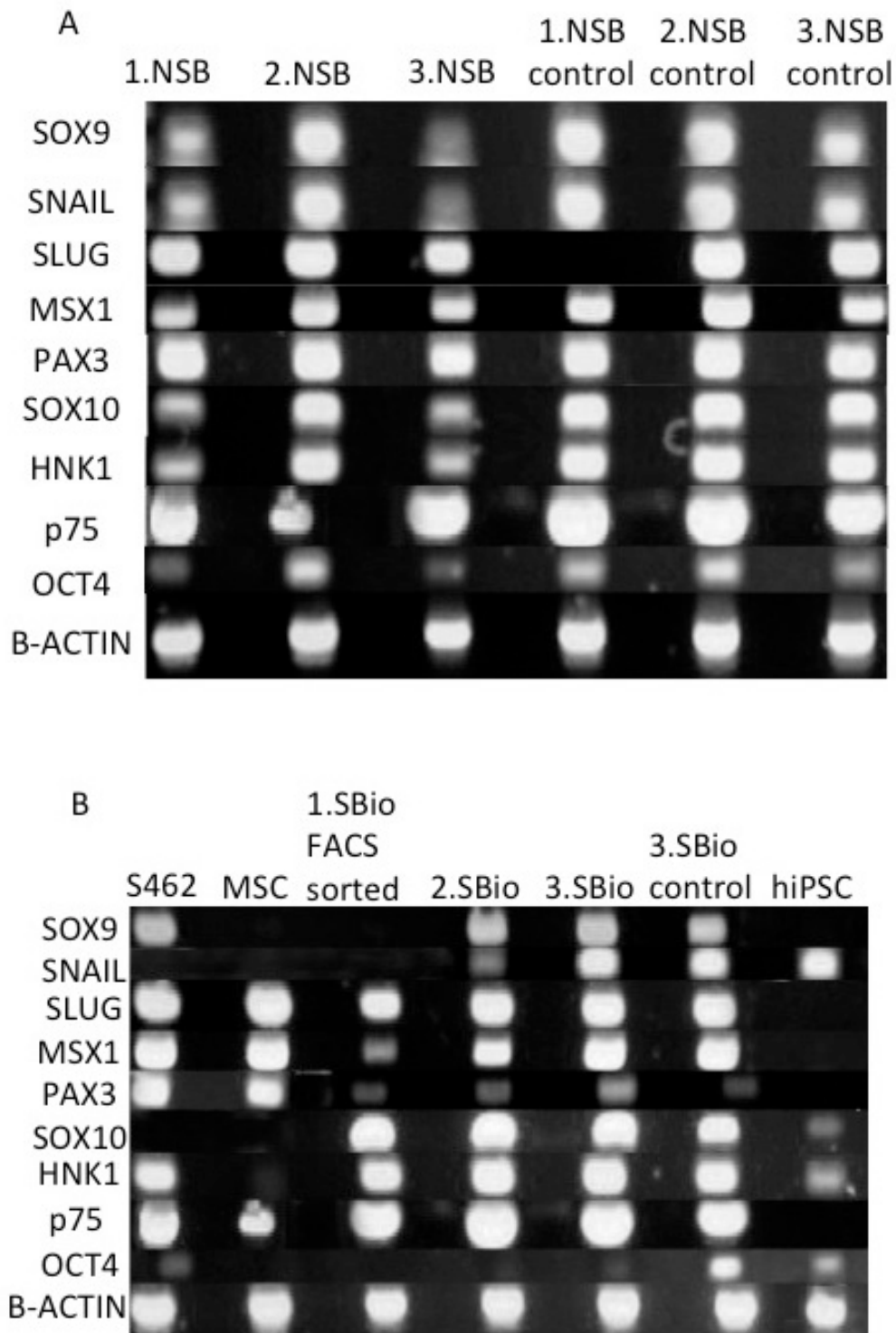


Figure 4-4: Exemplary demonstration of separated PCR products of neural plate border-, early NCSCs-, late NCSCs-markers, Oct4 and β -Actin through gel electrophoresis in a 1 % agarose gel.

Ten different RT-PCR products of seven approaches of cDNA (A) NSB samples, their respective control samples w/o NC inducers, (B) S462, MSC, SBio samples, their related control samples w/o NC inducers and hiPSC were loaded on gel.

All samples and related controls of both NCSC differentiation experiments, including the 1.SBio FACSorted sample were positive for both late NCSC markers *HNK1* and *p75* as well as for *SOX10*, which indicates migratory NC cells (Hari et al. 2012; Britsch et al. 2001). However, it has to be mentioned that the cDNA bands of all late NCSC markers for the NSB control samples were stronger compared to that of treated NSB samples (see Figure 4-4 A). S462 expressed only the genes *HNK1* and *p75*, while MSC displayed a signal for *p75* marker; and in hiPSCs low expression of *SOX10* and *HNK1* was monitored.

As expected, the pluripotent cell marker *OCT4* was active in hiPSCs. Surprisingly, a clear signal for this marker also appeared in all NSB samples, NSB controls, SBio control as well in S462 cells. In 2.SBio and 3.SBio cells expression of *OCT4* still occurred in a lower extent, but was not further active in 1.SBio FACSorted and MSCs (Figure 4-4 A-B).

4.1.2.2 ICC staining for HNK1 and p75

Immunofluorescence staining was performed to identify and quantify NC-like cells obtained from NSB and SBio treatment by the presence of the late NCSC markers HNK1 and p75. Analysis of stained NSB and SBio samples was carried out with Columbus Image Data Storage and Analysis System (see section 3.4.6). Figure 4-5 A-F shows cells after 12 days treatment with NSB, while SBio treated cells are displayed in Figure 4-5 a-f. In Figure 4-5 A, a cells are presented as brightfield, in B, b the DAPI stained nuclei are shown, while C, c and D, d visualize surface receptor HNK1 and surface receptor p75, respectively. Both surface markers are shown in E, e and all markers are displayed in F, f. Due to approximately 80 - 90 % cell loss of NSB samples, which occurred during the staining process (section 3.4.5), the analysis for NSB treatment was not significant. However, a minor population of remaining NSB cells were positive for p75 (Figure 4-5 D), but only a few cells showed expression for the HNK1 marker (indicated as low signal; shown in Figure 4-5 C) resulting in the detection of some HNK1⁺p75⁺ cells (Figure 4-5 F). In contrast, the majority of SBio cells were positive for the surface receptor HNK1 (Figure 4-5 c) as well as for p75 (Figure 4-5 e) leading to a high amount of HNK1⁺p75⁺ cells shown in Figure 4-5 e. The calculated percentage of double positive cells for NSB and SBio cells are shown in Figure 4-6 A. Combinational treatment with SB431542 and BIO led to a mean value and standard deviations (MV ± Std) of 68.22 ± 11.2 % cells, which expressed both surface receptors HNK1 and p75, while from

residual NSB cells, the MV of double positive cells for both NCSC surface markers was only 13.68 ± 4.91 %.

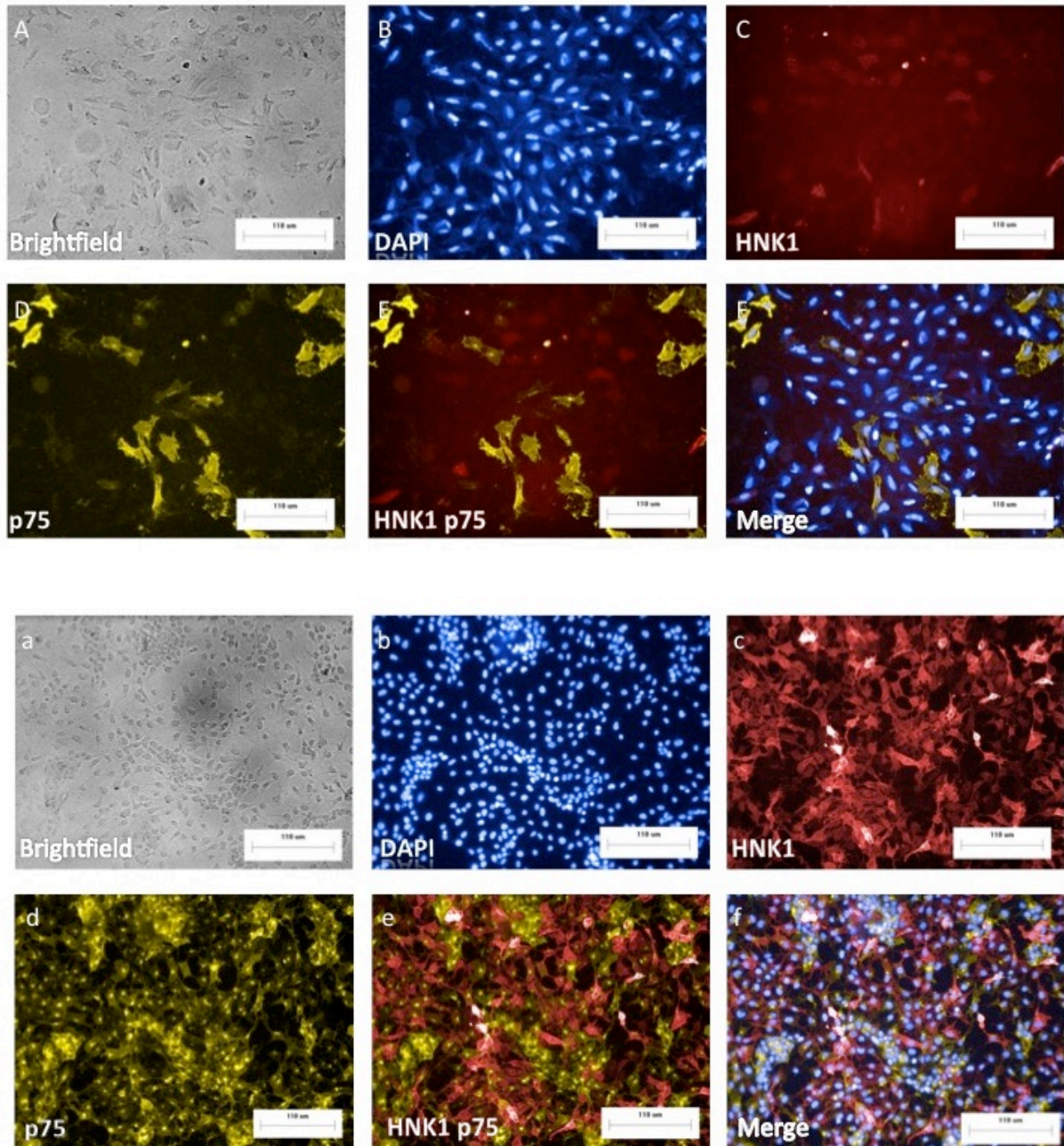


Figure 4-5: Exemplary fluorescence pictures of ICC staining of NSB and SBio treated cells for NCSC marker.

(A-F) NSB and (a-f) SBio cells were immunofluorescently labeled with antibodies for HNK1 (C, c), p75 (D, d) and both markers are visualized in (E, e). (B, b) represents DAPI stained Nuclei and all markers are shown in (F, f). All pictures are shown in 20 x original magnification. Scale bar = 110 µm in all pictures.

Another method employed to quantify HNK1 and p75 double positive cells was FACS analysis. Each experiment was performed in triplicate, however, one experiment of the NSB experiment failed. Therefore the MV of only two measurements for NSB samples and related NSB controls were taken into account. For the SBio experiments, the MV of three experiments of SBio treated cells was calculated. But for the SBio controls (Figure 4-6 B, C) the MV of only two approaches were calculated, because cells of one SBio control could not be maintained in culture. The values of the NSB samples were very similar and yielded as $MV 7.4 \pm 1.8 \%$ of $HNK1^+p75^+$ cells, but unexpectedly, results of untreated NSB controls were divergent. The first measurement of untreated NSB control yielded 9.03% $HNK1^+p75^+$ cells, while the second analysis detected 24.7% $HNK1^+p75^+$ positive cells ($MV 16.86 \pm 11.08 \%$). The MV of $HNK1^+p75^+$ population from SBio treatment was $35.2 \pm 18.24 \%$, while the MV of untreated SBio cells was $8.40 \pm 4.53 \%$. FACS-analysis detected that our hiPSCs cell line was also positive for the surface receptor HNK1 with 98% , shown in Figure 4-6 D.

To obtain a highly enriched pure NCSC-like cell population, SBio cells were sorted for both NCSC markers $HNK1^+$ and $p75^+$. These 1.SBio cells were already in passage 32 (117 d). Figure 4-7 depicts representative FACS plots of treated SBio cells. FACS analyzed 47.7% (Figure 4-7 A) double positive cells for HNK1 and p75 of 1.SBio cells. Cell sorting was carried out to high purity (94.6%), which was confirmed by Re-FACS analysis (Figure 4-7 B). Repeated cell sorting after 7 days of cell expansion verified that only 65.9% of these FACSorted SBio cells showed expression of both NCSC markers ($MV \pm Std$ for each marker are presented in Figure 4-7 C).

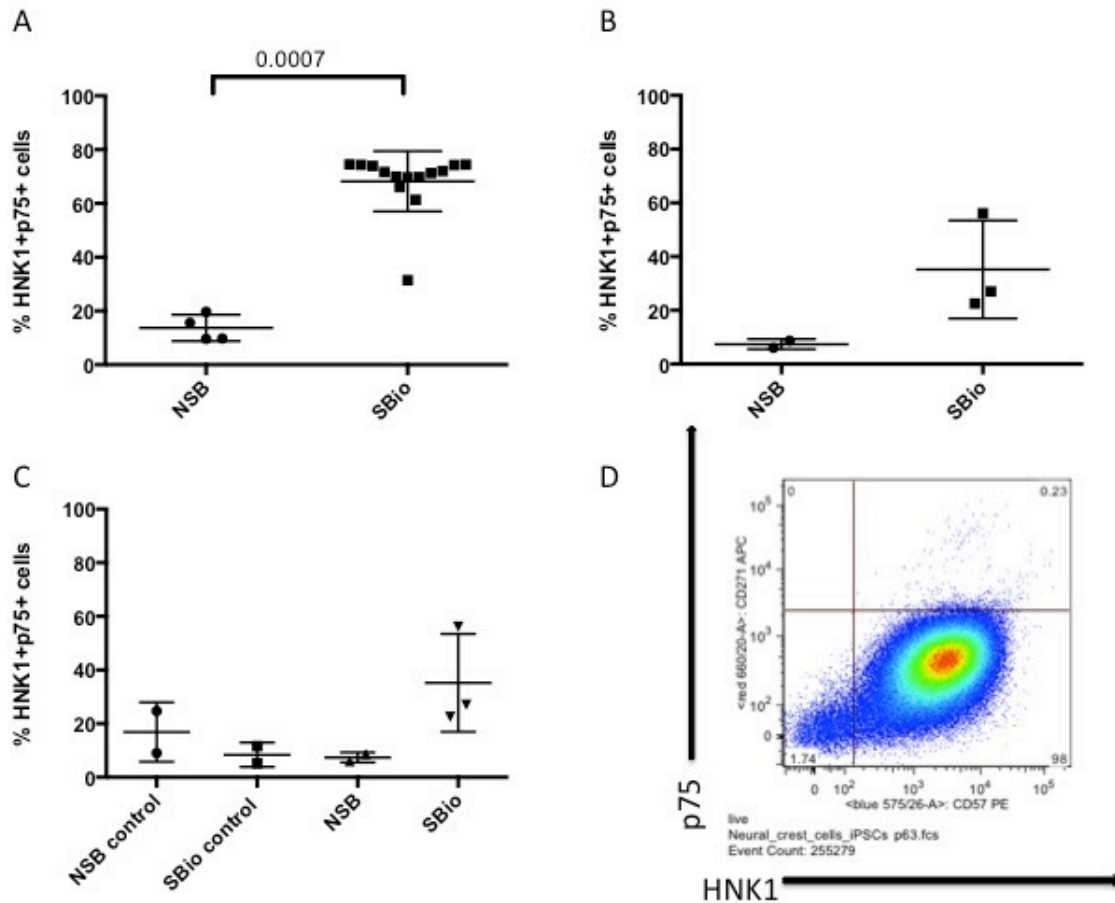


Figure 4-6: Expression of both surface receptors HNK1 and p75 in NSB and SBio treated cells.

(A) represents ICC staining of NSB (n=4) and SBio cells (n=14)(B,C) shows FACS analysis (B) of NSB (n=2) and SBio cells (n=3), while (C) compares NSB control (n=2) with NSB (n=2) and SBio control (n=3) with SBio cells (n=3) for concomitant expression of HNK1 and p75 by FACS analysis. (D) presents a dot plot of FACS analysis of undifferentiated hiPSCs for HNK1 and p75 surface markers. Statistical analysis between groups was performed using Mann-Whitney U test, parameters within one group were compared by Wilcoxon test. Data are presented as mean values, with error bars representing standard deviations.

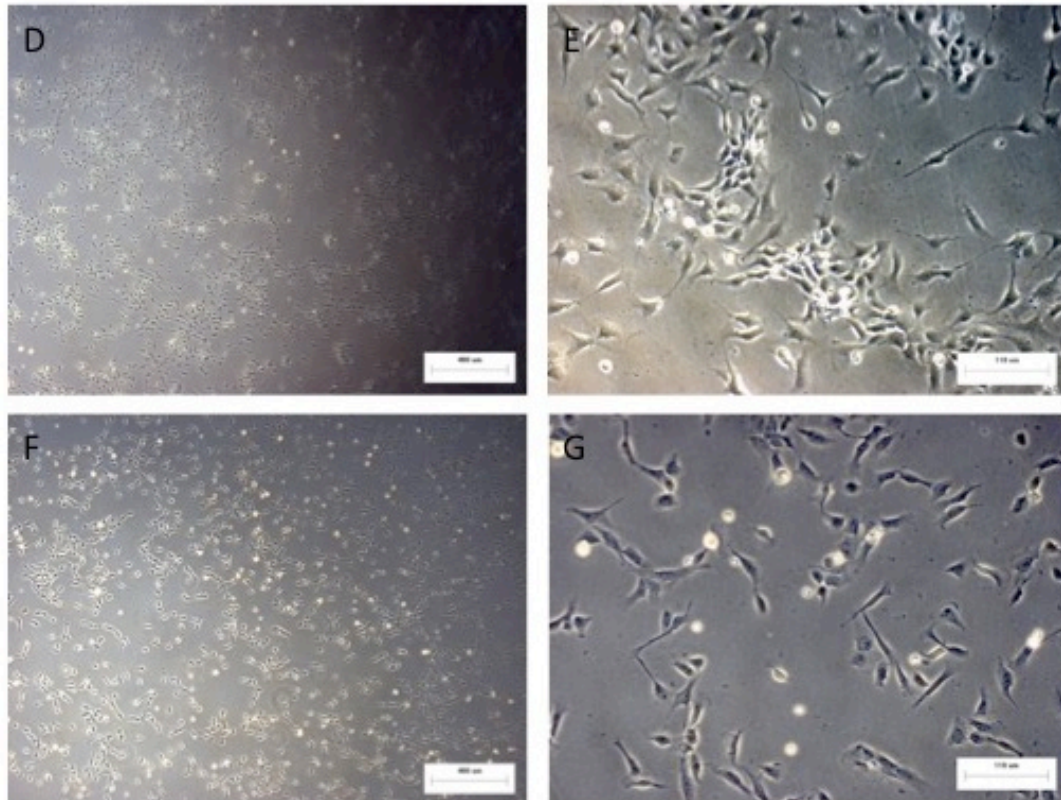
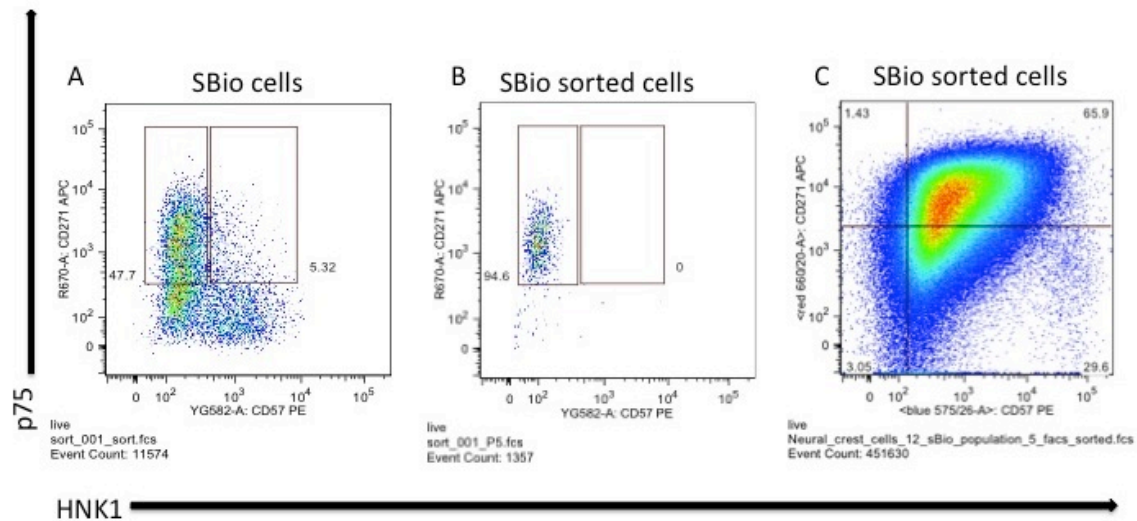


Figure 4-7: FACS based characterization of HNK1 and p75 double positive SBio cells.

(A) displays 47.7 % HNK1+p75⁺ FACS sorted SBio cells. (B) Re-FACS analysis reveals high purity cell sort for both markers with 94.6 %. (C) shows percentage for both NCSC markers of SBio FACS sorted cells after 7 days expansion. (D-E) displays morphology of unsorted SBio cells, while (F-G) demonstrates morphology of FACSsorted SBio cells, documented by phase contrast microscopy. (D and F) pictures are shown in 5 × magnification, while (E and G) are presented in 20 x magnification. Scale bar = 400 μm in D, F and scale bar = 110 μm in E, G.

4.1.2.3 Comparison of Real time PCR with ICC data for p75 and HNK1

Surprisingly, real time PCR indicated that relative transcript level of mRNA products of HNK1 isolated from SBio samples was only 10.68 (MV = 9.33 ± 3.92) times increased compared to untreated SBio controls, while relative transcript levels of mRNA products of p75 were 220.36 (MV = 472.5 ± 761) higher than in untreated cells (Figure 4-8 A).

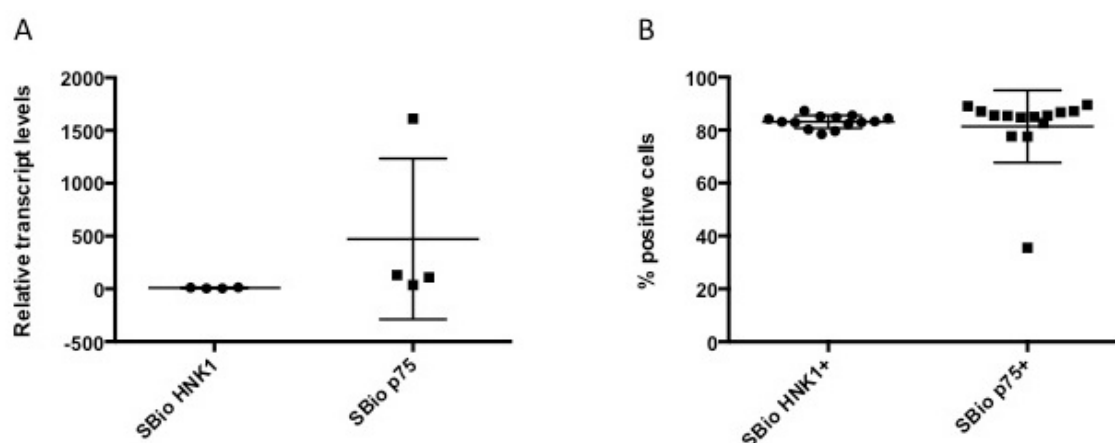


Figure 4-8: Evaluation of HNK1 and p75 in SBio cells by Real time PCR analysis and ICC staining

Percentage of HNK1 and p75 received by (A) Real time PCR based on mRNA level (n=4) and (B) ICC staining of the surface markers (n=14) in SBio cells. Statistical analysis between groups was performed using Mann-Whitney U test, parameters within one group were compared by Wilcoxon test. Data are presented as mean values, with error bars representing standard deviations.

These results contradict analysis received from the ICC evaluation, where intensity of SBio cells showed that 83.16 ± 2.42 % were positive for the HNK1 receptor and 81.36 ± 13.66 % for the p75 receptor. The MV \pm Std for each receptor in SBio samples obtained from real time PCR analysis is shown in Figure 4-8 A and MV \pm Std obtained from ICC evaluation is presented in Figure 4-8 B.

According to our results obtained by ICC and FACS analysis, hiPSCs treated with SB431542 BIO showed higher yield of NC-like cells compared to hiPSCs treated with Noggin SB431542.

4.2 NCSC multipotency proofed by induced osteogenic differentiation

NCSCs are a transient multipotent cell population, derived from the neural ectoderm in vertebrate embryos. This unique population possesses the ability to evolve into various types of cell lineages. To characterize the developmental potential of hiPSC-derived sorted HNK1⁺p75⁺ cells obtained from SB431242, BIO treatment was the next step of this experiment. Therefore a standard osteogenic differentiation protocol for MSCs was performed with the hiPSC-derived sorted HNK1⁺p75⁺ population. Additionally concomitant osteogenic differentiation with MSCs and hEpi-NCSCs was carried out to function as a comparison to the SBio and SBio FACSorted cells. Figure 4-9 A-E shows the mineralization process of SBio cells, Figure 4-10 A-E of SBio FACSorted cells, Figure 4-11 A-E of MSCs and Figure 4-12 A-E of hEpi-NCSCs during a time period of 28 days. Their respective controls cultivated under non-osteogenic conditions were marked in small letters (a-e).

SBio osteo sample: During the first two weeks, no change in morphology was observed and cells continued to proliferate, even an increased cell death rate was observed (Figure 4-9 A-C). After two weeks cell aggregates developed and mineralization process started, indicated by light opaque cell aggregates (indicated by white arrows in Figure 4-9 C), which developed into a thick dark layer onto the cell layer (indicated by black arrows in Figure 4-9 D). After 4 weeks, matrix layers were distributed through the whole plates that appeared dark, opaque (indicated by black arrows in Figure 4-9 F).

SBio control sample: High cell loss was observed during the first two weeks (Figure 4-9 a-c). After three weeks cells regenerated and grew as 3-dimensional clusters forming cell aggregates (indicated by black arrows in Figure 4-9 d). A thick light opaque layer on the cell layer was monitored, which started to get connected by filaments with each other after 4 weeks (indicated by black arrows Figure 4-9 e).

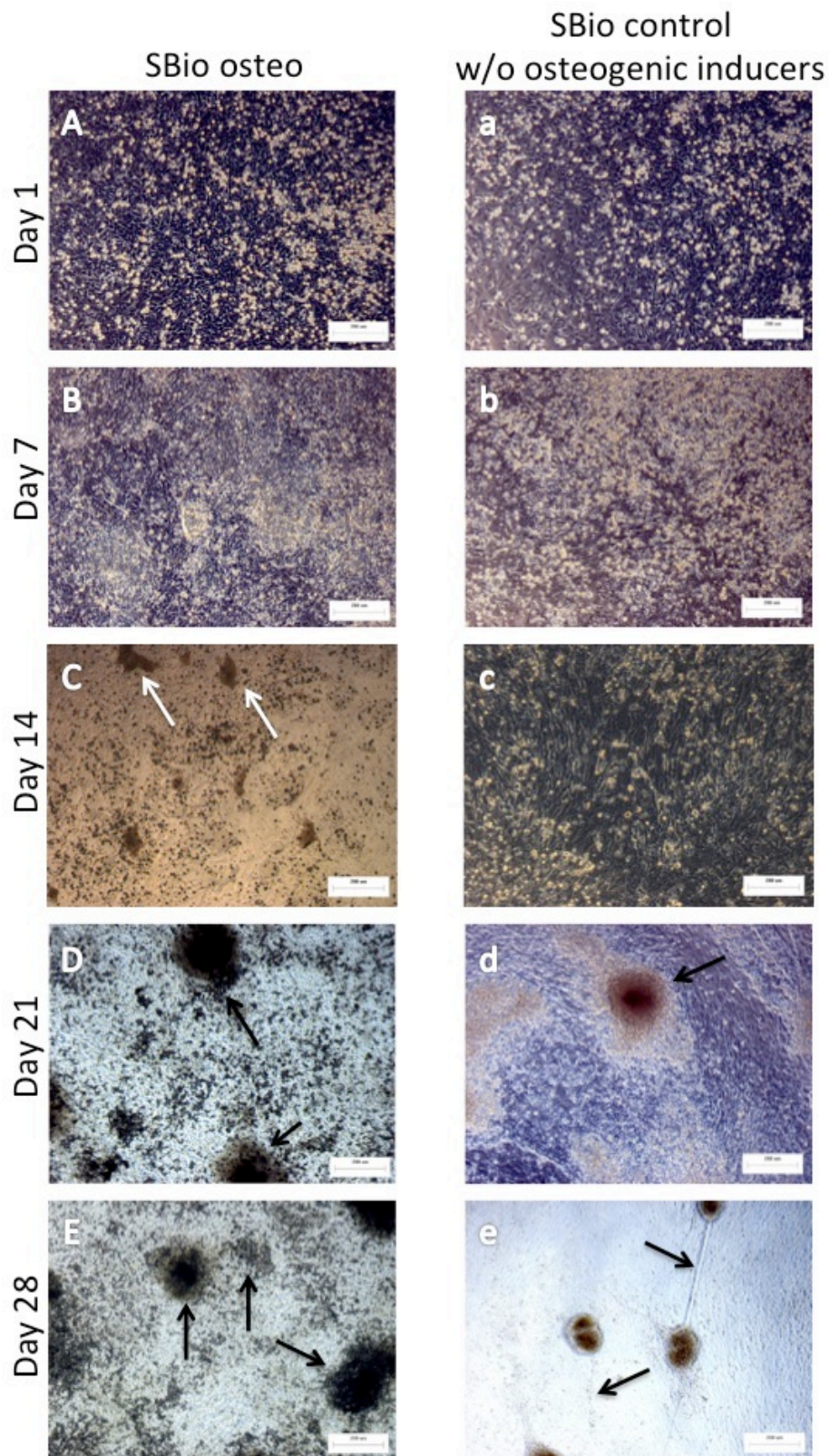


Figure 4-9: Morphological changes of SBio cells during osteogenic differentiation

Morphological alterations during osteogenesis documented by phase contrast microscopy over a time period of 28 days. (A-E) SBio cells cultivated in osteogenic media, while (a-e) SBio cells supplemented in non-osteogenic media. All pictures are shown in 10 × magnification. Scale bar = 200 μm in all pictures.

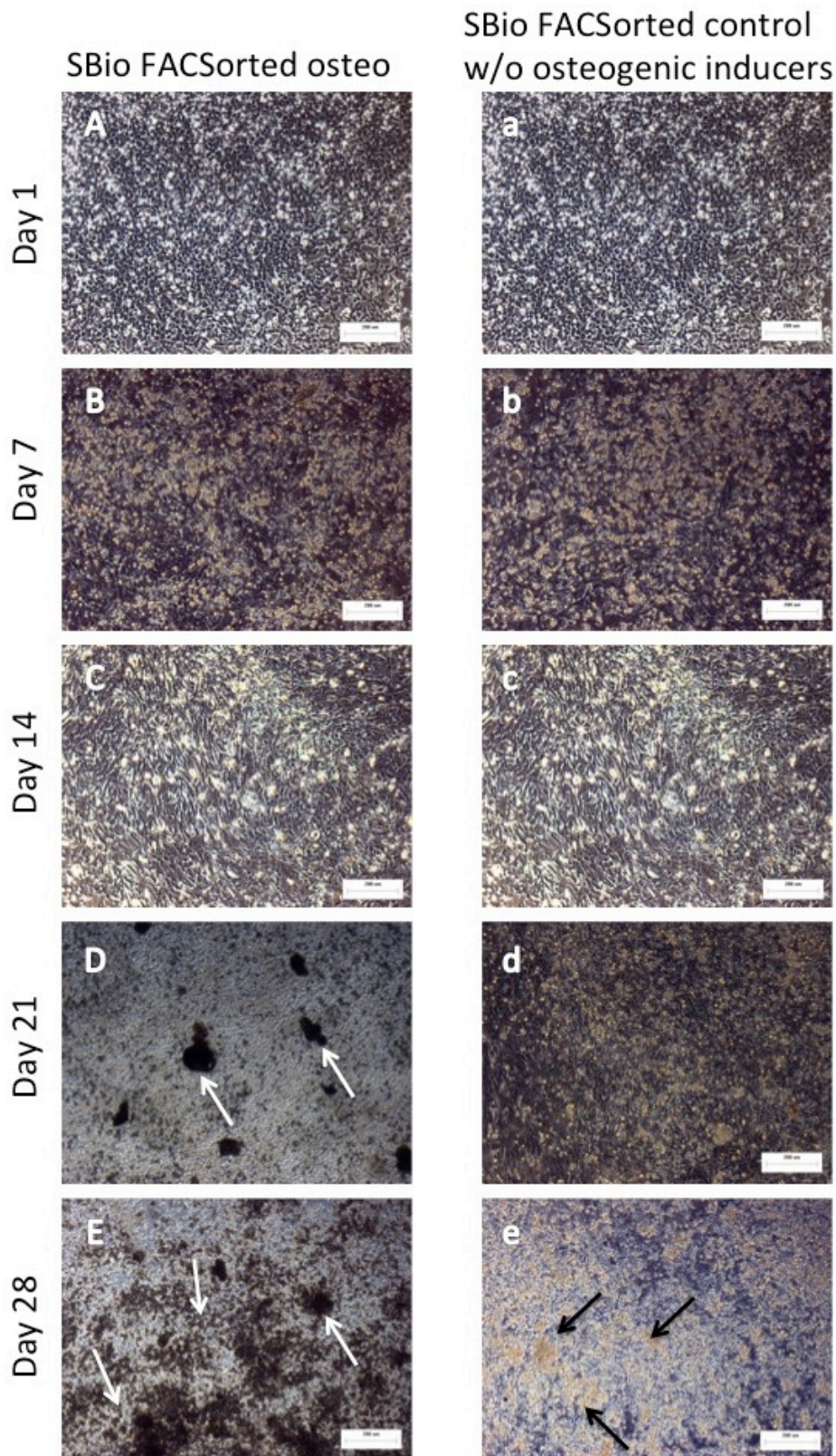


Figure 4-10: Morphological changes of SBio FACSsorted cells during osteogenic differentiation

Morphological alterations during osteogenesis documented by phase contrast microscopy over a time period of 28 days. (A-E) SBio FACSsorted cells cultivated in osteogenic media, while (a-e) SBio FACSsorted cells supplemented in non-osteogenic media. All pictures are shown in 10 × magnification. Scale bar = 200 µm in all pictures.

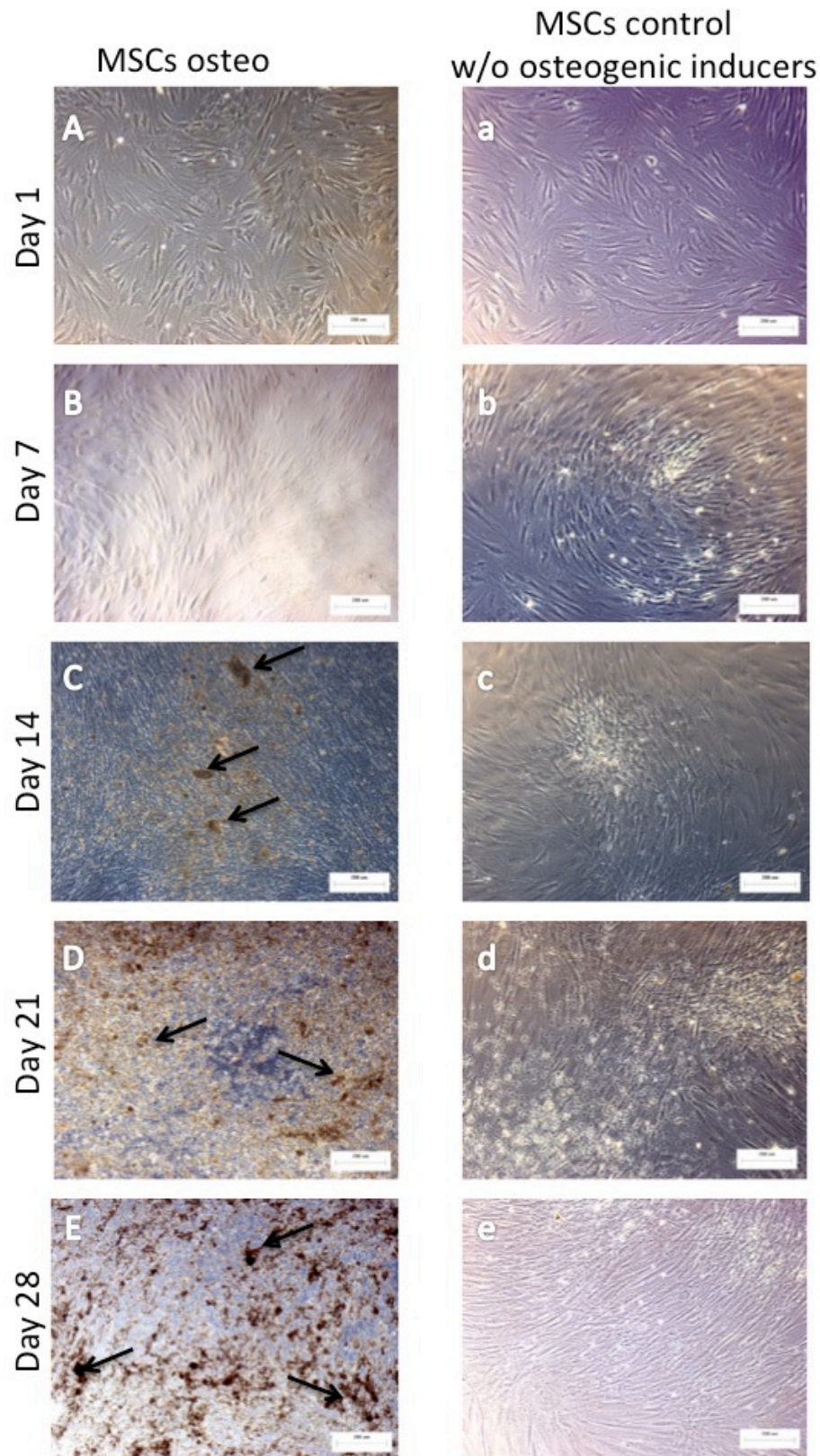


Figure 4-11: Morphological changes of MSCs during osteogenic differentiation

Morphological alterations during osteogenesis documented by phase contrast microscopy over a time period of 28 days. (A-E) MSCs cultivated in osteogenic media, while (a-e) MSCs supplemented in non-osteogenic media. All pictures are shown in 10 × magnification. Scale bar = 200 µm in all pictures.

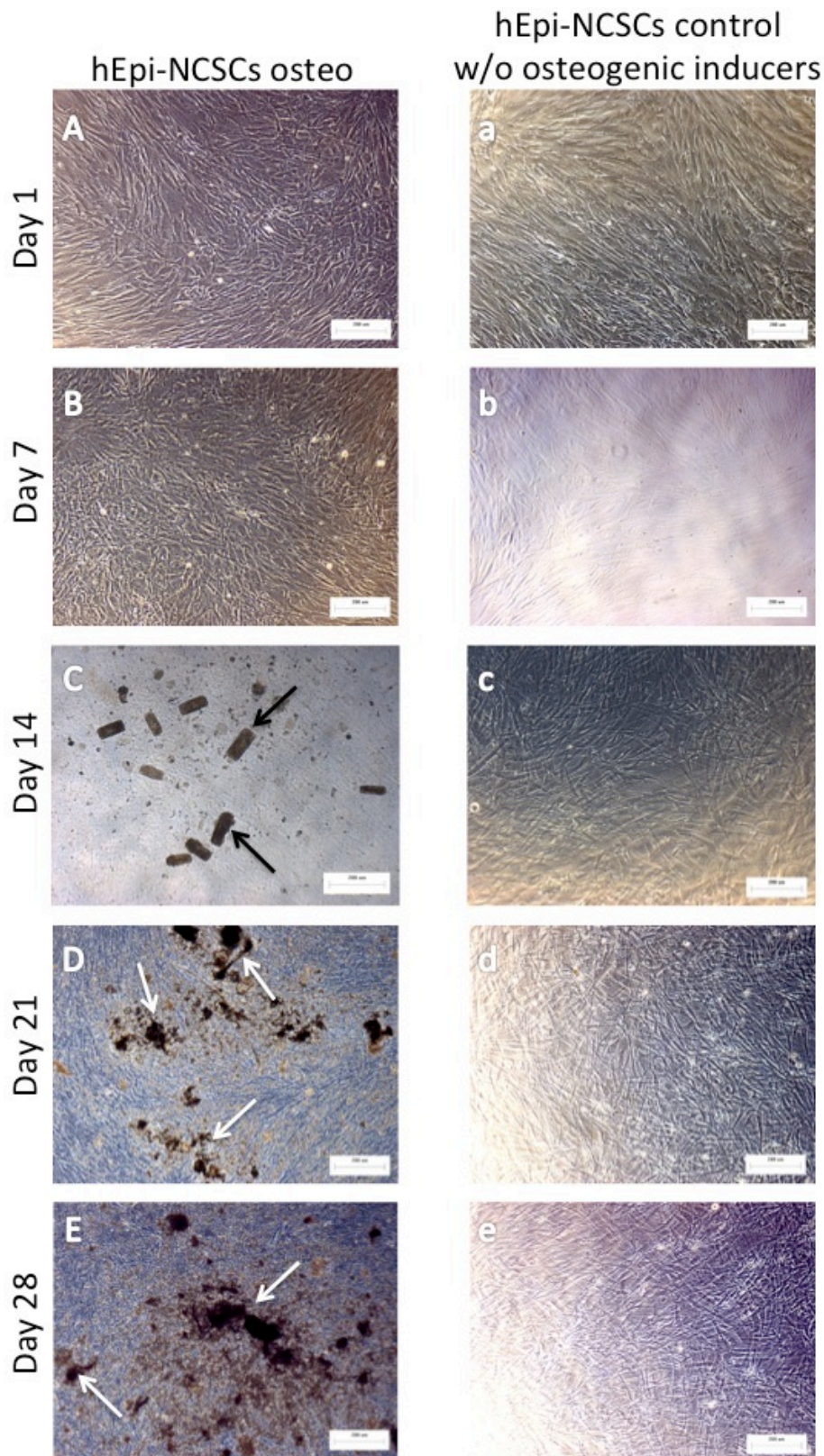


Figure 4-12: Morphological changes of hEpi-NCSCs cells during osteogenic differentiation

Morphological alterations during osteogenesis documented by phase contrast microscopy over a time period of 28 days. (A-E) MSCs cultivated in osteogenic media, while (a-e) MSCs supplemented in non-osteogenic media. All pictures are shown in 10 × magnification. Scale bar = 200 µm in all pictures.

SBio FACSorted osteo sample: Cells proliferated even though high cell loss was observed for the first two weeks (Figure 4-10 A-C). Cell density was very high from the beginning of the second week. Mineralization was monitored in the third week (indicated by white arrows in Figure 4-10 D), implied as dark, opaque deposits that unevenly spread at some areas of the well in the 4th week (indicated by white arrows in Figure 4-10 E).

SBio FACSorted control sample: Cell proliferation was monitored for the first two weeks leading to increased cell density (Figure 4-10 a-c). Compared to SBio FACSorted supplemented in osteogenic induction media, an extremely high cells loss was observed until the third week (Figure 4-10 d) and cells started to overgrow in cell layers in the 4th week (indicated by black arrows in Figure 4-10 e).

MSC osteo sample: There was no morphology change detected for the first two weeks for MSCs. However cells markedly decreased cell proliferation within the second week and morphological changes from small, spindle-like to large, flattened, cuboidal could be observed (Figure 4-11 C). Strong matrix development and a reduction in cell density were observed after three weeks (indicated by black arrows in Figure 4-11 C-D). After 4 weeks only a thick opaque matrix cell layer covered the whole area of wells and almost no cells could be detected (indicated by black arrows in Figure 4-11 E).

MSC control sample: Cells proliferated for the first 6 to 7 days until they reached confluence (Figure 4-11 a-c). Due to contact inhibition, cell growth was down-regulated and cells kept their characteristic small longitudinal fibroblast-like cell shape under proliferative conditions (Figure 4-11 d-e).

hEpi-NCSC osteo sample: hEpi-NCSCs proliferated for the first 7 days (Figure 4-12 A-C). In the second week cells began to secrete extracellular matrix (ECM), which resembled a rectangular form (indicated by black arrows in Figure 4-12 C). From all cell types, lowest calcified ECM formation was observed in hEpi-NCSCs, where ECM was only observed in the center of wells (indicated by white arrows in Figure 4-12 D-E) correlating with highest cell density within the culture vessel.

hEpi-NCSC control sample: Cell growth behavior of hEpi-NCSCs showed similar patterns compared to MSCs cultivated in non-osteogenic media. After cells were

confluent from the second week, cell proliferation was down-regulated due to contact inhibition and cells kept their longitudinal fibroblast-like cell shape (Figure 4-12 c-e).

4.2.1 Qualitative ALP staining and quantitative ALP activity assay

As previously mentioned ALP is a well-known osteoblast differentiation marker at an early stage. To verify the presence of ALP, NBT-BCIP staining was applied after one week of osteogenic differentiation (Figure 4-13 A-d). Additionally, ALP assay was performed, in which ALP hydrolyzed the p-nitrophenyl phosphate substrate to deliver the yellow colored end product p-nitrophenol that is photometric quantified (Figure 4-13 E-F). ALP staining with BCIP/NBT indicates that (A) SBio cells, (B) SBio FACSsorted cells, (C) MSCs, and (D) hEpi-NCSCs and their respective control are positive for the enzyme ALP, indicated by the indigo color change. As visible in Figure 4-13 A-D, ALP activity in SBio cells and their related untreated control seems to be stronger compared to SBio FACSsorted cells, MSCs, and hEpi-NCSCs. However, ALP staining of osteogenic stimulated MSCs and SBio FACSsorted cells appeared more intense compared to osteogenic induced hEpi-NCSCs. For each cell type, the correlated control sample cultivated in non-osteogenic media showed weaker indigo coloration compared to their osteogenic treated sample. This observation correlates to the measured ALP activity measurements presented in Figure 4-13 E-F. SBio cells showed highest ALP activity with a MV of 0.11 ± 0.01 U/ μ l, indicating that these cells tend to differentiate towards osteogenic differentiation. MV of ALP activity in their untreated control sample was 0.04037 ± 0.01304 U/ μ l. ALP activity in MSC osteogenic induced cells is 10 times lesser (MV 0.01530 ± 0.01235 U/ μ l) than in SBio osteogenic induced cells. MSC untreated cells (MV 0.005153 ± 0.001940 U/ μ l) and SBio FACSsorted cells supplemented in osteogenic media (MV 0.006153 ± 0.001468 U/ μ l) possess half of the ALP activity of MSC osteogenic induced cells. hEpi-NCSC supplemented in mineralization media (MV = 0.002739 ± 0.001720 U/ μ l) showed half of ALP activity than all other previously mentioned samples and untreated hEpi-NCSCs had an ALP activity MV of 0.001554 ± 0.002142 U/ μ l. The lowest ALP activity was measured in untreated FACSsorted SBio cells with a MV of 0.0007346 ± 0.0006583 U/ μ l. The difference of ALP activity in SBio cells ($p=0.0022$), SBio FACSsorted cells ($p=0.0022$), MSCs ($p<0.0001$) cultivated in mineralization media is significant in relation to their respective untreated control sample (Figure 4-13 E).

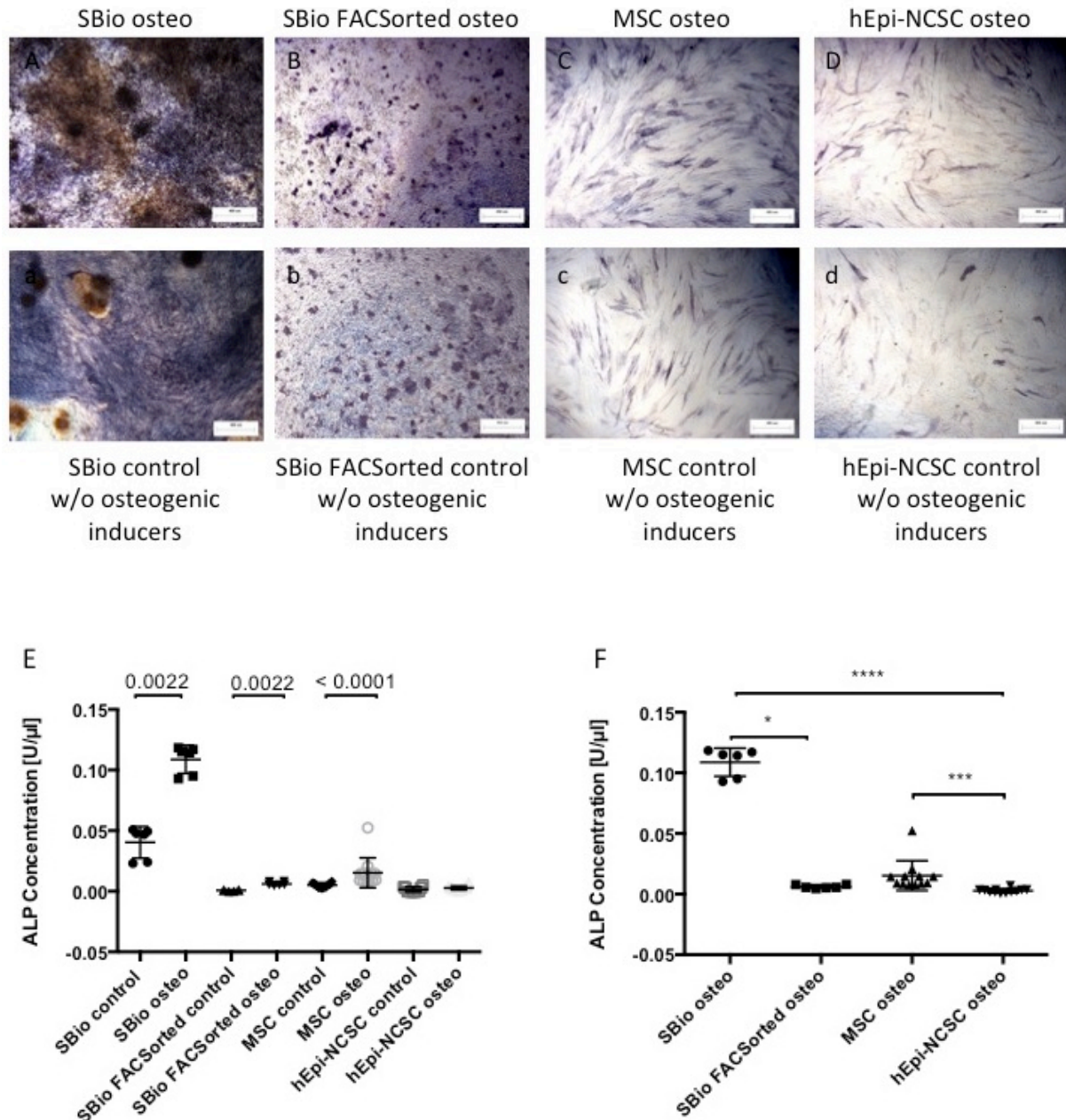


Figure 4-13: Osteogenic differentiation of SBio cells, SBio FACSsorted cells, MSCs and hEpi-NCSCs after 7 days cultivation represented by positive Alkaline phosphatase staining and Alkaline phosphatase activity analysis.

(A) SBio cells, (B) SBio FACSsorted cells, (C) MSCs and (D) hEpi-NCSCs compared to their respective control (a-d). All pictures were documented by phase contrast microscopy and are shown in 5 × magnification. Scale bar = 400 μm represents in all pictures. (E) displays absorption of p-Nitrophenol of SBio cells (n=6), SBio FACSsorted (n=6), MSCs (n=12) and hEpi-NCSCs (n=12) in relation to corresponding untreated control. (F) shows comparison of degraded pNPP absorption of osteogenic induced cells from each cell type. Statistical analysis between groups was performed using Mann-Whitney U test, parameters within one group were compared by Wilcoxon test. Data are presented as mean values, with error bars representing standard deviations, *p<0.012, ***p<0.0001.

In addition, there was a significant difference in ALP activity between osteogenic induced SBio cells ($p < 0.012$) and osteogenic induced SBio FACSsorted cells (Figure 4-13 F). Moreover, osteogenic induced SBio cells ($p < 0.0001$) and osteogenic induced MSCs ($p < 0.0001$) showed significant difference in ALP activity compared to osteogenic induced hEpi-NCSCs (Figure 4-13 F). These results led to the assumption, that SBio cells incline more towards osteogenesis, followed by MSCs, SBio FACSsorted cells, while less mineralization is expected in hEpi-NCSCs.

4.2.2 Alizarin red staining

Osteogenic differentiation was compared in 28-days cultures of (A) SBio cells, (B) SBio FACSsorted cells, (C) MSCs and hEpi-NCSCs cultured in mineralization media and compromised to their relevant untreated control (Figure 4-14 a-d).

As shown in Figure 4-14 A-D, strong Alizarin staining of mineralized matrix occurred only in osteogenic treated cells, while no staining was observed in their respective control (Figure 4-14 a-d). To estimate intensity of stained calcified ECM, discoloration of Alizarin red was carried out with Cetylpyridiniumchlorid and measured at 562 nm. Figure 4-14 E depicts the compromise between osteogenic induced cells in relation to their accordant untreated control, whereas Figure 4-14 F compares the osteogenic induced samples among themselves.

The results obtained from the ALP assay correlate to the results of Alizarin red staining presented in Figure 4-14. Cell aggregates on SBio osteogenic induced cells were stained dark red (Figure 4-14 A), while no coloration was observed on non-osteogenic treated cell aggregates (Figure 4-14 a). Similar patterns of mineralization was also detected on SBio FACSsorted cells, MSCs, hEpi-NCSCs (Figure 4-14 B-D) cultivated osteogenic, indicated by dark red staining. Respective controls supplemented in non-osteogenic media remained unstained (Figure 4-14 b-d). Highest Alizarin red absorption was detected in SBio ($MV = 1.733 \pm 0.4651$) cells, followed by MSC ($MV = 1.146 \pm 0.3175$), and hEpi-NCSC ($MV = 0.8303 \pm 0.3112$). Contrary to our prospect, lowest absorbance was measured in SBio FACSsorted cells ($MV = 0.6537 \pm 0.3330$), indicating that least mineralization occurred.

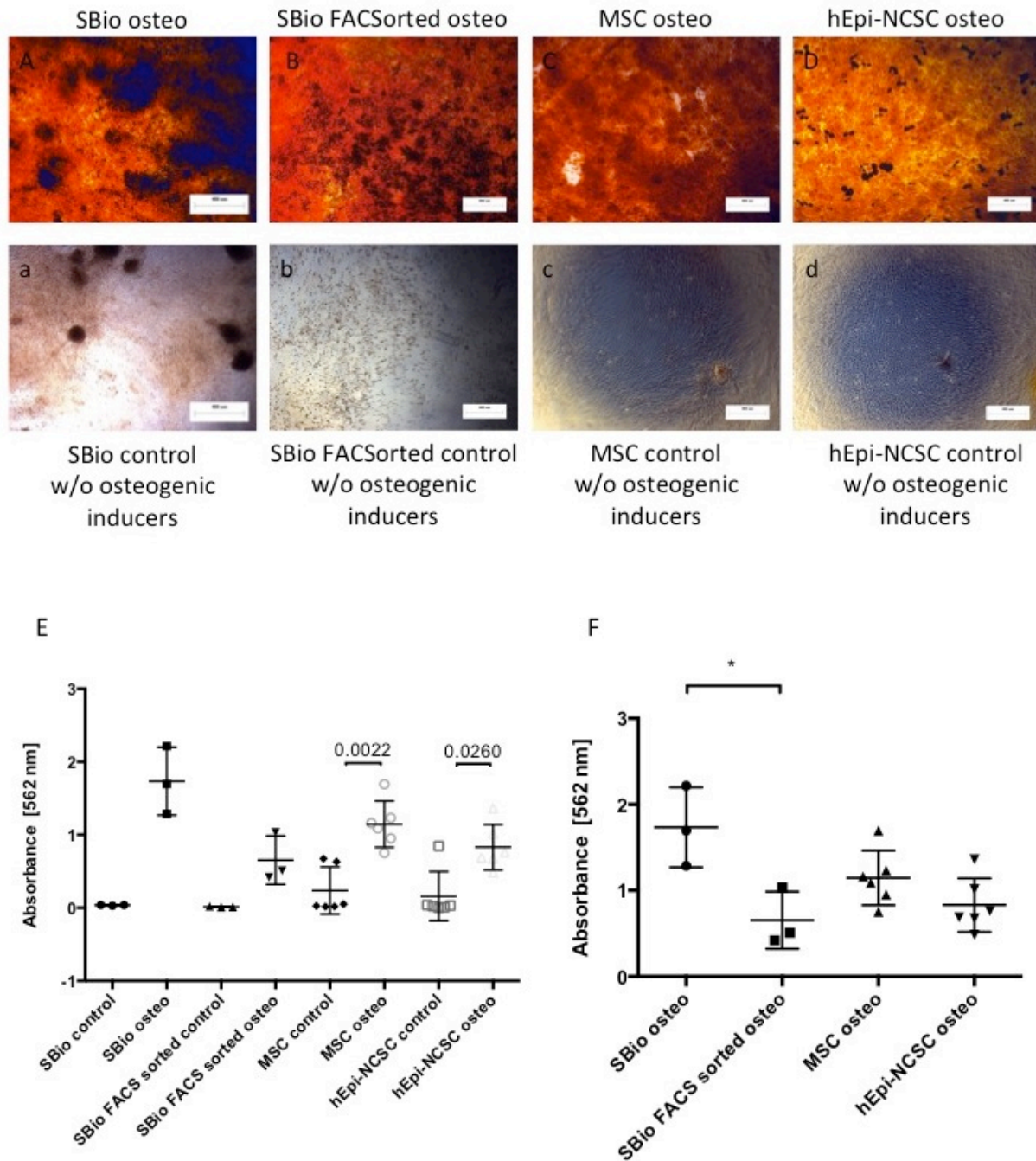


Figure 4-14: Osteogenic differentiation of SBio cells, SBio FACSsorted cells, MSCs and hEpi-NCSCs after 28 days cultivation represented by positive Alizarin red staining.

(A) SBio cells, (B) SBio FACSsorted cells, (C) MSCs and (D) hEpi-NCSCs compared to their respective control (a-d). All pictures were documented by phase-contrast microscopy and are shown in 5 × magnification. Scale bar = 400 μm in all pictures. (E) displays absorption of destained Alizarin red of SBio cells (n=6), SBio FACSsorted (n=6), MSCs (n=12) and hEpi-NCSCs (n=12) in relation to corresponding untreated control. (F) Comparison of achromatized Alizarin red absorption of osteogenic induced samples from each cell type. Statistical analysis between groups was performed using Mann-Whitney U test, parameters within one group were compared by Wilcoxon test. Data are presented as mean values, with error bars representing standard deviations, *p<0.012.

Absorbance of all control samples was extensively decreased in reference to their mineralized supplemented sample. Among the untreated samples, MSC showed highest absorbance ($MV = 0.2363 \pm 0.3236$), followed by hEpi-NCSCs ($MV = 0.1580 \pm 0.3379$), SBio cells ($MV = 0.03502 \pm 0.005593$), and FACSorted cells possessed lowest absorbance with a MV of 0.01378 ± 0.005889 .

To compare cell types in relation to each other, SBio cells with highest absorbance were used as a reference and set to 100 %. In correlation to ECM formation of SBio cells, mineralization of MSCs was 66.13 %, hEpi-NCSCS showed 47.91 %, and SBio cells 37.72 % maintained in osteo-inductive media. In untreated control samples calcified mineralization accounted 13.64 % for MSC controls, 9.12 % for hEpi-NCSC controls, 2.02 % for SBio controls and 0.80 % for SBio FACSorted controls.

Thus, we conclude that osteogenic induction was successful in all cell types. Unsorted SBio cells showed highest potential to differentiate towards osteogenic lineage compared to FACSorted SBio cells and even in relation to MSCs and hEpi-NCSCs.

5 Discussion

Aim of this thesis was to establish and characterize a hiPS cell-based model system for the generation of human NC-like cell population. Several methods for NCSC-generation are available, which involve hiPSCs co-cultured with mouse stromal cell line PA6 (Mizuseki et al. 2003; Pomp et al. 2005; Jiang et al. 2008), embryoid body (Zhou & Snead 2008) as well as neural rosette formation (Lazzari et al. 2006). However, most of these protocols are very time consuming with experimental design exceeding 4 weeks and the majority of cells tend to differentiate towards neuroectodermal lineage characterized by *PAX6*⁺ expression (Callaerts et al. 1997), while only a minor cell amount gives rise to NCSC-like cells distinguished by *HNK1*⁺*p75*⁺ expression (Pomp et al. 2008b; Lee et al. 2007; Elkabetz et al. 2008). Additionally, use of stromal feeder cells provides undefined culture conditions and might also cause contaminations, which might have a negative effect on NC development (Chimge & Bayarsaihan 2010). NC differentiation under defined culture conditions within a reduced time period, and a feasible higher yield of *HNK1*⁺*p75*⁺ cells is of high demand in NCSC research. To fulfill these conditions, hiPSCs-derived NC generation through targeting several intracellular pathways might be constituted as a promising tool. In order to find the most effective NCSC differentiation method for an improved yield of *HNK1*⁺*p75*⁺ cells, two already published protocols were selected, performed, and investigated.

5.1 NCSC differentiation by modifying signaling pathways

Both protocols yielded NC-like cell population from hiPS cell line by modifying signaling pathways within a time frame of 12 days. Further, cells were cultivated as adherent cells, which enabled observations of morphological changes occurring during the differentiation process. While G. Lee (Lee et al. 2010) induced NCSC formation through dual SMAD inhibition and neural differentiation media, L. Menendez (Menendez et al. 2011) applied SMAD-2/-3 inhibition combined with canonical WNT activation.

5.1.1 Dual Smad inhibition was not sufficient for enhanced production of NC-like cell population

This method is based on the NCSC differentiation protocol published by G. Lee (Lee et al. 2010), which evolved from a neural induction system. Previous findings described the crucial role of SMAD signaling in neural induction by mammalian noggin⁷ and recombinant Noggin (Lee et al. 2007; Elkabetz et al. 2008), while another research group discovered hESC neural induction in an EB promoted by the small molecule SB431542 (Smith et al. 2008). The underlying mechanism of SB431542 is the inhibition of Lefty/Activin/TGF- β pathways through blocking of phosphorylation of ALK4, ALK5 and ALK7 receptors (Inman et al. 2002). Due to these findings, Chambers developed a defined feeder-free hESC neural induction system by combining recombinant Noggin and the drug SB431542. Unexpectedly, Chambers observed that this culture model also efficiently generates cells of NC fate (Stuart M. Chambers 2009). Based on these findings, Lee established a defined feeder-free culture system for NCSC differentiation from hiPSCs. Previous to NCSC induction, Lee dissociated undifferentiated hiPSCs into single cells and re-plated onto matrigel coated culture wells in conditioned medium containing Rock-inhibitor Y-27632, which supports survival of dissociated cells (Stuart M. Chambers 2009; Lee et al. 2010a). To work under defined culture conditions, we cultivated single hiPSCs in mTeSR-1 media supplemented with Rock-inhibitor Y-27632. After 48 hours media switch from mTeSR-1 media to KSR:N2 media gradient containing Noggin and SB431542 (NSB) was carried out over a time frame of 12 days (Lee et al. 2010a). One major drawback that occurred during NCSC differentiation through dual SMAD inhibition was the high cell density, which was observed from day 5. Additionally, media change was only performed every second day starting from day three (section 1.2.3.1). The yellow color change of the media might be an indication that cells performed high metabolism and that nutrient supply was not sufficient (data not shown). In addition to the reduced nutrition inadequate inhibitor concentration might have a negative effect on NC differentiation. Regarding cell density, the protocol points out that a lower cell density might decrease cell viability, whereas an excessive cell density significantly lowers NC differentiation (Lee et al. 2010a). Chamber also examined that by increasing cell density, more cells became neural progenitor cells expressing *PAX6*⁺, while by reducing cell density development of *PAX6*⁻ NC progeny was favored (Stuart M. Chambers 2009). Therefore, it is expected that 3-dimensional cell

growth (see Figure 4-2 B-C) might significantly minimize differentiation towards NC lineage. As expected, the cell population showed high heterogeneity of neuroectoderm cultures as visible in Figure 4-2 B-C (Stuart M. Chambers 2009; Lee et al. 2010a; Menendez et al. 2011) from which NCSC-like cells were quantified via FACS analysis. Lee denoted in his protocol, that approximately 15 – 40 % (Lee et al. 2010a) of the Noggin/SBio431542 (NSB) treated cells should be positive for HNK1⁺p75⁺, which was not achieved in our experiments. The mean value (MV) of HNK1⁺p75⁺ NSB cells was clearly under the estimated value (MV = 7.4 ± 1.88 %; shown in Figure 4-6 B-A) after 12 days treatment. In opposition to our expectations, untreated NSB control samples showed a higher yield of HNK1⁺p75⁺ cell population (MV= 16.86 ± 11.08 %; presented in Figure 4-6 C), whereby only in one sample of the two induced approaches a high proportion of HNK1⁺p75⁺ cells was measured (24.7 % see Figure 4-6 C). These values correlated to the cDNA bands, which were visualized by gel-electrophoresis. cDNA bands for *HNK1* and *p75* of untreated NSB control samples were thicker compared to that of treated NSB samples (Figure 4-4 A). Even by omitting the high value received by FACS analysis of untreated NSB control sample, NSB treatment did not show an improved yield of HNK1⁺p75⁺ cells compared to untreated NSB control samples ($p=0.3333$). There are no exact explanations for these results other than that spontaneous NC differentiation might occur in untreated NSB control or that the treated NSB sample was interchanged with the untreated control, but both options are very improbable. Moreover, even if the ICC staining was not significant due to high cell loss, the remaining NSB cells still exhibited a MV of 13.68 ± 4.91 % HNK1⁺p75⁺ cells (compare Figure 4-6 A), which ranged in the lower expectations of the NSB protocol (Lee et al. 2010a).

Recently, a research group published a modification of dual SMAD inhibition method (Kreitzer et al. 2013). They used the synthetic small molecule inhibitor LDN-193189 for BMP type-1 receptors ALK2 and ALK3 to substitute Noggin (Yu et al. 2008). Another abbreviation of the protocol was that NC-differentiation was carried out within 10 days instead of 12 days. Based on the observation that the two applied hiPSCs cell lines expressed HNK1, only cells expressing p75⁺ were selected as NC-like cells. However, they also observed that the majority of cells were neural precursor cells expressing *PAX6*. They presumed NC-like cell production at higher yields developed from fewer neural precursor cells in a shortened time frame due to the knowledge that lower

iPSC-seeding density promotes differentiation of neural precursor and NC cell types (Stuart M. Chambers 2009). For this purpose, they retained the neural priming step, but reduced NC formation phase time by half. Neural-primed cells were cultivated in a KSR:N2 media gradient over a time period of 4 days leading to a NC-system formation method of 5 instead of 10 days. Approximately 80 % of the NC-like cells expressed p75 as analyzed by FACS (Kreitzer et al. 2013).

Comparing our results to the previously mentioned outcomes of Kreitzers group, we came to the conclusion that an intermediate BMP level within 12 days does not lead to a difference ($p = 0.3333$ via FACS) of NC-like cell formation compared to untreated control samples (compare Figure 4-6 C). Therefore a large production of NC-like cells was not achieved by applying the dual SMAD inhibition model system. In order to verify this assumption and the reproducibility of results, the experiment should be repeated several times under identical conditions. However, the modified method developed by Kreitzer might be a time-reducing and cost-effective technology for hiPSCs-derived NC formation through dual SMAD blockage (Kreitzer et al. 2013), which should also be tested.

5.1.2 Intermediate BMP level combined with canonical WNT activation improved NC differentiation

The second method was based on the NCSC specification protocol according to L. Menendez (Menendez et al. 2011). Menendez constructed her protocol similar to the NCSC formation method designed by Lee (Lee et al. 2010a) but modified the NC differentiation model system by including the canonical WNT signaling (Menendez et al. 2011; Menendez et al. 2013). Canonical WNT signaling is known as a key regulatory pathway crucial in NC lineage generation in vertebrate development (Wilson et al. 2001; García-Castro et al. 2002; Patthey et al. 2009). By summarizing both theories, Menendez protocol for NC differentiation from hESCs and hiPSCs implies blocking of GSK, the antagonist of WNT signaling with the small molecule BIO and inhibition of Activin A/SMAD signaling with SB431542 (Menendez et al. 2011; Menendez et al. 2013).

According to our expectations intermediate BMP signaling in conjunction with canonical WNT signaling produced a higher yield of NC-like cells than the dual SMAD inhibition system (Lee et al. 2010a). Even if the predicted value of $> 90\%$ HNK1⁺p75⁺ cell population (Menendez et al. 2011) was not achieved, ICC evaluation resulted in a quite

high amount of NC-like cells ($MV = 68.22 \pm 11.20 \%$; presented in Figure 4-6 A), while FACS analysis measured a lower percentage of cells expressing HNK1⁺p75⁺ ($MV = 35.2 \pm 18.24 \%$; shown in Figure 4-6 B-C; $p=0.2$ via FACS of SBio and SBio control samples). An explanation for the differences between these two analytical techniques might arise from the intensity measurement for ICC evaluation (see section 3.4.6) as well as during the adjustment of the fluorescence frame (see sections 3.4.6 – 3.4.9) for FACS analysis. Both methods have to be manually adjusted by the user. This assumption is underlined by the fact that our hiPSCs cell line was HNK1⁺ analyzed by FACS measurement (see Figure 4-6 D), which was also reported by another research group for two other hiPSCs cell lines (Kreitzer et al. 2013). As previously mentioned, Kreitzers group conducted NC differentiation analysis by p75⁺ expression (Kreitzer et al. 2013). Consequently, the possibility exists that by adjusting the fluorescence frame only for p75 cells, the results would be in concordance with ICC evaluation because the strong signals for HNK1⁺ might falsify the FACS measurements.

Beside these deviations of results gained from both practices, FACS analysis clarified that there was a difference between SBio treated cells ($MV = 35.2 \pm 18.24 \%$; shown in Figure 4-6 B-C) and untreated cells, which displayed a minor amount of HNK1⁺p75⁺ cells ($MV = 8.40 \pm 4.53 \%$; shown in Figure 4-6 C). Already during cell cultivation, we could observe that cells treated with SBio not only survived under new culture conditions, they also changed from colony forming cells (Figure 4-1 A) into single cells after the second EDTA cell passing (Figure 4-3 B).

In contrast, only few cells of untreated SBio control cells could be maintained in culture and these remaining cells continued to grow in colonies (Figure 4-3 c). In this regard, it has to be mentioned that the applied conditioned media in the Menendez protocol is the defined hiPSCs culture media StemPro but without Activin A. Therefore, hiPSCs of L. Menendez were already maintained in StemPro media (Menendez et al. 2011; Menendez et al. 2013), while our hiPSCs master culture was cultivated in mTeSR-1 media. StemPro and mTeSR-1 media are two commercial hiPSC media, which support hiPSCs maintenance in culture, while retaining differentiation capabilities. They differ in their supplements in respect to different components and concentrations of specific growth factors (Akopian et al. 2010). As hiPSCs are known for their sensitivity to any changes related to cultivation conditions, we assumed that media switch from mTeSR-1 to conditioned media used for Menendez protocol led to poor survival of our untreated

hiPSC SBio control cells (Figure 4-3 c). Furthermore, we tried to cultivate our hiPSCs cells within StemPro media but as these cells had to be maintained at least for three passages in this new media, the time frame was too short for this new culture conditions adaption. With regard of these culture conditions, the opportunity persists that hiPSCs already maintained in StemPro media might affect a higher yield of HNK1⁺p75⁺ cells than hiPSCs cultured in mTeSR-1 media. Importantly, it has to be taken into consideration that our hiPSCs cells were not only exposed to new influences induced by the two inhibitors but also had to adapt to new media conditions during NC-lineage formation.

Aside from modulation of intracellular signaling the handling of cell culture is very crucial for a successful NC-lineage formation system (Stuart M. Chambers 2009; Lee et al. 2010a; Kreitzer et al. 2013). This was indicated by the third approach of SBio treatment, which produced a higher yield of NC-like cells (56.1 % shown in Figure 4-6 B-C) compared to the other two approaches that showed lower yields of HNK1⁺p75⁺ cells (compare Figure 4-6 B-C). Therefore, optimizing the handling of cells during differentiation process is significant e.g. cell densities when NC-differentiation is induced, as well as passaging and cell-seeding density during NC-differentiation process. To figure out optimized handling of cell culture, it is recommended to repeat the experiment under identical conditions to ensure reproducibility of results.

A further advantage of this protocol is that inhibition of SMAD-1, -5 and -8 by Noggin was not required, which was also denoted by Menendez (Menendez et al. 2011). Menendez assumed that the basal level of SMAD-1, -5 and -8 must be very low in this system and that WNT activation affected major impact on NC differentiation. This outcome allows omission of Noggin. The ability to omit Noggin enables a cost-effective NC differentiation protocol, as small molecules are less expensive than recombinant Noggin (Menendez et al. 2011). This aspect is crucial for the perspective to generate high numbers of NCSCs for cell replacement therapies in future.

As previous mentioned, our experiment did not achieve > 90 % HNK1⁺p75⁺ cells. The minor amount of NC-like cells (47.7 % Figure 4-7 A) resulted in the requirement of cell-sorting step to obtain a homologous cell population. Thus, the great advantage of omitting a FACS-assisted purification step could not be ensured (Menendez et al. 2011). Subsequently FACSorted SBio cells were further expanded to achieve a high yield of cells

for osteogenic differentiation. Surprisingly, after one week of expansion, of cells re-analyzed by FACS only 65.9 % of SBio cells were positive for HNK1 and p75 expression (see Figure 4-7 C). This might demonstrate that both markers are not constantly expressed or that previous FACSorting harmed cells indicated by a modified gene expression.

Interestingly, levels of mRNA expression for HNK1 were only 10.68 times increased, while mRNA level of p75 was 220.36 increased (see section 4.1.2.3). The outcome on mRNA level for p75 correlated to the results published by Menendez that showed elevated levels of 230-240 (Menendez et al. 2011). With respect of these outcomes, the question emerged how fast the conversion of protein translation from HNK1 mRNA is and how long the half-life of HNK1 mRNA is.

However, SBio cells expressed all NC markers such as *SOX9*, *SNAIL*, *SLUG*, *HNK1*, *p75* and *SOX10* (Sauka-Spengler & Bronner-Fraser 2008; Jiang et al. 2009; Lee et al. 2010a; Menendez et al. 2011), visualized by the presence of cDNA in gel-electrophoresis (see Figure 4-4 B).

Summarizing our findings, we can conclude that combination of activating canonical WNT signaling, and inhibition of Activin A/SMAD signaling represents an effective system for a successful enrichment of cells with genetic and phenotypic properties of NCSCs. These findings, however, should be optimized by further recapitulations.

5.2 SBio cells exhibited highest potential for mineralization

In the second part of the study, osteogenic differentiation was induced followed by mineralization formation to proof multipotency characteristic for NCSCs in SBio and FACSorted SBio cells (Hall 2000). MSCs and hEpi-NCSCs functioned as control references due to their known multipotency. As previously mentioned, MSCs are multipotent adult stem cells with the ability to differentiate into various mesodermal cell type including osteoblasts (Friedenstein et al. 1974). The second control reference is hEpi-NCSCS isolated from hair follicles that also retain their multipotency to differentiate towards osteogenic lineage (Clewes et al. 2011).

Based on the application of tissue culture plates we were able to analyze osteogenic potential of SBio cells, FACSorted SBio cells, hMSCs and hEpi-NCSCSs by Alkaline phosphatase (ALP) assay and histochemical staining for mineral deposit. Osteoblast

phenotype and matrix maturation is reflected by enhanced enzymatic ALP activity (Sila-Asna et al. 2007; Allen 2003; Kulterer et al. 2007). Even if the exact mechanism of ALP in osteogenesis is not clarified (Siffert 1950; Golub et al. 1992), it is suspected that ALP releases P_i by hydrolyzing phosphate substrates and participates in mineralization induction (Balcerzak et al. 2003). NBT/BCIP staining method revealed that all cell types showed basal ALP activity. This was verified as all osteogenic induced cell types and respective non-treated controls were stained after 7 days (compare Figure 4-13 A-d).

However strongest color signal was detected in unsorted SBio osteogenic initiated cells, followed by its respective untreated control sample (Figure 4-13 A and a). It seemed that ALP coloration of SBio FACSorted, MSCs and hEpi-NCSCs mineralized samples was slightly more intense compared to their respective untreated control samples (Figure 4-13 B-D and b-d). ALP assay confirmed that highest ALP activity was measured in SBio mineralized cells, which was significant higher than its respective untreated control that possessed secondary highest ALP activity, followed by osteogenic induced MSCs samples (Figure 4-13 E). Untreated MSCs and SBio FACSorted cells showed similar ALP activity (Figure 4-13 E-F), followed by hEpi-NCSCs mineralized sample and the corresponding untreated control (Figure 4-13 E) and lowest ALP activity was detected in SBio untreated control (Figure 4-13 E). Mature osteoblasts secrete and deposit mineral matrix comprising mainly calcium phosphate in form of hydroxyapatite that characterizes the final phase of osteoblast differentiation (zur Nieden et al. 2003). In our experiment, we observed matrix deposition by phase contrast microscopy in all osteogenic treated cell types in the second week of the differentiation process (Figure 4-9 C, Figure 4-11 C and Figure 4-12 C) except for SBio FACSorted, where matrix development was observed in the third week (Figure 4-10 D). This observation is in concordance with previous reports of osteogenic induced MSCs, where mineralization was also observed after two weeks (Mathews et al. 2011). To analyze mineral matrix accumulation, Alizarin Red staining was performed (Figure 4-14 A-d). Highest potential for mineralization formation under osteogenic condition was assumed in pure FACSorted SBio cells. But in opposition to our expectations, enhanced mineralization deposition was measured in unsorted SBio cells, which was significantly ($p=0.0117$) higher than SBio FACSorted cells (Figure 4-14 F). Additionally, mineralization formation of unsorted SBio cells even exceeded that of osteogenic induced MSCs and hEpi-NCSCs (Figure 4-14 E-F). These findings, in combination of the results of the ALP staining and

the ALP assay indicated that unsorted SBio cells show the highest mineralization potential (Figure 4-14 A, E and F; Figure 4-13 A, E and F). Based on the hypothesis that the fluorescence frame of the FACS was wrongly adjusted due to the strong HNK1⁺ signal, we can speculate that another cell type than the target type of the heterologous cell population was FACSorted, which does not possess multipotency like NC-like cells. Moreover, Menendez proofed that hiPSCs differentiated NC-like cells are capable to perform mineralization formation (Menendez et al. 2011).

Further, it would be interesting to investigate which cell types were present beside HNK1 p75 double positive cells in the heterologous SBio population (Jiang et al. 2009; Lee et al. 2010a; Menendez et al. 2011).

Lower osteogenic potential in SBio FACSorted cells might arise due to FACSorting. Menendez emphasized that one main benefit of the established method is the omission of FACSorting (Menendez et al. 2011). Her statement comprises that FACSorting might harm cells at various levels due to damage caused by hydrodynamic stress during the cell-sorting process (Mollet et al. 2007). Hence, we might assume that this stress might lead to cell mutation, which might modify multipotency resulting in decreased osteogenic differentiation. Therefore, FACSorting should be avoided if possible (Menendez et al. 2011). The decreased amount of 65.9 % HNK1⁺p75⁺ cells one week after FACSorting (Figure 4-7 C) might be an indication of this previously mentioned assumption or that NCSC do not constantly express both NC-markers. In addition, an important aspect that has to be taken into account is the high cell passage of these particular mineralized induced SBio cells. This cell population was already in passage 32 (117 days after NC differentiation), when mineralization was initiated. Menendez only assures for 100 days (< 25 passages) maintenance of NCSC features (Menendez et al. 2011; Menendez et al. 2013). It would be interesting to which extent osteogenic differentiation would have been observed with fresh NC induced cells. To confirm the assumption that hiPSCs derived NC-like cells are able to differentiate towards osteogenic lineage, several replications of mineralization experiments should be carried out. Additionally, other osteopromotive substances such as BMP (2, 4 and 7), TGF- β 1, active Vitamin D, parathyroid hormone (reviewed in Zuk et al., 2001), VEGF, IGF-1 and FGF2 (Huang et al. 2010) should be supplemented to mineralization media to improve osteogenic differentiation potential. Other studies dealing with culture surfaces coated

with chitosan (Mathews et al. 2011) or titanium (Maeda et al. 2007) reported beneficial effects in mineralization process during osteoblast differentiation derived from hMSCs.

6 Conclusion

This work compared two NCSC-lineage formation methods by modifying intracellular signaling pathways from a feeder-free hiPSCs cell line under adherent cell culture conditions. We aimed to investigate, which method is more effective in generating a high amount of NC-like cells from hiPSCs indicated by HNK1⁺p75⁺ expression. The first method is based on dual SMAD inhibition provided by recombinant Noggin and SB431542 (NSB) and cultivated in KSR/N2 media. Here, we did not achieve the predicted value of 15 – 20 % HNK1⁺p75⁺ cells (Lee et al. 2010b) in three different biological approaches. Importantly, NSB treated cells did not differ from untreated NSB control cells for HNK1⁺p75⁺ expression measured by FACS analysis ($p=0.3333$).

In contrast, the second method, based on activated canonical WNT signaling and blocking of TGF- β pathway, improved NC differentiation ($p=0.2$), even though the predicted value of more than 90 % was not reached in three different biological approaches (Menendez et al. 2011). To proof and optimize NC differentiation procedure the method should be recapitulated several times and also be tested in different hiPSCs cell lines (Kreitzer et al. 2013). One disadvantage of this approach in terms of NC-characterization was the application of FACS analysis for HNK1⁺p75⁺ expression. Thereby, the possibility persists that errors might occur during this procedure by the user who has to adjust the fluorescence frame manually.

As previously mentioned, Kreitzer investigated that his used hiPSCs cell lines were positive for HNK1. This was also observed for our applied hiPSCs cell line. Kreitzer selected NC-like cells by the presence of p75 for his modified dual SMAD inhibition model system to generate NC cells from hiPSCs (Kreitzer et al. 2013). Based on this outcome, NC-characterization of both methods should be carried out on p75 expression in order to reduce erroneous measurements by FACS-analysis. This assumption is also reinforced by the observation that unsorted SBio cells possessed a significant higher potential for mineralization formation ($p = 0.00117$) compared to FACSorted SBio cells that co-expressed HNK1⁺p75⁺.

Finally, we came to the conclusion that combinational SMAD-2, -3 blocking and canonical WNT signaling represent an auspicious instrument to produce NC-like cells

confirmed by morphological appearance, genetic expression of NC-markers and multipotency.

The aim of this study was to compare two methods in order to investigate, which method yields the highest amount of hiPSCs-derived NC-lineage formation. The improved method should serve as a tool for the generation of NC-derived tissue in NC research. The next goal is to optimize cultivation conditions to establish unlimited numbers of hiPSCs induced NC-like cells. This *in vitro* NC-differentiation model allows new opportunities to investigate basic biology of NC cells or NC derivatives in human development (Kreitzer et al. 2013). Moreover, hiPSCs-derived NC-like cells enable differentiation into various cell types such as peripheral nerves, smooth muscle cells (Kreitzer et al. 2013), astrocytes, chondrocytes and osteocytes (Menendez et al. 2011), evoking great attraction in regenerative medicine. In future, this NC-like generation cell system might be interpreted as a promising source for cell and tissue replacement therapies (Kreitzer et al. 2013). Particularly, reprogramming of patient-specific cells into hiPSCs could be further differentiated into NC-derived tissue to replace damaged or lost tissue. Especially, examination of the mechanism of NC biology and associated neurocristopathies in a patient-specific manner opens new avenues to speed-up the development of new drugs and therapeutic approaches in the treatment of NC disorders (Lee et al. 2010b; Menendez et al. 2011; Müntz 2012; Kreitzer et al. 2013). As mentioned in section 1.2.5, G. Lee generated the first hiPSCs-derived NCSCs *in vitro* model from Familial Dysautonomia (FD) patients (Lee et al. 2009; Lee & Studer 2011). One major hallmark of this genetic disorder is the degeneration of the neural crest derivatives autonomic and sensory neurons. FD patients possess a tissue specific mRNA processing defect, which is caused by a point mutation in the *IKB-KAP* gene (I-k-B kinase complex associated protein), reducing the amount of normal IKBKAP protein. The *in vitro* cellular model from FD reprogrammed hiPSCs enabled the generation of neural crest precursor cells, which showed reduced levels of intact *IKBKAP* transcripts, an aberrant migration behavior, as well as deficiencies in their differentiation processes (Lee et al. 2009; Milet & Monsoro-Burq 2012). Based on these properties, various drugs have been designed and tested on these hiPSCs-FD-derived NCSCs, resulting in the creation of a substance that reestablishes the *IKBKAP* mRNA processing defects in these affected cells (Milet & Monsoro-Burq 2012). This study clearly demonstrates in which extent hiPSCs-derived

NCSCs models in a patient-specific manner accelerates the discovery of new therapy strategies, which might be significant to treat neurocristopathies in clinical applications.

7 Literature

- Adewumi, O. et al., 2007. Characterization of human embryonic stem cell lines by the International Stem Cell Initiative. *Nature biotechnology*, 25(7), pp.803–16.
- Akopian, V. et al., 2010. Comparison of defined culture systems for feeder cell free propagation of human embryonic stem cells. *In vitro cellular & developmental biology. Animal*, 46(3-4), pp.247–58.
- Allen, M.J., 2003. Biochemical Markers of Bone Metabolism in Animals: Uses and Limitations. *Veterinary Clinical Pathology*, 32(3), pp.101–113.
- Van Amerongen, R. & Nusse, R., 2009. Towards an integrated view of Wnt signaling in development. *Development (Cambridge, England)*, 136(19), pp.3205–14.
- Amit, M. et al., 2003. Human feeder layers for human embryonic stem cells. *Biology of reproduction*, 68(6), pp.2150–6.
- Antony, A.C. & Hansen, D.K., 2000. Hypothesis: folate-responsive neural tube defects and neurocristopathies. *Teratology*, 62(1), pp.42–50.
- Atmani, H. et al., 2002. Phenotypic effects of continuous or discontinuous treatment with dexamethasone and/or calcitriol on osteoblasts differentiated from rat bone marrow stromal cells. *Journal of cellular biochemistry*, 85(3), pp.640–50.
- Balcerzak, M. et al., 2003. The roles of annexins and alkaline phosphatase in. , 50(4), pp.1019–1038.
- Banerjee, C. et al., 1997. Runt homology domain proteins in osteoblast differentiation: AML3/CBFA1 is a major component of a bone-specific complex. *Journal of cellular biochemistry*, 66(1), pp.1–8.
- Bellmeyer, A. et al., 2003. The protooncogene c-myc is an essential regulator of neural crest formation in xenopus. *Developmental cell*, 4(6), pp.827–39.

- Bellows, C.G., Heersche, J.N. & Aubin, J.E., 1990. Determination of the capacity for proliferation and differentiation of osteoprogenitor cells in the presence and absence of dexamethasone. *Developmental biology*, 140(1), pp.132–8.
- Bettters, E. et al., 2010. Analysis of early human neural crest development. *Developmental biology*, 344(2), pp.578–92.
- Bolande, R.P., 1997. Neurocristopathy: its growth and development in 20 years. *Pediatric pathology & laboratory medicine : journal of the Society for Pediatric Pathology, affiliated with the International Paediatric Pathology Association*, 17(1), pp.1–25.
- Boskey, A.L., Wright, T.M. & Blank, R.D., 1999. Collagen and bone strength. *Journal of bone and mineral research : the official journal of the American Society for Bone and Mineral Research*, 14(3), pp.330–5.
- Britsch, S. et al., 2001. The transcription factor Sox10 is a key regulator of peripheral glial development. , pp.66–78.
- Brokhman, I. et al., 2008. Peripheral sensory neurons differentiate from neural precursors derived from human embryonic stem cells. *Differentiation; research in biological diversity*, 76(2), pp.145–55.
- Bronner, M.E. & LeDouarin, N.M., 2012. Development and evolution of the neural crest: an overview. *Developmental biology*, 366(1), pp.2–9.
- Burger, E.H. & Klein-Nulend, J., 1999. Mechanotransduction in bone--role of the lacuno-canalicular network. *FASEB journal: official publication of the Federation of American Societies for Experimental Biology*, 13 Suppl, pp.S101–12.
- Callaerts, P., Halder, G. & Gehring, W.J., 1997. PAX-6 in development and evolution. *Annual review of neuroscience*, 20, pp.483–532.
- Caplan, A.I. & Correa, D., 2011. The MSC: an injury drugstore. *Cell stem cell*, 9(1), pp.11–5.

- Cárcamo, J. et al., 1994. Type I receptors specify growth-inhibitory and transcriptional responses to transforming growth factor beta and activin. *Molecular and cellular biology*, 14(6), pp.3810–21.
- Carpenter, M.K. et al., 2004. Properties of four human embryonic stem cell lines maintained in a feeder-free culture system. *Developmental dynamics: an official publication of the American Association of Anatomists*, 229(2), pp.243–58.
- Carpenter, M.K., Rosler, E. & Rao, M.S., 2003. Characterization and differentiation of human embryonic stem cells. *Cloning and stem cells*, 5(1), pp.79–88.
- Cheng, S.L. et al., 1994. Differentiation of human bone marrow osteogenic stromal cells in vitro: induction of the osteoblast phenotype by dexamethasone. *Endocrinology*, 134(1), pp.277–86.
- Cheung, M. et al., 2005. The transcriptional control of trunk neural crest induction, survival, and delamination. *Developmental cell*, 8(2), pp.179–92.
- Chimge, N.-O. & Bayarsaihan, D., 2010. Generation of neural crest progenitors from human embryonic stem cells. *Journal of experimental zoology. Part B, Molecular and developmental evolution*, 314(2), pp.95–103.
- Clevers, H., 2006. Wnt/beta-catenin signaling in development and disease. *Cell*, 127(3), pp.469–80.
- Clewes, O. et al., 2011. Human epidermal neural crest stem cells (hEPI-NCSC)--characterization and directed differentiation into osteocytes and melanocytes. *Stem cell reviews*, 7(4), pp.799–814.
- Daley, G.Q., 2010. Stem cells: roadmap to the clinic. *The Journal of clinical investigation*, 120(1), pp.8–10.
- Davis, R.L., Weintraub, H. & Lassar, A.B., 1987. Expression of a single transfected cDNA converts fibroblasts to myoblasts. *Cell*, 51(6), pp.987–1000.
- Denker, H.-W., 2009. Induced pluripotent stem cells: how to deal with the developmental potential. *Reproductive biomedicine online*, 19 Suppl 1, pp.34–7.

- Le Douarin, N.M. et al., 2004. Neural crest cell plasticity and its limits. *Development (Cambridge, England)*, 131(19), pp.4637–50.
- Draper, J.S. et al., 2004. Recurrent gain of chromosomes 17q and 12 in cultured human embryonic stem cells. *Nature biotechnology*, 22(1), pp.53–4.
- Drukker, M., 2006. *Stem Cell Tools and Other Experimental Protocols*, Elsevier.
- Duband, J.L. et al., 1995. Epithelium-mesenchyme transition during neural crest development. *Acta anatomica*, 154(1), pp.63–78.
- Ducy, P. et al., 1997. Osf2/Cbfa1: A Transcriptional Activator of Osteoblast Differentiation. *Cell*, 89(5), pp.747–754.
- Eisenmann, D.M., 2005. Wnt signaling. *WormBook: the online review of C. elegans biology*, pp.1–17.
- Elkabetz, Y. et al., 2008. Human ES cell-derived neural rosettes reveal a functionally distinct early neural stem cell stage. *Genes & development*, 22(2), pp.152–65.
- Endo, Y., Osumi, N. & Wakamatsu, Y., 2002. Bimodal functions of Notch-mediated signaling are involved in neural crest formation during avian ectoderm development. *Development (Cambridge, England)*, 129(4), pp.863–73.
- Evans, M.J. & Kaufman, M.H., 1981. Establishment in culture of pluripotential cells from mouse embryos. *Nature*, 292(5819), pp.154–156.
- Fortuna, R. et al., 1980. Enzymatic characterization of the matrix vesicle alkaline phosphatase isolated from bovine fetal epiphyseal cartilage. *Calcified tissue international*, 30(3), pp.217–25.
- Friedenstein, A.J. et al., 1974. Stromal cells responsible for transferring the microenvironment of the hemopoietic tissues. Cloning in vitro and retransplantation in vivo. *Transplantation*, 17(4), pp.331–40.
- García-Castro, M.I., Marcelle, C. & Bronner-Fraser, M., 2002. Ectodermal Wnt function as a neural crest inducer. *Science (New York, N.Y.)*, 297(5582), pp.848–51.

- Glavic, A. et al., 2004. Interplay between Notch signaling and the homeoprotein Xiro1 is required for neural crest induction in *Xenopus* embryos. *Development (Cambridge, England)*, 131(2), pp.347–59.
- Golub, E.E. et al., 1992. The role of alkaline phosphatase in cartilage mineralization. *Bone and mineral*, 17(2), pp.273–8.
- Gore, A. et al., 2011. Somatic coding mutations in human induced pluripotent stem cells. *Nature*, 471(7336), pp.63–7.
- Gurdon, J.B., 1962. The developmental capacity of nuclei taken from intestinal epithelium cells of feeding tadpoles. *Journal of embryology and experimental morphology*, 10(December), pp.622–40.
- Hacein-Bey-Abina, S. et al., 2003. LM02-associated clonal T cell proliferation in two patients after gene therapy for SCID-X1. *Science (New York, N.Y.)*, 302(5644), pp.415–9.
- Hall, B.K., 2000. The neural crest as a fourth germ layer and vertebrates as quadroblastic not triploblastic. *Evolution and Development*, 2(1), pp.3–5.
- Hansen, D., Lou, H.C. & Olsen, J., 2000. Serious life events and congenital malformations: a national study with complete follow-up. *Lancet*, 356(9233), pp.875–80.
- Hari, L. et al., 2012. Temporal control of neural crest lineage generation by Wnt/ β -catenin signaling. *Development (Cambridge, England)*, 139(12), pp.2107–17.
- Hitomi, K., Torii, Y. & Tsukagoshi, N., 1992. Increase in the activity of alkaline phosphatase by L-ascorbic acid 2-phosphate in a human osteoblast cell line, HuO-3N1. *Journal of nutritional science and vitaminology*, 38(6), pp.535–44.
- Huang, X. & Saint-Jeannet, J.-P., 2004a. Induction of the neural crest and the opportunities of life on the edge. *Developmental biology*, 275(1), pp.1–11.
- Huang, X. & Saint-Jeannet, J.-P., 2004b. Induction of the neural crest and the opportunities of life on the edge. *Developmental biology*, 275(1), pp.1–11.

- Huang, Z. et al., 2010. Modulating osteogenesis of mesenchymal stem cells by modifying growth factor availability. *Cytokine*, 51(3), pp.305–10.
- Hussein, S.M. et al., 2011. Copy number variation and selection during reprogramming to pluripotency. *Nature*, 471(7336), pp.58–62.
- Inman, G.J. et al., 2002. SB-431542 Is a Potent and Specific Inhibitor of Transforming Growth Factor- β Superfamily Type I Activin Receptor-Like. , 62(1), pp.65–74.
- Jiang, X. et al., 2009. Isolation and characterization of neural crest stem cells derived from in vitro-differentiated human embryonic stem cells. *Stem cells and development*, 18(7), pp.1059–70.
- Jiang, X. et al., 2008. Isolation and characterization of neural crest stem cells derived from in vitro-differentiated human embryonic stem cells. *Stem cells and development*, 18(7), pp.1059–70.
- Jones, N.C. & Trainor, P.A., 2005. Role of morphogens in neural crest cell determination. *Journal of neurobiology*, 64(4), pp.388–404.
- Kang, L. & Gao, S., 2012. Pluripotency of induced pluripotent stem cells. *Journal of animal science and biotechnology*, 3(1), p.5.
- Kee, Y. & Bronner-Fraser, M., 2005. To proliferate or to die: role of Id3 in cell cycle progression and survival of neural crest progenitors. *Genes & development*, 19(6), pp.744–55.
- Kim, J.B. et al., 2009. Direct reprogramming of human neural stem cells by OCT4. *Nature*, 461(7264), pp.649–643.
- Körbling, M., Estrov, Z. & Champlin, R., 2003. Adult stem cells and tissue repair. *Bone marrow transplantation*, 32 Suppl 1(S1), pp.S23–4.
- Koshihara, Y. et al., 1987. In vitro calcification in human osteoblastic cell line derived from periosteum. *Biochemical and biophysical research communications*, 145(2), pp.651–7.

- Kreitzer, F.R. et al., 2013. A robust method to derive functional neural crest cells from human pluripotent stem cells. , 2(2), pp.119–131.
- Kulterer, B. et al., 2007. Gene expression profiling of human mesenchymal stem cells derived from bone marrow during expansion and osteoblast differentiation. *BMC genomics*, 8, p.70.
- LaBonne, C. & Bronner-Fraser, M., 1998. Neural crest induction in *Xenopus*: evidence for a two-signal model. *Development (Cambridge, England)*, 125(13), pp.2403–14.
- Lagasse, E. et al., 2000. Purified hematopoietic stem cells can differentiate into hepatocytes in vivo. *Nature medicine*, 6(11), pp.1229–34.
- Lagna, G. et al., 1996. Partnership between DPC4 and SMAD proteins in TGF-beta signalling pathways. *Nature*, 383(6603), pp.832–6.
- Lazzari, G. et al., 2006. Direct derivation of neural rosettes from cloned bovine blastocysts: a model of early neurulation events and neural crest specification in vitro. *Stem cells (Dayton, Ohio)*, 24(11), pp.2514–21.
- Lee, G. et al., 2010a. Derivation of neural crest cells from human pluripotent stem cells. *Nature protocols*, 5(4), pp.688–701.
- Lee, G. et al., 2010b. Derivation of neural crest cells from human pluripotent stem cells. *Nature protocols*, 5(4), pp.688–701.
- Lee, G. et al., 2007. Isolation and directed differentiation of neural crest stem cells derived from human embryonic stem cells. *Nature biotechnology*, 25(12), pp.1468–75.
- Lee, G. et al., 2009. Modelling pathogenesis and treatment of familial dysautonomia using patient-specific iPSCs. *Nature*, 461(7262), pp.402–6.
- Lee, G. & Studer, L., 2011. Modelling familial dysautonomia in human induced pluripotent stem cells. *Philosophical transactions of the Royal Society of London. Series B, Biological sciences*, 366(1575), pp.2286–96.

- Lewis, J.L. et al., 2004. Reiterated Wnt signaling during zebrafish neural crest development. *Development (Cambridge, England)*, 131(6), pp.1299–308.
- Light, W. et al., 2005. Xenopus Id3 is required downstream of Myc for the formation of multipotent neural crest progenitor cells. *Development (Cambridge, England)*, 132(8), pp.1831–41.
- Lister, R. et al., 2011. Hotspots of aberrant epigenomic reprogramming in human induced pluripotent stem cells. *Nature*, 471(7336), pp.68–73.
- Liu, Y. & Xiao, A., 2011. Epigenetic regulation in neural crest development. *Birth defects research. Part A, Clinical and molecular teratology*, 91(8), pp.788–96.
- Maeda, M. et al., 2007. In vitro mineralization by mesenchymal stem cells cultured on titanium scaffolds. *Journal of biochemistry*, 141(5), pp.729–36.
- Marchant, L. et al., 1998. The inductive properties of mesoderm suggest that the neural crest cells are specified by a BMP gradient. *Developmental biology*, 198(2), pp.319–29.
- Mathews, S. et al., 2011. Chitosan enhances mineralization during osteoblast differentiation of human bone marrow-derived mesenchymal stem cells, by upregulating the associated genes. *Cell proliferation*, 44(6), pp.537–49.
- Mayor, R., Guerrero, N. & Martínez, C., 1997. Role of FGF and noggin in neural crest induction. *Developmental biology*, 189(1), pp.1–12.
- Mayor, R., Morgan, R. & Sargent, M.G., 1995. Induction of the prospective neural crest of Xenopus. *Development (Cambridge, England)*, 121(3), pp.767–77.
- McLaren, A., 2001. Ethical and social considerations of stem cell research. *Nature*, 414(6859), pp.129–31.
- Menendez, L. et al., 2013. Directed differentiation of human pluripotent cells to neural crest stem cells. *Nature protocols*, 8(1), pp.203–12.

- Menendez, L. et al., 2011. Wnt signaling and a Smad pathway blockade direct the differentiation of human pluripotent stem cells to multipotent neural crest cells.
- Milet, C. & Monsoro-Burq, A.H., 2012. Embryonic stem cell strategies to explore neural crest development in human embryos. *Developmental biology*, 366(1), pp.96–9.
- Miron, R.J. & Zhang, Y.F., 2012. Osteoinduction: a review of old concepts with new standards. *Journal of dental research*, 91(8), pp.736–44.
- Miyazono, K., Kamiya, Y. & Morikawa, M., 2010. Bone morphogenetic protein receptors and signal transduction. *Journal of biochemistry*, 147(1), pp.35–51.
- Mizuseki, K. et al., 2003. Generation of neural crest-derived peripheral neurons and floor plate cells from mouse and primate embryonic stem cells. *Proceedings of the National Academy of Sciences of the United States of America*, 100(10), pp.5828–33.
- Mollamohammadi, S. et al., 2009. A simple and efficient cryopreservation method for feeder-free dissociated human induced pluripotent stem cells and human embryonic stem cells. *Human reproduction Oxford England*, 24(10), pp.2468–2476.
- Mollet, M. et al., 2007. Acute hydrodynamic forces and apoptosis: a complex question. *Biotechnology and bioengineering*, 98(4), pp.772–88.
- Monsoro-Burq, A.-H., 2003. Neural crest induction by paraxial mesoderm in *Xenopus* embryos requires FGF signals. *Development*, 130(>14), pp.3111–3124.
- Morrison, S.J., Shah, N.M. & Anderson, D.J., 1997. Regulatory mechanisms in stem cell biology. *Cell*, 88(3), pp.287–98.
- Motohashi, T. et al., 2007. Multipotent cell fate of neural crest-like cells derived from embryonic stem cells. *Stem cells (Dayton, Ohio)*, 25(2), pp.402–10.
- Münst, S., 2012. Neural crest development in a human embryonic stem cell-based model system.

- Nakashima, K. et al., 2002. The Novel Zinc Finger-Containing Transcription Factor Osterix Is Required for Osteoblast Differentiation and Bone Formation. *Cell*, 108(1), pp.17–29.
- Neirinckx, V. et al., 2013. Concise review: adult mesenchymal stem cells, adult neural crest stem cells, and therapy of neurological pathologies: a state of play. *Stem cells translational medicine*, 2(4), pp.284–96.
- Zur Nieden, N.I., Kempka, G. & Ahr, H.J., 2003. In vitro differentiation of embryonic stem cells into mineralized osteoblasts. *Differentiation; research in biological diversity*, 71(1), pp.18–27.
- Nuttelman, C.R., Tripodi, M.C. & Anseth, K.S., 2004. In vitro osteogenic differentiation of human mesenchymal stem cells photoencapsulated in PEG hydrogels. *Journal of biomedical materials research. Part A*, 68(4), pp.773–82.
- O’Rahilly, R. & Müller, F., 2007. The development of the neural crest in the human. *Journal of anatomy*, 211(3), pp.335–51.
- Okita, K., Ichisaka, T. & Yamanaka, S., 2007. Generation of germline-competent induced pluripotent stem cells. *Nature*, 448(7151), pp.313–7.
- Patthey, C., Edlund, T. & Gunhaga, L., 2009. Wnt-regulated temporal control of BMP exposure directs the choice between neural plate border and epidermal fate. *Development (Cambridge, England)*, 136(1), pp.73–83.
- De Peppo, G.M. & Marolt, D., 2012. State of the Art in Stem Cell Research: Human Embryonic Stem Cells, Induced Pluripotent Stem Cells, and Transdifferentiation. *Journal of Blood Transfusion*, 2012, pp.1–10.
- Peter, S.J. et al., 1998. Osteoblastic phenotype of rat marrow stromal cells cultured in the presence of dexamethasone, beta-glycerolphosphate, and L-ascorbic acid. *Journal of cellular biochemistry*, 71(1), pp.55–62.
- Pomp, O. et al., 2005. Generation of peripheral sensory and sympathetic neurons and neural crest cells from human embryonic stem cells. *Stem cells (Dayton, Ohio)*, 23(7), pp.923–30.

- Pomp, O. et al., 2008a. PA6-induced human embryonic stem cell-derived neurospheres: a new source of human peripheral sensory neurons and neural crest cells. *Brain research*, 1230, pp.50–60.
- Pomp, O. et al., 2008b. PA6-induced human embryonic stem cell-derived neurospheres: a new source of human peripheral sensory neurons and neural crest cells. *Brain research*, 1230(null), pp.50–60.
- Rathjen, J. et al., 2002. Directed differentiation of pluripotent cells to neural lineages: homogeneous formation and differentiation of a neurectoderm population. *Development (Cambridge, England)*, 129(11), pp.2649–61.
- Raven, C., 1945. *Induction by medial and lateral pieces of the archenteron roof, with special reference to the determination of the neural crest*, Utrecht: N.V.A Oosthoek's Uitgevers-Maatschappij.
- Rosler, E.S. et al., 2004. Long-term culture of human embryonic stem cells in feeder-free conditions. *Developmental dynamics: an official publication of the American Association of Anatomists*, 229(2), pp.259–74.
- Sanchez-Ramos, J. et al., 2000. Adult bone marrow stromal cells differentiate into neural cells in vitro. *Experimental neurology*, 164(2), pp.247–56.
- Sarić, T., Frenzel, L.P. & Hescheler, J., 2008. Immunological barriers to embryonic stem cell-derived therapies. *Cells, tissues, organs*, 188(1-2), pp.78–90.
- Sato, T., Sasai, N. & Sasai, Y., 2005. Neural crest determination by co-activation of Pax3 and Zic1 genes in *Xenopus* ectoderm. *Development (Cambridge, England)*, 132(10), pp.2355–63.
- Sauka-Spengler, T. & Bronner-Fraser, M., 2008. A gene regulatory network orchestrates neural crest formation. *Nature reviews. Molecular cell biology*, 9(7), pp.557–68.
- Schneuwly, S., Klemenz, R. & Gehring, W.J., Redesigning the body plan of *Drosophila* by ectopic expression of the homoeotic gene Antennapedia. *Nature*, 325(6107), pp.816–8.

- Selleck, M. a et al., 1998. Effects of Shh and Noggin on neural crest formation demonstrate that BMP is required in the neural tube but not ectoderm. *Development (Cambridge, England)*, 125(24), pp.4919–30.
- Shakhova, O. & Sommer, L., 2010. Neural crest-derived stem cells. *StemBook*, pp.1–20.
- Shi, Y. & Massagué, J., 2003. Mechanisms of TGF-beta signaling from cell membrane to the nucleus. *Cell*, 113(6), pp.685–700.
- Siffert, B.R.S., 1950. THE ROLE OF ALKALINE PHOSPHATASE IN O S T E O G E N E S i S (From the Departments of Orthopedic Surgery and Pathology , The Mount Sinai Hospital , New York).
- Sila-Asna, M. et al., 2007. Osteoblast differentiation and bone formation gene expression in strontium-inducing bone marrow mesenchymal stem cell. *The Kobe journal of medical sciences*, 53(1-2), pp.25–35.
- Smith, A.G., 2001. E MBRYO -D ERIVED S TEM C ELLS : Of Mice and Men.
- Smith, A.G. et al., 1988. Inhibition of pluripotential embryonic stem cell differentiation by purified polypeptides. *Nature*, 336(6200), pp.688–90.
- Smith, A.G. & Hooper, M.L., 1987. Buffalo rat liver cells produce a diffusible activity which inhibits the differentiation of murine embryonal carcinoma and embryonic stem cells. *Developmental biology*, 121(1), pp.1–9.
- Smith, J.R. et al., 2008. Inhibition of Activin/Nodal signaling promotes specification of human embryonic stem cells into neuroectoderm. *Developmental biology*, 313(1), pp.107–17.
- Stojkovic, M. et al., 2004. Derivation, growth and applications of human embryonic stem cells. *Reproduction (Cambridge, England)*, 128(3), pp.259–67.
- Stuart M. Chambers, 2009. Highly efficient neural conversion of human ES and iPS cells by dual inhibition of SMAD signaling. , 27(3), pp.275–280.

- Tada, M. et al., 2001. Nuclear reprogramming of somatic cells by in vitro hybridization with ES cells. *Current biology : CB*, 11(19), pp.1553–8.
- Takahashi, K. et al., 2007. Induction of pluripotent stem cells from adult human fibroblasts by defined factors. *Cell*, 131(5), pp.861–872.
- Takahashi, K. & Yamanaka, S., 2006. Induction of pluripotent stem cells from mouse embryonic and adult fibroblast cultures by defined factors. *Cell*, 126(4), pp.663–76.
- Tenenbaum, H.C., 1987. Levamisole and inorganic pyrophosphate inhibit beta-glycerophosphate induced mineralization of bone formed in vitro. *Bone and mineral*, 3(1), pp.13–26.
- Thiery, J.P., 2002. Epithelial-mesenchymal transitions in tumour progression. *Nature reviews. Cancer*, 2(6), pp.442–54.
- Thomas, S. et al., 2008. Human neural crest cells display molecular and phenotypic hallmarks of stem cells. *Human molecular genetics*, 17(21), pp.3411–25.
- Thomson, J. a., 1998. Embryonic Stem Cell Lines Derived from Human Blastocysts. *Science*, 282(5391), pp.1145–1147.
- Uccelli, A., Moretta, L. & Pistoia, V., 2008. Mesenchymal stem cells in health and disease. *Nature reviews. Immunology*, 8(9), pp.726–36.
- Vazin, T. & Freed, W.J., 2010. Human embryonic stem cells: derivation, culture, and differentiation: a review. *Restorative neurology and neuroscience*, 28(4), pp.589–603.
- Wennberg, C. et al., 2000. Functional characterization of osteoblasts and osteoclasts from alkaline phosphatase knockout mice. *Journal of bone and mineral research : the official journal of the American Society for Bone and Mineral Research*, 15(10), pp.1879–88.
- Wilmut, I. et al., 1997. Viable offspring derived from fetal and adult mammalian cells. *Nature*, 385(6619), pp.810–3.

- Wilson, S.I. et al., 2001. The status of Wnt signalling regulates neural and epidermal fates in the chick embryo. *Nature*, 411(6835), pp.325–30.
- Woodbury, D. et al., 2000. Adult rat and human bone marrow stromal cells differentiate into neurons. *Journal of neuroscience research*, 61(4), pp.364–70.
- Wrana, J.L. et al., 1994. Mechanism of activation of the TGF-beta receptor. *Nature*, 370(6488), pp.341–7.
- Wu, J., Yang, J. & Klein, P.S., 2005. Neural crest induction by the canonical Wnt pathway can be dissociated from anterior-posterior neural patterning in *Xenopus*. *Developmental biology*, 279(1), pp.220–32.
- Yamanaka, S., 2012. Induced pluripotent stem cells: past, present, and future. *Cell stem cell*, 10(6), pp.678–84.
- Yamanaka, S. & Blau, H.M., 2010. Nuclear reprogramming to a pluripotent state by three approaches. *Nature*, 465(7299), pp.704–12.
- Yanfeng, W., Saint-Jeannet, J.-P. & Klein, P.S., 2003. Wnt-frizzled signaling in the induction and differentiation of the neural crest. *BioEssays: news and reviews in molecular, cellular and developmental biology*, 25(4), pp.317–25.
- Yu, P.B. et al., 2008. BMP type I receptor inhibition reduces heterotopic ossification. , 14(12), pp.1363–1369.
- Zaehres, H. et al., 2010. Induction of pluripotency in human cord blood unrestricted somatic stem cells. *Experimental hematology*, 38(9), pp.809–18, 818.e1–2.
- Zeisberg, M. & Kalluri, R., 2004. The role of epithelial-to-mesenchymal transition in renal fibrosis. *Journal of molecular medicine (Berlin, Germany)*, 82(3), pp.175–81.
- Zhou, Y. & Snead, M.L., 2008. Derivation of cranial neural crest-like cells from human embryonic stem cells. *Biochemical and biophysical research communications*, 376(3), pp.542–7.

Zuk, P.A. et al., 2001. Multilineage cells from human adipose tissue: implications for cell-based therapies. *Tissue engineering*, 7(2), pp.211–28.

Curriculum Vitae

Personal information

First name/Surname	Song-hi Kneutgen
Address	Pannierstraße 15 12047 Berlin
E-mail	Song-hi@hotmail.de
Nationality	German
Date of birth	31. January 1981
Gender	Female

Work and Scientific Experience

Dates	April 2012-January 2013
Occupation or position held	Internship, 10 months
Main activities	Master thesis „NCSC differentiation from hiPSCs“ Induced pluripotent stem cells (iPSC), Cell culture, Neural crest stem cell differentiation, Osteogenic differentiation, RNA isolation, PCR, RT-PCR, ICC, Alkaline phosphatase staining & biochemical assay, Alizarin Red staining
Group leader	Dr. Andreas Kurtz
Name of employers	Berlin Brandenburg Zentrum für regenerative Therapien, Charité Berlin

Dates	November 2011-March 2012
Occupation or position held	Internship, 5 months
Main activities	Cell culture, FACS
Group leader	Prof. Dr. Hermann Lage
Name of employers	Institut für Pathologie, Charité Berlin
Dates	July 2011-September 2011
Occupation or position held	Internship, 11 weeks
Main activities	ChIP (from cell suspensions, tissue and FFPE), Real time PCR
Group leader	Dr. Gerda Egger
Name of employers	Institut für Pathologie, Medizinische Universität Wien
Dates	April 2009 – June 2009
Occupation or position held	Internship, 3 months
Main activities	Bachelor thesis „ Evaluation of Standardised Meal Test by Exemplary Biomarkers for the Assessment of Insulin Treatment and Underlying Beta-Cell Function“, Clinical Research
Group leader	Prof. Andreas Pfützner
Name of employers	Ikfe CRO GmbH, Institut für klinische Forschung und Entwicklung, Mainz
Type of business	Clinical Research

Dates February 2007 – March 2007

Occupation or position held Internship, 2 months

Group leader Dr. Johannes Schumacher

Name of employers Institut für Humangenetik, Poliklinik Bonn

Dates June 2004 – July 2004

Occupation or position held Internship, 6 weeks

Name of employers Institut für Tierwissenschaft, Bonn

Education and training

Dates Since April 2010

Title of qualification awarded Master of Science

Field of studies Molecular Biology – Molecular Medicine

Molecular Medicine, Epigenetics, Stem cells, Virology, Protein structure

Relevant professional knowledge and experience (laboratory internship, literature)

Name and type of organisation Universität Wien

Providing education and training Dr. Karl-Lueger Ring 1, 1010 Vienna

Dates	October 2006 – October 2009
Title of qualification awarded	Bachelor of Science
Field of Studies	Molecular Biology
	Molecular Medicine, Microbiology, Cell Biology, Laboratory Internships
Name and type of organisation	Hochschule Bonn-Rhein-Sieg
Providing education and training	Von-Liebig-Straße 20, 53359 Rheinbach
Dates	October 2004 – July 2007
Title of qualification awarded	Biologisch-Technische - Assistentin
Field of Studies	Biology
	Microbiology, Zoology, Botanic, Cell Biology, Laboratory Internships
Name and type of organisation	Rheinische Akademie Köln gGmbH
Providing education and training	Vogelsanger Straße 295, 50825 Köln
Dates	October 2000 – October 2002
Field of Studies	Economy
Name and type of organisation	Humboldt Universität Berlin
Providing education and training	Unter den Linden 6, 10117 Berlin
Dates	August 1991 – July 2000
Title of qualification awarded	School leaving examination

Name and type of organisation Ernst Kalkuhl Gymnasium, Bonn

Personal skills and competences

Mother tongue German

Other language English

Organizational skills and competences Teamwork and Conflict Management, Quality Management

Additional activities

Dates April 2010 – October 2010

Position Waitress

Name of employers Kimchi Princess, Berlin

Dates Decembre 2009

Position Sales woman

Name of employers Christmas Market

Dates October 2002 – March 2003

Position Waitress

Name of employers Cafe Melitta Sundström, Berlin